ROLE OF THE RHOA/ROCK PATHWAY IN HYPERTENSION ASSOCIATED WITH DIABETES

by

MILLY YUSHU RAO

B.Sc., The University of Washington, 2009

A THESIS SUBMITTED IN PARTIAL FULFILLMENT OF

THE REQUIREMENTS FOR THE DEGREE OF

MASTER OF SCIENCE

in

THE FACULTY OF GRADUATE STUDIES

(Pharmaceutical Sciences)

THE UNIVERSITY OF BRITISH COLUMBIA

(Vancouver)

October 2011

Abstract

Hypertension is the most common cardiovascular complication associated with diabetes mellitus. The RhoA/ROCK pathway has been implicated in the regulation of vascular smooth muscle contractile responses associated with hypertension and diabetes. Here we wished to determine the role of the RhoA/ROCK pathway in vascular smooth muscle contractile responses in different types of diabetic models and its contribution to diabetes-associated hypertension.

Our results suggest that the involvement of ROCK may be more important in U-46619- than in PE-induced contractile responses in endothelium denuded mesenteric resistance arteries from control rats. On the other hand, as found in our previous work and other reports, PE-induced contractile responses were attenuated by inhibition of ROCK in rat superior mesenteric arteries, suggesting that ROCK is likely to play an essential role in PE-induced contraction in superior mesenteric arteries.

Blood pressure in GK rats was normalized by one-week treatment with fasudil, a known ROCK inhibitor, suggesting that the elevated blood pressure in GK rats may be due to enhanced ROCK pathway. However, agonist-induced contractile responses in GK mesenteric resistance arteries were not augmented compared to control arteries, and moreover, expression of ROCK/RhoA as well as activity of ROCK were similar between control and GK arteries. The specific causes of the discrepancy remain unknown.

In the presence of L-NAME, ROCK inhibitor significantly attenuated contraction induced by PE or U-46619 in mesenteric resistance arteries from GK rats, suggesting that agonist-induced contractile responses in mesenteric resistance arteries from GK rats were likely to be ROCK-mediated. This was further supported by Western blotting results, in that

phosphorylation of MYPT was significantly increased by U-46619. Interestingly, U-46619-induced contraction in mesenteric resistance arteries from control rats was no longer sensitive to inhibition of ROCK in the presence of L-NAME, although the reasons were unclear.

In conclusion, results from the GK rat study do not support the hypothesis that activation of the RhoA/ROCK pathway contributes to the development of diabetes-associated hypertension in GK rats by enhancing vascular smooth muscle contractile responses. To further investigate this study, a more ROCK selective ROCK inhibitor is needed.

Preface

All animal work conducted in this thesis was approved by the University of British Columbia Animal Care Ethics Committee, protocol # A07-0707.

Table of Contents

List of Figures

LIST OF ABBREVIATIONS

°C	degrees Celsius
μ	micro (1×10^{-6})
μm	micron (1×10^{-6} meter)
ANOVA	analysis of variance
ATP	adenosine triphosphate
BSA	bovine serum albumin
GTP	guanosine triphosphate
GDP	guanosine diphosphate
EGTA	ethylene glycol bis(β-aminoethyl ether) N,N'-tetraacetic acid
g	gram
H-1152	(S)-(+)-2-Methyl-1-[(4-methyl-5 isoquinolinyl) sulfonyl]-homopiperazine, 2HCl
HCl	hydrogen chloride
kg	kilogram
Ki	inhibition constant, concentration for half maximal inhibition
L	liter
L-NAME	NG-Nitro-L-arginine methyl ester hydrochloride
m	milli (1×10^{-3})
Min	minute
M	molar
PAGE	polyacrylamide gel electrophoresis
SDS	sodium dodecyl sulfate

SEM	standard error of the mean
TEMED	N,N,N’N’-tetramethylethylenediamine
U-46619	9,11-Dideoxy-9a,11a-methanoepoxy prostaglandin
Y-27632	(R)-(+)-*trans*-N-(4-Pyridyl)-4-(1-aminoethyl)-cyclohexanecarboxamide, 2HCl
Fasudil	HA-1077, 5-Isoquinolinesulfonyl)homopiperazine, 2HCl

Acknowledgements

I am heartily thankful to my supervisor, Dr. Kathleen MacLeod, for her patience, guidance, and encouragement throughout the course of studies at UBC. Without her kindness and support, my completion of this Master degree and the precious experiences gained throughout the training would not be possible.

My gratitude also goes to my supervisory committee members for their time and constructive suggestions: Drs. Stelvio Bandiera, Roger Brownsey, Brian Rodrigues, and Ujendra Kumar.

I also cannot forget to express appreciation to my fellow lab colleagues Dr. Guorong Lin, Hesham Soliman, and Girish Bankar. Thank you all for your constant assistance and endless support throughout my graduate training.

Finally, I am deeply grateful to my parents and friends. Thank you very much for your advice and love.

Chapter 1: INTRODUCTION

1.1 Diabetes mellitus

Diabetes mellitus is a well known disease with a long history; the earliest known record is from 1552 B.C.. The symptoms were first recognized as excessive thirst, weight loss and the production of large quantities of honey-sweet urine. The name diabetes was provided by the ancient Greek physician Arataeus of Cappodocia around 70 A.D.. Later on in 1670, Thomas Willes, a physician to King Charles, discovered that the urine and blood from a person with diabetes had a sweet taste, so he added 'mellitus' derived from the Latin word for honey (Canadian Diabetes Association, 2011).

In the late 19th century, Joseph von Mering and Oskar Minkovski first noted that dogs that are pancreatectomized developed hyperglycemia, suggesting there is something in the pancreas that might regulate glucose levels (Canadian Diabetes Association, 2011). This work was continued and expanded by the Canadian researchers Sir Frederick Grant Banting and John James Richard MacLeod. Together with their colleagues, they found that the pancreactomy-induced diabetes in dogs could be reversed by providing them extracts from healthy pancreatic islets, and that the hormone insulin produced from the pancreatic β-cells is the key player controlling glucose levels (Banting, Best et al. 1922). The discovery of insulin for the treatment of diabetes is indeed one of the major milestones of the 20th century.

1.2 Classification of diabetes

Type 1 diabetes mellitus, known as insulin-dependent diabetes, accounts for about 10% of all diagnosed diabetes cases. People are usually diagnosed with type 1 diabetes at an early age (Canadian Diabetes Association, 2011). The pathogenesis of type 1 diabetes has been attributed to three proposed mechanisms: genetic susceptibility, autoimmunity, and environmental factors (Krolewski, Warram et al. 1987; Rossini, Mordes et al. 1988). The genetic susceptibility leads to a slow and progressive immunological attack on pancreatic β-cells due to a genetic defect. The autoimmunity is widely accepted to be a T-cell mediated response, which can occur spontaneously or can be triggered by environmental factors including viruses and chemicals. All these would lead to progressive destruction of β-cells, resulting in insulin deficiency. Insulin injection is the only treatment that is effective in type 1 diabetic patients.

Type 2 diabetes on the other hand makes up 90% of all diagnosed cases. Unlike type 1 diabetes, the onset of type 2 diabetes is relatively later. However, due to the prevalence of obesity and lack of exercise, the incidence of type 2 diabetes in children has dramatically increased (Canadian Diabetes Association, 2011). It is thought to be due to over-nutrition and subsequent insulin resistance (Prentki and Nolan 2006). Obesity is found in 50-90% of all type 2 diabetic patients (Del Valle, Adair et al. 1997). Through a compensatory response to over-nutrition and obesity-associated insulin resistance, increased amounts of insulin are secreted by β-cells, leading to hyperinsulinemia. With time, β-cells fail to maintain hypersecretion of insulin to overcome the insulin resistance, which results in hyperglycemia (Del Valle, Adair et al. 1997). This eventually leads to insulin deficiency similar to the conditions in type 1 diabetes. Therefore, in the later stages of type 2 diabetes, patients also

require insulin injection. The major causes of type 2 diabetes have been attributed to genetic predisposition, environmental factors and lifestyle choices. In addition, certain ethnic populations have been suggested to be more prone to type 2 diabetes (Pimenta, Korytkowski et al. 1995).

1.3 Diabetes associated cardiovascular complications and increased vascular smooth muscle contractile response

Diabetes mellitus associated cardiovascular complications, such as hypertension, cardiomyopathy, cardiac hypertrophy, and coronary atherosclerosis are recognized to be the major cause of morbidity and mortality (Tenenbaum, Fisman et al. 1999). Approximately 65% of diabetic patients die from cardiovascular complications (Grundy, Benjamin et al. 1999). Factors including obesity and insulin resistance in type 2 diabetes are usually associated with an increased risk of cardiovascular disease (Vega 2001). Among these diabetes-associated cardiovascular complications, hypertension (BP > 140/90 mm Hg) is the most commonly seen one; up to 60% of the diabetic population has a dual diagnosis of type 2 diabetes together with hypertension, and it is twice as common in diabetic patients as in the non-diabetic population (Sowers and Epstein 1995). Not only is hypertension associated with type 2 diabetes, it is also seen in patients with type 1 diabetes; a study conducted by Collado-Mesa et al. has shown that 24% of 3250 type 1 diabetic patients from European countries had hypertension, and only a few of them were on treatment, suggesting the undermanagement of hypertension in Type 1 diabetes (Collado-Mesa, Colhoun et al. 1999). Hypertension is characterized by a high arterial pressure level caused by elevated peripheral vascular

resistance attributable to increased vascular smooth muscle contractility, arterial wall remodeling (thickening), and reduced vasodilation (Loirand, Guerin et al. 2006). Although both type 1 and type 2 diabetes are associated with hypertension, the causes are different. In type 1 diabetes, nephropathy is the most frequent cause of hypertension (Lago, Singh et al. 2007). In contrast, in type 2 diabetes, hypertension usually occurs without abnormalities in renal function, but instead, it is often associated with obesity and insulin resistance, resulting in the activation of the sympathetic nervous and the renin–angiotensin systems (Lago, Singh et al. 2007).

1.4 RhoA/Rho kinase pathway

Abnormalities in the regulatory apparatus mediating contractile responses of smooth muscle have been suggested to be a major cause of augmentation in vascular tone (Noma, Oyama et al. 2006; Puetz, Lubomirov et al. 2009). Among multiple complex contractile pathways, the RhoA/Rho kinase (ROCK) pathway has been implicated in the regulation of vascular smooth muscle contractility associated with hypertension and diabetes (Somlyo and Somlyo 1994; Chitaley, Weber et al. 2001; Somlyo and Somlyo 2003; Xie, Gong et al. 2010). In addition, the RhoA/ROCK pathway also regulates other important cellular functions, such as differentiation, proliferation, and migration in various organs including vessels, brain, lungs, and heart (Somlyo and Somlyo 1994; Somlyo and Somlyo 2003; Loirand, Guerin et al. 2006).

RhoA is a member of the Rho family of monomeric GTPases, which cycle between an inactive GDP-bound form and an active GTP-bound form (Budzyn, Marley et al. 2006).

When agonists bind to their receptors, the receptors couple to G proteins, leading to the activation by G proteins of a protein called guanine nucleotide exchange factor (GEF), which increases the low dissociation rate of GDP, allowing GTP to bind to RhoA (Somlyo and Somlyo 2000; Puetz, Lubomirov et al. 2009; Aittaleb, Boguth et al. 2010) (fig. 1). Upon activation, Rho is translocated to the plasma membrane from the cytosol, and its interaction with the membrane is facilitated by the hydrophobic geranyl-geranyl tail attached to its C-terminus (Budzyn, Marley et al. 2006). Activated GTP-RhoA at the plasma membrane can then activate its downstream effectors. There are many types of agonists that can activate RhoA through various G-protein-coupled receptors, including α-adrenoceptor agonists, thromboxane A_2, endothelin, thrombin, angiotensin and more, and the two major types of G-proteins these receptors couple to are $G\alpha_{12/13}$ and $G\alpha_q$ (Somlyo and Somlyo 2003). The important players in RhoA activation, GEFs, have been suggested to be direct downstream effectors of G proteins, and consist of three major domains: the DBL homology (DH) domain responsible for the activity of GEFs, the pleckstrin homology (PH) domain in charge of protein-protein and protein-phosphoinositide lipid interactions as well as the localization of GEFs, and the regulators of G protein signaling-like domain (RGSL) required for the coupling of G-protein-receptors to GEFs (Kozasa, Jiang et al. 1998; Kozasa 2001; Rossman, Cheng et al. 2003; Aittaleb, Boguth et al. 2010).

During RhoA inactivation, GTPase-activating proteins (GAPs) catalyze the hydrolysis of active RhoA-bound GTP (Bernards and Settleman 2004; Bos, Rehmann et al. 2007). Inactive RhoA resides predominantly in the cytoplasm, and exists in two forms: free GDP-RhoA and GTPase-dissociation inhibitor (GDI)-GDP-RhoA (Somlyo and Somlyo 2003). GDI captures the prenylated C-terminus of GDP-bound RhoA in its hydrophobic pocket, and at the same

time, its N-terminus interacts with the switch-1 and switch-2 regions of RhoA, inhibiting nucleotide exchange until activated by GEFs (Longenecker, Read et al. 1999). However, the mechanisms by which GDIs dissociate from RhoA are largely undefined. Inactivation of RhoA can also be promoted by phosphorylation of its Ser188 site, which enhances its interaction with GDIs rather than decreasing the activity of GEFs (Ellerbroek, Wennerberg et al. 2003).

One of the well-identified downstream targets of RhoA is ROCK, which is a serine/threonine kinase with a molecular mass of 160 kD (Loirand, Guerin et al. 2006). ROCK sequences are composed of a kinase domain located at the N-terminus, a Rho-binding domain (RBD) within a coiled-coil region, and a C-terminal pleckstrin-homology (PH) domain (Loirand, Guerin et al. 2006) (fig. 2). Two isoforms of ROCK have been identified: ROCK 1 (also known as ROCKβ) and ROCK 2 (also known as ROCKα) (Riento and Ridley 2003; Loirand, Guerin et al. 2006). ROCK 1 and ROCK 2 are greatly homologous, with an identity of 65% in overall amino acid sequence, 58% in the RBD, and 92% in the kinase domain (Nakagawa, Fujisawa et al. 1996). Both ROCK 1 and 2 are expressed in vascular smooth muscle and in heart, with a higher mRNA expression of ROCK 2 in brain and skeletal muscle (Leung, Chen et al. 1996; Nakagawa, Fujisawa et al. 1996; Wibberley, Chen et al. 2003). Although ROCK isoforms are primarily distributed in the cytoplasm, they are partially translocated to the plasma membrane when activated by RhoA (Leung, Manser et al. 1995; Matsui, Amano et al. 1996). The main fraction of ROCK is soluble, and the mechanisms for the subcellular localization of ROCK still remain unclear. Amano *et al.* have shown that the truncated ROCK lacking the C-terminal portion was constitutively active, suggesting that the C-terminal portion of ROCK is responsible for ROCK autoinhibition

(Amano, Chihara et al. 1999). When active GTP-RhoA binds to the RBD of ROCK, it stimulates the phosphotransferase activity of ROCK by disrupting the interaction between kinase and the inhibitory C-terminal region (Feng, Ito et al. 1999). Independently of RhoA, lipid messengers such as arachidonic acid (AA) and spingosine phosphorylcholine (SPC) can efficiently promote ROCK activity by interacting with the negative regulatory C-terminal region of ROCK (Feng, Ito et al. 1999). Furthermore, ROCK can also be activated by cleavage of the autoinhibitory region, resulting in the release of a truncated and active form (Loirand, Guerin et al. 2006). ROCK 1 is cleaved by caspase-3 at its cleavage site DETD, and ROCK 2 is cleaved by proapoptotic protease granzyme B at IGLD, since the consensus sequence for caspase 3 cleavage is not present in ROCK 2 (Sin, Chen et al. 1998; Kosako, Goto et al. 1999; Amano, Fukata et al. 2000).

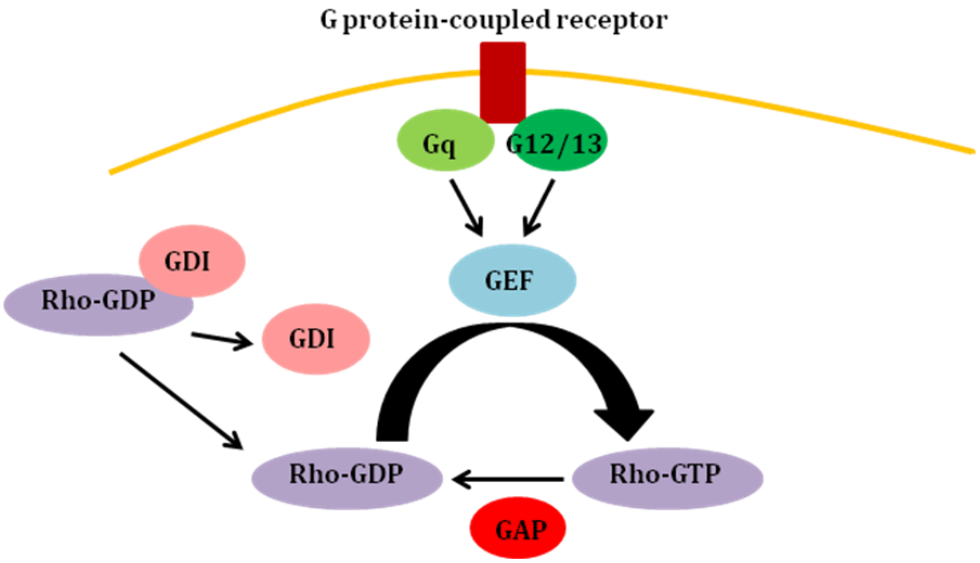

Figure 1: Regulation of Rho activity. RhoGEFs activate Rho by promoting the exchange of GDP for GTP. GDI and GAP negatively regulate the activity of Rho.

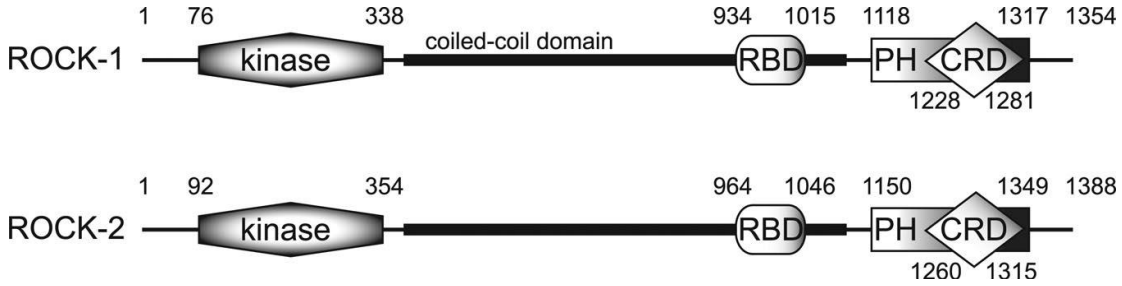

Figure 2: The molecular structure of ROCK isoforms (Loirand, Guerin et al. 2006).

1.5 ROCK inhibitors

The two commonly used ROCK inhibitors are Y-27632 and H-1152. The inhibitory constant (Ki) of Y-27632 is 0.2-0.3 μM for ROCK and 10 μM for protein kinase C (PKC), whereas the Ki value of H-1152 for ROCK is 0.0016 μM and 9.27 μM for PKC (Sasaki, Suzuki et al. 2002). It has been suggested that Y-27632 at a concentration of 10 μM or less is sufficient to inhibit ROCK activity (Somlyo and Somlyo 2003). A third ROCK inhibitor used in this study was Fasudil, a clinically available ROCK inhibitor that inhibits ROCK by competing for the ATP binding site (Dong, Yan et al. 2010). Compared to H-1152 and Y-27632, fasudil is less selective both in intact arteries and in vitro (Tamura, Nakao et al. 2005; Rattan and Patel 2008). However, the major active metabolite of fasudil, hydroxyfasudil, has been shown to be more selective toward ROCK than fasudil (Hattori, Shimokawa et al. 2004). Hydroxylfasudil also has a longer elimination half-life, 5 hours, than fasudil, 1 hour. A review study has pointed out that although ROCK inhibitors are not perfectly selective for ROCK, their activity against ROCK is much greater than against PKC, which in most cases is sufficient for evaluating ROCK functions (Somlyo and Somlyo 2003). Nonetheless, the relative selectivity of ROCK inhibitors has only been tested against a limited number of the many kinases in mammalian systems, so that we cannot rule out the possibility that they may also inhibit other kinases that have not yet been tested. It is worth to mention the major drawback of these ROCK inhibitors, which is that they are not ROCK isoform selective. In other words, all three ROCK inhibitors mentioned here lack the ability to inhibit one of the ROCK isoforms more than the other.

1.6 Ca^{2+}-dependent contraction of vascular smooth muscle

Multiple regulatory processes are involved in modulating vascular smooth muscle contraction, one of which is known as the Ca^{2+}-dependent contraction. In response to specific stimuli, the intracellular Ca^{2+} concentration increases, leading to increased association of Ca^{2+} and calmodulin. The Ca^{2+}-calmodulin complex then activates myosin light chain kinase (MLCK), which in turn phosphorylates myosin light chain (MLC) at Ser19, activating myosin ATPase, which facilitates the cycling of cross-bridges, leading to contraction (fig. 3) (Horowitz, Menice et al. 1996). Activation of receptors such as the α_1-adrenoceptor, which are members of the family of G-protein-coupled receptors, can induce smooth muscle contraction through the Ca^{2+}-dependent pathway (Budzyn, Marley et al. 2006). Activation of G-protein-coupled receptors promotes the breakdown by phospholipase C (PLC) of phosphatidylinositol-4,5-bisphosphate (PIP_2) to produce inositol 1,4,5-triphosphate (IP_3) and diacylglycerol (DAG) (Somlyo and Somlyo 2000). IP_3 binds to IP_3 receptors on Ca^{2+} channels in the sarcoplasmic reticulum, an organelle responsible for storing Ca^{2+}, triggering the release of Ca^{2+} (Somlyo and Somlyo 2000). The intracellular Ca^{2+} concentration can also be increased by the influx of Ca^{2+} from the extracellular space through Ca^{2+} channels upon agonist stimulation (Lee, Webb et al. 2004). In addition, α_1-adrenoceptor and other G-protein-coupled receptor agonists are also thought to have an impact on the Ca^{2+} sensitization-induced smooth muscle contraction, another key pathway modulating vascular smooth muscle contraction, which is discussed in the next section.

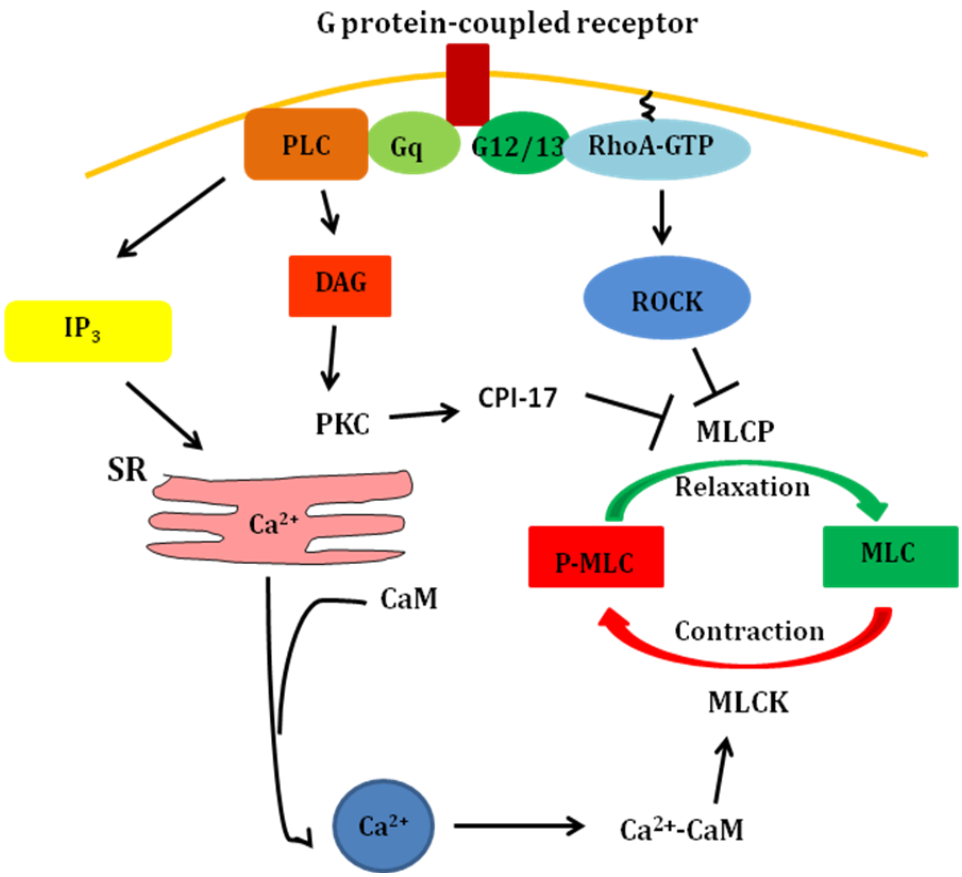

Figure 3: Mechanisms of vascular smooth muscle contraction. Activated G-protein-coupled receptor increases intracellular [Ca^{2+}] via multiple cellular signaling responses, leading to vascular smooth muscle contraction. This is a Ca^{2+}-dependent mechanism. On the other hand, G-protein-coupled receptor agonists can also activate PLC and RhoA, which in turn activate PKC and ROCK, respectively. Activated ROCK phosphorylates and inactivates MLCP, which leads to an increased proportion of phosphorylated MLC and hence increasing contraction. The RhoA/ROCK-mediated pathway occurs independently of changes in intracellular [Ca^{2+}], and therefore is known as Ca^{2+} sensitization. PKC is also involved in Ca^{2+} sensitization by activating CPI-17, which results in MLCP inactivation and increased contraction.

1.7 Ca^{2+} sensitization and contraction

The state of MLC phosphorylation can be regulated by myosin light chain phosphatase (MLCP) in addition to MLCK (Somlyo, Wu et al. 1999; Solaro 2000; Somlyo and Somlyo 2000). MLCP dephosphorylates MLC, promoting smooth muscle relaxation. MLCP is composed of three subunits: a 37-kD catalytic subunit of type 1 phosphatase (PP1), a 20-kD variable subunit of unknown function, and a 110- to 130-kD myosin-binding subunit (MYPT). MYPT interacts with both PP1 and the variable subunits leading to the formation of the holoenzyme of MLCP, which has higher affinity towards phosphorylated MLC than does isolated PP1 (Ito, Nakano et al. 2004). Dissociation of MLCP or inhibition of MLCP activity allows MLC to remain phosphorylated, promoting contraction without a change in intracellular Ca^{2+} concentration, which is known as Ca^{2+} sensitization (fig. 3) (Lee, Webb et al. 2004). Multiple complex cell signaling pathways regulate MLCP activity, and increased vascular smooth muscle contractile responses caused by inhibition of MLCP may eventually lead to hypertension (Chitaley, Weber et al. 2001).

1.7.1 Inhibition of MLCP by dissociation of the holoenzyme

As mentioned above, the holoenzyme formed by the interaction between PP1 and MYPT has a 3-15 fold increase in affinity towards phosphorylated MLC (Ito, Nakano et al. 2004). Thus, dissociation of the MLCP holoenzyme would attenuate the activity of MLCP. It has been reported that AA can cause the dissociation of the holoenzyme, leading to inhibition of MLCP (Gong, Fuglsang et al. 1992).

1.7.2 Inhibition of MLPC by MYPT phosphorylation

One of the major mechanisms for inhibition of MLCP activity is through phosphorylation of MYPT, which results in inhibition of its ability to dephosphorylate MLC (Lee, Webb et al. 2004). A number of studies have demonstrated that inhibition of ROCK alleviated agonist-induced phosphorylation of MYPT in isolated arteries or cultured vascular smooth muscles from several animal models, suggesting that MLCP activity is regulated by ROCK (Mukai, Shimokawa et al. 2001; Seko, Ito et al. 2003; Moriki, Ito et al. 2004; Tsai and Jiang 2006). Phosphorylation of MYPT at Thr696 has been recognized as a major inhibitory phosphorylation site (Chen, Chen et al. 1994; Shimizu, Ito et al. 1994; Takizawa, Koga et al. 2002; Takizawa, Niiro et al. 2002). However, some studies have reported that they found no significant changes in the degree of phosphorylation of Thr696 after agonist stimulation in rabbit portal vein and vas deferens, femoral artery or cultured smooth muscle cells (Kitazawa, Eto et al. 2003; Niiro, Koga et al. 2003; Woodsome, Polzin et al. 2006). Somlyo et al. have suggested that the difficulty in detecting phosphorylation of Thr696 may be due to rapid dephosphorylation at Thr696 site, while on the other hand, Ito et al. have proposed that the nature of Thr696 phosphorylation may differ from tissue/cell to tissue/cell (Somlyo and Somlyo 2003; Ito, Nakano et al. 2004). Besides ROCK, several other kinases, such as integrin-linked kinase (ILK), p21-activated protein kinase (PAK), zipper-interacting protein kinase (ZIPK), myotonic dystrophy protein kinase (DMPK), raf-1, and a ZIP-like kinase are able to phosphorylate MYPT at the Thr696 site (MacDonald, Borman et al. 2001; Muranyi, Zhang

et al. 2001; Niiro and Ikebe 2001; Broustas, Grammatikakis et al. 2002; Muranyi, MacDonald et al. 2002; Takizawa, Koga et al. 2002; Grassie, Moffat et al. 2011).

Thr853 of MYPT has been identified as another important phosphorylation site for inhibiting MLCP activity. Phosphorylation of MYPT at Thr853 is believed to be a specific target of ROCK, whereas Thr696 can be targeted by many different kinases (Grassie, Moffat et al. 2011). Woodsome et al. have shown that agonist-induced phosphorylation of Thr853 in cultured vascular smooth muscle cells was attenuated significantly by Y-27632, suggesting that the other major phosphorylation site of MYPT, Thr853, is highly regulated by ROCK (Woodsome, Polzin et al. 2006).

1.7.3 Inhibition of MLPC by CPI-17 phosphorylation

MLCP activity can also be attenuated by the inhibitor known as CPI-17 (PKC-potentiated myosin phosphatase inhibitor of 17 kDa). CPI-17 is able to inhibit the activity of the holoenzyme of MLCP or the MYPT-PP1 complex as well as that of isolated PP1, and the phosphorylation of CPI-17 at Thr38 enhances its inhibitory activity about 1000 fold due to greater affinity to PP1 (Ito, Nakano et al. 2004). As its name implies, the phosphorylation of Thr38 in CPI-17 is mediated by PKC. This has been shown to be the major mechanism of Ca^{2+} sensitization by PKC under physiological conditions (Somlyo and Somlyo 2003). There are many isoforms in the PKC superfamily, and all of them are able to bind to CPI-17 (Zemlickova, Johannes et al. 2004). The PKC isoforms are categorized into three groups: classic or conventional PKCs including PKC-α, -βI, -βII, and-γ, novel PKCs including PKC-δ, -ε, -η, and -θ, and atypical PKCs including PKC-ζ

and -λ (Carmena and Sardini 2007). Among those, the activation of classic PKCs is Ca^{2+} dependent, while that of novel and atypical PKCs is Ca^{2+} independent (Carmena and Sardini 2007). Nonetheless, only a few of the PKC isoforms, such as PKC-α and PKC-ε, have been implicated in Ca^{2+} sensitization and contraction in response to agonist in vascular smooth muscles from control and STZ-diabetic animals (Mueed, Zhang et al. 2005). Interestingly, a recent study has reported that inhibition of ROCK by Y-27632 was able to diminish high glucose-induced phosphorylation of CPI-17 in cultured vascular smooth muscle cells, suggesting a role for the RhoA/ROCK pathway in regulating the activity of CPI-17 in addition to PKC (Xie, Su et al. 2006) (fig. 2). Pang et al. have reported that agonist-induced CPI-17 phosphorylation was not affected by PKC inhibition, but significantly attenuated by Y-27632 or RhoA inhibition in cultured rabbit aortic cells, further suggesting that the regulation of CPI-17 can be mediated by ROCK (Pang, Guo et al. 2005). In contrast, studies done by Tsai et al. have reported that phenylephrine (PE)-induced CPI-17 phosphorylation was not inhibited by Y-27632, but was by PKC inhibition in rat tail artery strips (Tsai and Jiang 2006). Seko et al. have also demonstrated that Y-27632 was not able to block angiotensin II (AngII)-induced CPI-17 phosphorylation in cultured rat aortic cells (Seko, Ito et al. 2003). These data reveal a discrepancy about whether CPI-17 phosphorylation is ROCK-mediated, which seems to differ from one species/tissue/cell type to another; different experimental preparations and agonist choice also seem to have an influence on CPI-17 phosphorylation.

1.8 Actin polymerization and contraction

In addition to MLCP, vascular smooth muscle contraction is also regulated by actin polymerization or formation of polymeric forms of actin from free monomeric forms, and such remodeling is often triggered by extracellular stimuli (Chen, Pavlish et al. 2006). In unstimulated smooth muscles, actin is composed of filamentous actin (F-actin; polymer) and approximately 25% of globular actin (G-actin; free monomer), whereas in striated muscles, only 11-13% of actin exists as G-actin; thus, a large pool of G-actin is available for polymerization into F-actin in smooth muscles (Cipolla, Gokina et al. 2002). The dynamic regulation of actin has been implicated in smooth muscle contraction in normotensive rats and rats with chronic portal hypertension. It has been suggested that the formation of actin filaments resulting from actin polymerization form cross-bridges with MLC serving as an anchor to the plasma membrane, which strengthens the contractile machinery to facilitate smooth muscle contraction (Gunst and Zhang 2008). Several pieces of evidence have suggested that increased polymerization of G- to F-actin or an increased ratio of F- to G-actin is involved in agonist-induced vascular smooth muscle contraction, and that this is regulated by the RhoA/ROCK pathway (Maekawa, Ishizaki et al. 1999; Chen, Pavlish et al. 2006; Tsai and Jiang 2006; Bernard 2007; Corteling, Brett et al. 2007). When ROCK is activated, it activates LIM kinase, a downstream effector of ROCK, which phosphorylates and inhibits the activity of an actin depolymerizing factor called cofilin (Bernard 2007). Thus, actin polymerization increases, leading to an increased F- to G-actin ratio.

1.9 ROCK and enhanced vascular smooth muscle contractility in hypertension and diabetes

As mentioned, hypertension is a major cardiovascular complication associated with diabetes. Uehata *et al.* have demonstrated that inhibition of ROCK was able to normalize blood pressure in several animal models of hypertension, including the spontaneously hypertensive rat, renal hypertensive rat, and DOCA-salt rat, suggesting a role for the RhoA/ROCK pathway in the development of hypertension (Uehata, Ishizaki et al. 1997). Hirata's group has demonstrated that Ang II-induced vasoconstriction was enhanced in aortic rings from obese zucker rats (OZ), a model of insulin resistance, which was normalized by treatment with ROCK inhibitor (Nishimatsu, Suzuki et al. 2005). Didion *et al.* and Nuno *et al.* have shown that the enhanced agonist-induced contractions in different types of type 2 diabetic models, the db/db mouse and TallyHo mouse models, were attenuated by inhibiting ROCK activity using ROCK inhibitors (Didion, Lynch et al. 2005; Nuno, Harrod et al. 2009). Similarly, in the chronic stage of streptozotocin (STZ)-induced type 1 diabetes in mice, Matsumoto *et al.* demonstrated that treatment with ROCK inhibitor successfully reduced endothelin-1 (ET-1)-induced contraction (Matsumoto, Kakami et al. 2008). These results suggest that ROCK may contribute to altered vascular contractile function in diabetes and conditions of insulin resistance (Nishimatsu, Suzuki et al. 2005; Didion, Lynch et al. 2007; Matsumoto, Kakami et al. 2008; Nuno, Harrod et al. 2009; Matsumoto, Ishida et al. 2010). However, blood pressure was not measured in those investigations, and a possible contribution of ROCK to hypertension in diabetes through enhancing vascular smooth muscle contractile response has not been determined. Furthermore, many studies have examined vascular smooth muscle contractile dysfunction in large arteries such as aorta from

diabetic animals, but only a few have used resistance arteries. Mesenteric resistance arteries are a suitable model for studies of vascular smooth muscle contractile response in hypertension, since the mesenteric circulation plays a pivotal role in the peripheral control of blood pressure.

1.10 Goto-Kakizaki (GK) rat model

The GK rat is a model of type 2 diabetes generated by inbreeding of non-diabetic Wistar rats with impaired glucose tolerance, which offers us a convenient non-obese model for study of type 2 diabetes-associated cardiovascular complications (El-Omar, Yang et al. 2004). GK rats inherit a stable form of type 2 diabetes reportedly characterized by mild hyperglycemia, hyperinsulinemia, and peripheral insulin resistance without obesity or severe hyperlipidemia (El-Omar, Yang et al. 2004). Brondem et al. have demonstrated that mesenteric small arteries isolated from GK rats showed increased contractile responses to NA compared to control Wistar rats, while the endothelial function of those arteries was normal, suggesting hypercontractility of vascular smooth muscles from GK rats. (Brondum, Kold-Petersen et al. 2008). The question of whether GK rats develop hypertension or not has not been resolved. A study done by El-Omar et al. claimed that the GK rat model is a type 2 diabetic model without confounding factors like obesity and hypertension (El-Omar, Yang et al. 2004). Based on results from Kobayashi et al., GK rats had lower systolic blood pressure at 12 weeks compared to control Wistar rats, and at 36 weeks, the blood pressure was normalized (Kobayashi, Matsumoto et al. 2004). However, Gronholm et al. have reported that GK rats had higher systolic blood pressure compared to nondiabetic Wistar rats (Gronholm, Cheng et

al. 2005). Moreover, a study done by Witte et al. has also shown that GK rats exhibited mild hypertension (Witte, Jacke et al. 2002). Interestingly, the GK rats used in our preliminary studies were mildly hypertensive, and acute inhibition of ROCK by H-1152 attenuated elevated blood pressure in those GK rats, suggesting that ROCK may contribute to the development of hypertension in this model (fig. 4).

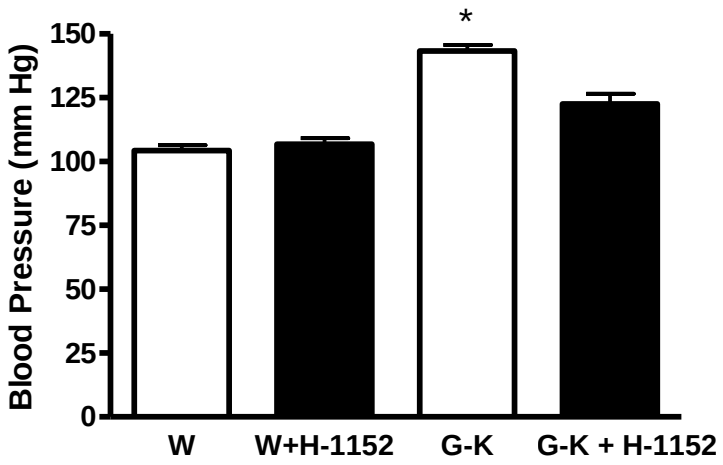

Figure 4: Effect of H-1152 on blood pressure in control (W) and GK rats. Blood pressure was measured before administration of H-1152 (0.2 mg/kg, intraperitoneal), and then it was measured again every 2 to 3 minutes for 30 minutes following administration of H-1152. Data shown are means ± SEM. N = 4, 5. *, $p < 0.05$ compared to corresponding control group (one-way ANOVA).

1.11 Streptozotocin (STZ)-induced rat model

STZ-diabetic rat models are widely used in diabetes research not only due to their low cost, but also the better control of the duration and severity of the disease. STZ is a glucosamine-nitrosourea antibiotic that is structurally similar to glucose, which is taken up preferentially by the glucose transporter, GLUT2, in pancreatic β-cells (Bugger and Abel 2009). This results in β-cell destruction, which leads to insulin deficiency, a condition resembling poorly controlled type 1 diabetes (Szkudelski 2001; Bugger and Abel 2009). The development of cardiovascular dysfunction has been shown to begin as early as 5 days after the injection of STZ (Schaan, Dall'Ago et al. 2004). Abnormalities such as depressed blood pressure, heart rate, cardiac output, and endothelial dysfunction have been found to be associated with type 1 diabetes (Smith, Paulson et al. 1997; Cheng, Cheng et al. 2004; Schaan, Dall'Ago et al. 2004). Nagareddy et al. have suggested that the hypotensive nature of STZ-diabetic rats was induced by elevated iNOS activity, and that inhibition of iNOS improved blood pressure in these animals (Nagareddy, McNeill et al. 2009).

1.12 Research hypothesis

Strong evidence has suggested a role of the RhoA/ROCK pathway in the development of hypertension associated with diabetes. However, the involvement of the RhoA/ROCK pathway in agonist-induced vascular smooth muscle contractile responses in diabetes-associated hypertension has not been investigated. Also, not many studies have used resistance arteries, such as mesenteric resistance arteries, to investigate vascular smooth

muscle contractile responses. The resistance arteries have an essential role in the peripheral regulation of blood pressure.

The main hypothesis of the present study is:

Activation of the RhoA/ROCK pathway contributes to the development of diabetes-associated hypertension by enhancing vascular smooth muscle contractile responses.

To test this hypothesis, mesenteric resistance arteries were isolated from both control and diabetic (STZ-diabetic and GK) rats, and mounted in a wire myograph for the measurement of contractile responses to vasoconstrictors in the presence or absence of ROCK inhibitor. Moreover, changes in expression or activation of proteins associated with the RhoA/ROCK pathway were monitored.

1.13 Specific objectives

1. Compare agonist-induced contractile responses in superior mesenteric or resistance arteries from STZ-diabetic to control rats.
2. Measure the RhoA/ROCK pathway associated protein response to agonist stimulation in the presence or absence of ROCK inhibitor in superior mesenteric or resistance arteries.
3. Monitor body weight, blood glucose and insulin levels, and systolic blood pressure in GK rats.
4. Compare agonist-induced contractile responses in mesenteric resistance arteries from GK and control rats.
5. Measure the RhoA/ROCK pathway associated protein response to agonist stimulation in the presence or absence of ROCK inhibitor in mesenteric resistance arteries.

Chapter 2: MATERIALS AND METHODS

2.1 Animals

2.1.1 STZ-diabetic rats

Male Wistar rats weighing around 170 grams were obtained from the Center for Disease Modeling, UBC, Canada. The animals were housed and treated in accordance with the guidelines of the Canadian Council on Animal Care. To induce diabetes, the rats were lightly anesthetized with isoflurane and given a single tail vein injection of 60 mg/kg STZ in 0.1 M citrate buffer or citrate buffer alone as control. STZ-injected rats with blood glucose levels over 13 mM measured using a glucometer (UltraOne) one week after injection were considered diabetic. Animals were housed in pairs. STZ-diabetic rats and their age-matched control Wistar rats were housed under identical conditions and were given free access to food and water for 12 to 14 weeks.

2.1.2 GK rats

Six 10-week old male GK rats were obtained from Taconic, USA, and age and gender-matched control Wistar rats were obtained from Charles River, Canada. The animals were housed and treated in accordance with the guidelines of the Canadian Council on Animal Care. Both the control and GK rats were kept for 16 weeks, and the weeks were numbered by the age of the rat. For example, week 20 corresponds to the 10^{th} week of the study, when rats

were 20 weeks old. All animals were housed under identical conditions and were given free access to food and water.

Systolic blood pressure was measured in conscious rats using the non-invasive tail-cuff method. Briefly, the rats were placed in rodent restrainers of suitable sizes. The animals were then allowed several minutes to calm down inside the restrainers. The tail was inserted into an inflatable O-ring cuff and a VPR cuff containing a sensor. The cuffs were connected to a blood pressure system, CODA system, from Kent Scientific Corporation (Torrington, CT). The measurement began with the inflation of the cuffs, and upon gradual deflation, the reappearance of pulsations was detected by the sensor and recorded by the system.

Blood pressure was measured every two weeks on two days. The first day was a training day so that the animals became used to the equipment, while blood pressure was recorded on the second day. At 20 weeks of age (week 20), blood pressure was also measured on the third day, and the results were almost identical to those obtained on the previous day, suggesting that the blood pressure results from the second day were stable. At week 25, GK and corresponding control rats were treated with 25 mg/kg fasudil twice a day by oral gavage for 7 days followed by a 24-hour wash-out period. Blood pressure was measured within 2 hours after fasudil administration and after the wash-out period.

A blood sample was collected from the tail vein every week at the same time after 4-hour fasting for measurement of plasma insulin and glucose levels. After the animals were anesthetized with isoflurane gas, 300 μl of blood was collected from tail vein of each rat. Plasma was then separated from blood samples by centrifugation. Blood glucose was measured using a commercially available glucometer (UltraOne).

Four days after the final administration of fasudil,, animals were euthanized by an overdose of sodium pentobarbital.

2.1.2.1 Measurement of blood insulin level

Plasma insulin levels were measured using a commercially available kit from Linco (Sensitive Rat Insulin, Millipore). The assay is based on antigen-antibody interaction. In brief, a fixed concentration of labeled tracer antigen is incubated with a constant dilution of insulin antibody. Unlabeled antigen in insulin containing samples competes with labeled tracer antigen for the limited and constant number of binding sites on antibody. In other words, the amount of tracer bound to antibody would decrease as the concentration of unlabeled antigen increases in the samples.

2.2 Mesenteric artery isolation

The mesenteric artery bed was isolated and placed in physiological saline solution (PSS) of composition (mM): 130 NaCl, 4.7 KCl, 14.9 $NaHCO_3$, 1.6 $CaCl_2$, 1.18 KH_2PO_4, 1.17 $MgSO_4$, 0.026 EDTA, and 5.5 glucose) at room temperature. The pH of PSS was adjusted to 7.4 by aeration with 95% O_2/5% CO_2. The entire mesenteric artery bed with its attached small intestine and large intestine was isolated following the method described in the wire myoraph manual (Multi Wire Myograph System, DMT 620M). The proximal end of the small intestine section was pinned down on the left-hand side of a Petri dish coated with a layer of Sylgard without stretching the vessels, and the remaining intestine section was

pinned down in a counter-clockwise direction. While in this orientation, the mesenteric veins are usually uppermost, while the arteries are right underneath the veins. The arteries could also be distinguished from the veins by their more elastic and thicker vessel wall as well as their unique branch points; the branch points of arteries are usually V-shaped whereas those of veins are more U-shaped. The first- and second-order branches of mesenteric artery (approximate internal diameter 200-300 μm) as well as the superior mesenteric artery were excised. In order to maintain the natural properties of the arteries, the fat and connective tissues were carefully removed without stretching the vessels.

2.3 Contractile function measurement

An isolated mesenteric artery was cut into 2 mm rings. Each artery ring was then mounted in the chamber of a wire myograph (DMT 620M). In brief, an artery ring was threaded onto an ultra-thin stainless steel wire with a diameter of 40 μm, and secured on one side of the jaws in the myograph chamber. A second wire was passed into the vessel lumen and secured on the other side of the jaws. The jaws were then carefully moved apart to slightly stretch the vessel segment. The rings were then equilibrated for 60 minutes in PSS with solution changed every 20 minutes. During equilibration, the vessel rings were continuously aerated with 95% O_2/5% CO_2 and maintained at a temperature of 37 °C. Following equilibration, normalization was performed to determine the optimal internal circumference that a fully relaxed vessel segment would have at a specified tension set at 100 mm Hg or 13.3 kPa. Following normalization, the wake-up protocol was performed. Each vessel ring was stimulated with high potassium physiological saline solution (KPSS) (mM)

containing 74.7 NaCl, 60 KCl, 1.18 KH_2PO_4, 1.17 $MgSO_4$, 14.9 $NaHCO_3$, 5.5 glucose, 0.026 EDTA, and 1.6 $CaCl_2$, plus 10 μM noradrenaline (NA) for 3 minutes. After stimulation, the vessel rings were washed 4 times with regular PSS over 5 minutes. The stimulation with KPSS plus 10 μM NA was repeated for a second time. After KPSS and NA were washed out with PSS, the vessel rings were stimulated with 10 μM NA in regular PSS for 3 minutes, and then washed out with PSS over 5 minutes. Then, the vessel segments were stimulated with KPSS alone over a period of time until the contraction reached a plateau. Afterward, the artery rings were washed with PSS until they returned to baseline. The artery rings were stimulated for one last time with KPSS plus 10 μM NA for 3 minutes, and then washed out 5 or 6 times over 20 minutes with regular PSS. 100 mM KCl was added to each organ bath to induce a contraction, which was then set as 100% contraction for each vessel ring. The tissues were then washed for 30 minutes with regular PSS and endothelial function was assessed in some vessels. The endothelial function was tested by demonstrating its ability to relax in response to Ach after pre-contraction with 3 μM of NA.

2.4 Concentration-response curves

In STZ-diabetic and corresponding control rats, the endothelium was removed from each segment by rubbing the internal lumen of the vessel gently against a thin wire. On the other hand, endothelium remained intact in GK and corresponding control rats, but the contribution of nitric oxide (NO) secreted from endothelium was eliminated chemically by treatment with the non-specific nitric oxide synthase (NOS) inhibitor L-NAME (100 μM) for 30 minutes. Cumulative concentration-response curves to PE or U-46619 were obtained in artery rings.

The tissues were then washed for 30 minutes and treated with Y-27632 or H-1152 for 30 minutes, following which cumulative concentration-response curves to PE or U-46619 were obtained in the presence of Y-27632 or H-1152.

2.5 Experimental treatments on isolated mesenteric resistance/superior arteries from STZ or GK rats and their Wistar controls

For Western blotting studies, the artery rings from control and STZ-diabetic animals were divided into 4 groups: basal, 30 minutes ROCK inhibitor treated, 5 minutes agonist treated, and agonist plus ROCK inhibitor treated, where the arteries were pretreated with ROCK inhibitor for 35 min, with agonist added for the last 5 min. In GK and corresponding control rats, artery rings were divided into 6 groups: basal, 30 minutes ROCK inhibitor treated, 5 minutes agonist treated, agonist plus ROCK inhibitor treated, agonist plus 30 minutes L-NAME treated, and agonist plus L-NAME plus ROCK inhibitor treated.

After treatment, the artery rings were collected and frozen by immersion in acetone mixture (acetone containing 10% trichloroacetic acid (TCA) and 10 mM dithiothreitol (DTT)) cooled with dry ice, and stored at -70 °C.

2.6 Extraction of total protein from arteries

Before processing, the frozen tissues were gradually warmed to -20 °C, then 4 °C and finally washed several times with acetone to remove TCA. Afterward, the tissues were ground using a mini glass tissue homogenizer (Radnoti LLC, Monrovia, Ca) in EGTA buffer

containing 20 mM DTT and 0.5% SDS, followed by centrifugation at 10,000 rpm for 10 minutes. The supernatant was collected and used for protein determination and Western blotting.

2.7 Protein concentration determination

The concentration of protein in each sample was determined using the Bio-Rad Protein Assay based on the Bradford dye-binding procedure. In brief, a small aliquot of each tissue sample was diluted 30 times and loaded to each well of a 96-well plate. The Bio-Rad Protein Assay dye with a ratio of 1:5 was then added to each well containing sample. The absorbance was read at 595 nm for comparison with a BSA standard curve.

2.8 Western blotting analysis

Prior to electrophoresis, samples were made up to the same protein concentration in sample buffer containing 2% SDS, 120 mM tris-HCl pH 6.8, 10% glycerol, 5% β-Mercaptoethanol, 0.004% bromophenol blue. The samples were then boiled for 5 minutes. SDS-PAGE gels were casted according to Laemmli (Laemmli 1970). The composition of the resolving gel was as follows: 10% total acrylamide, tris-HCl pH 8.8, 0.1% SDS, 0.08% ammonium persulfate and 0.03% TEMED. The composition of the stacking gel was as follows: 4% total acrylamide, tris-HCl pH 6.8, 0.1% SDS, 0.08% ammonium persulfate and 0.05% TEMED. The gel-running tank was filled with running buffer containing 25 mM tris, 192 mM glycine, and 0.1% SDS. Equal amounts of protein were loaded into appropriate

wells in the stacking gels. Proteins were electrophoretically separated through the resolving gel under a constant voltage of 125 volts for about 80 minutes using a Bio-Rad Protein II electrophoresis unit. Following this, a Bio-Rad Criterion Blotter was used to transfer the resolved proteins to a PVDF membrane. Protein transfer was conducted at a constant voltage of 100 volts for 1 hour in ice-cold transfer buffer containing 25 mM tris, 192 mM glycine, and 20% methanol. The membrane was treated with 5% non-fat milk/0.05% Tween-TBS (TBST) for 30 min at room temperature to block any non-specific antibody binding. Afterward, the membranes were washed 3 times for 5 minutes/time with TBST, and then incubated with appropriate primary antibodies diluted in 5% BSA in TBST on a shaker at 4°C overnight. The following day, the membranes were washed 3 times for 5 minutes/time with TBST, and then incubated with appropriate horseradish peroxidase-conjugated secondary antibodies (1:4000; in 5% non-fat milk) for 1 hour on a shaker at room temperature. After washing 3 times for 5 minutes/time with TBST, the membranes were incubated with an enhanced chemiluminescence detection kit to develop the protein signals. The band intensity of each phosphorylated and total protein was analyzed by densitometry and normalized to GAPDH on the same membrane using ImageJ software (Java). The ratio of phosphorylated to total protein was determined by dividing each normalized phosphorylated protein to its corresponding normalized total protein.

2.9 Measurement of the degree of actin polymerization (F-/G-actin)

A commercially available assay kit (Cytoskeleton Inc.) was used to determine the ratio of F- to G-actin. In brief, each artery sample was homogenized using a mini glass tissue

homogenizer in F-actin stabilization buffer (37 °C) containing (mM) 50 piperazine-*N*,*N'*-bis (2-ethanesulfonic acid), pH 6.9, 50 NaCl, 5 $MgCl_2$, 5 EGTA, 5% glycerol, 0.1% Triton X-100, 0.1% Nonidet P-40, 0.1% Tween 20, 0.1% β-mercaptoethanol, 0.001% antifoam, 1 ATP, 1 μg/ml pepstatin, 1 μg/ml leupeptin, 10 μg/ml benzamidine, and 500 μg/ml tosyl arginine methyl ester. Supernatant was collected after ultracentrifugation (100,000 g, 1 h at 37 °C). The pellet was resuspended in ice-cold distilled water with 1 μM cytochalasin-D, and F-actin was dissociated by incubation of the suspension on ice for 1 hour. Supernatant (G-actin) and pellet suspension (F-actin) fractions were then diluted 5 times and analyzed by Western blotting technique with anti-actin antibody. The ratio of F- to G-actin was determined by dividing the band intensity of F-actin by its corresponding G-actin.

2.10 Statistical analysis

All data were presented as mean ± SEM. Agonist-induced concentration-response curves were logarithmically transformed and fitted to a sigmoidal dose-response curve for calculation of -logEC50 and maximum responses (Rmax). Rmax and –logEC50 values were compared to examine the effect of ROCK inhibitors on agonist-induced contractions in a given type of artery. For multiple comparisons of more than two experimental groups, one-way or two-way ANOVA followed by a Newman-Keuls or Bonferroni post-hoc test was conducted using GraphPad Prism5 (GraphPad Software). A P-value < 0.05 was considered statistically significant.

Chapter 3: RESULTS

3.1 PE-induced contractile responses in mesenteric resistance arteries from control and STZ-diabetic rats

We isolated mesenteric resistance arteries from STZ-diabetic male rats and their age-matched controls, and measured the contractile responses to agonist with or without ROCK inhibitor. We first tried PE, which is an α_1-adrenoceptor agonist. Based on our results, we observed a slight decrease in PE-induced contraction from STZ-diabetic arteries compared to control arteries; however this reduction was not statistically significant (fig. 5A). Studies have found that contractile responses to NA were significantly increased in aorta and mesenteric arteries from STZ-diabetic rats, and such hyperreactivity to NA has been shown to be mediated via the α-adrenoceptor, suggesting an important role of α-adrenoceptor stimulation in vascular smooth muscle contraction (Abebe, Harris et al. 1990; Abebe and MacLeod 1991; Taylor, Oon et al. 1994). Furthermore, in a preliminary study, the response of mesenteric arteries from control and diabetic rats to NA was significantly attenuated by 0.1 μM H-1152 or 1 μM Y-27632, implicating a role of ROCK in regulating contractile responses to α-adrenoceptor stimulation. However, as shown in figure 5B, 30-minute pre-treatment with 0.1 μM H-1152 did not reduce the PE-induced contraction in the control group. Similarly, this concentration of H-1152 appeared to have no effect on the response of arteries from diabetic rats to PE.

When the H-1152 concentration was increased to 1 μM, the maximum contractile response was attenuated significantly by 37% in resistance arteries from control animals (fig.

6A). In the STZ-diabetic resistance arteries, the contractile responses induced by PE were also reduced by 15% (fig. 6B).

Similarly, the less potent ROCK inhibitor Y-27632, at a concentration of 1 μM, didn't have any effect on PE-induced contraction in control animals (fig. 7A). However, an increased concentration of Y-27632 (10 μM) reduced PE-induced contraction by 49% in resistance arteries from control animals (fig. 7B).

3.1.1 Effect of PE with or without H-1152 on activity of ROCK in mesenteric resistance arteries

The catalytic subunit of MLCP, MYPT, is a major target of ROCK. When ROCK is activated, it phosphorylates MYPT at Thr853, which inhibits MLCP activity, leading to inhibition of MLC dephosphorylation and thereby increasing smooth muscle contraction (Somlyo and Somlyo 2003). Hence, MYPT phosphorylation can be used as a marker for ROCK activity.

Isolated mesenteric resistance arteries were treated with 0.1 μM H-1152, 30 μM PE (a concentration that induced a near-maximal contractile response), 0.1 μM H-1152 plus 30 μM PE, or were left untreated. Following treatment, arteries were homogenized and MYPT phosphorylation was determined using Western blotting. As shown in figure 8, there was no significant difference in basal MYPT expression or phosphorylation between control and STZ-diabetic resistance arteries. There was no increase in MYPT phosphorylation in response to 30 μM PE in either control or diabetic animals. Phosphorylation of MYPT was

decreased by 0.1 μM H-1152 in both the absence and presence of PE; however, this reduction was not statistically significant.

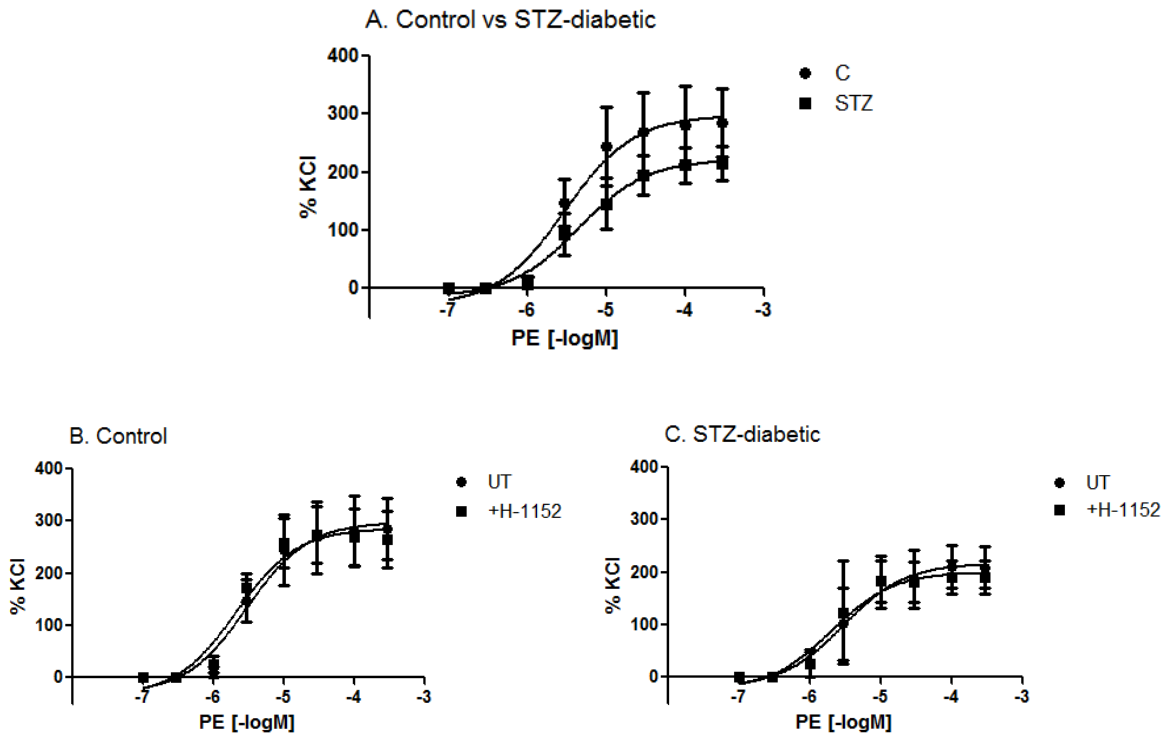

	C	C+H-1152	STZ	STZ+H-1152
LogEC50	-5.53 ±0.27	-5.68 ±0.23	-5.36 ±0.21	-5.7 ±0.31
Rmax	284.36 ± 30.32	263.38 ±23.39	209.03 ±18.88	190.53 ±22.18

Figure 5: A: Comparison of PE-induced contraction in mesenteric resistance arteries from control and STZ-diabetic rats (N = 5 in each group). B, C: PE-induced contractile responses in the absence and presence of 0.1 μM H-1152 in mesenteric resistance arteries from control and STZ-diabetic rats. Table shows log EC50 and Rmax derived from non-linear curve fitting of individual concentration-response curves. UT = untreated. Data shown are means ± SEM. N = 5, 2 (C). Results were analyzed using Student's unpaired t-test.

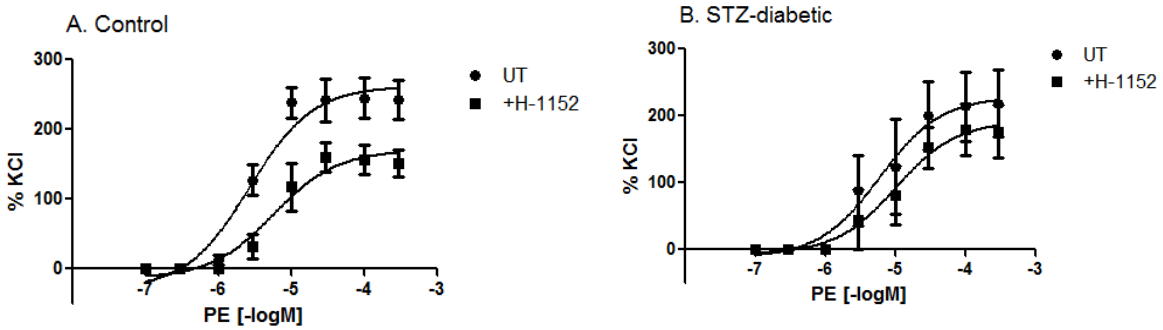

	C	C+H-1152	STZ	STZ+H-1152
LogEC50	-5.58 ±0.14	-5.25 ±0.18	-5.23 ±0.31	-4.50 ±0.26
Rmax	231.17 ±13.23	151.13 ±13.66 *	217.99 ±29.75	175.85 ±23.9

Figure 6: A, B: PE-induced contractile responses in the absence and presence of 1 μM H-1152 in mesenteric resistance arteries from control and STZ-diabetic rats. Table shows log EC50 and Rmax derived from non-linear curve fitting of individual concentration-response curves. UT = untreated. Data shown are means ± SEM. N = 5 in control, 3 in STZ. *, $p < 0.05$ compared to corresponding control group (Student's unpaired t-test).

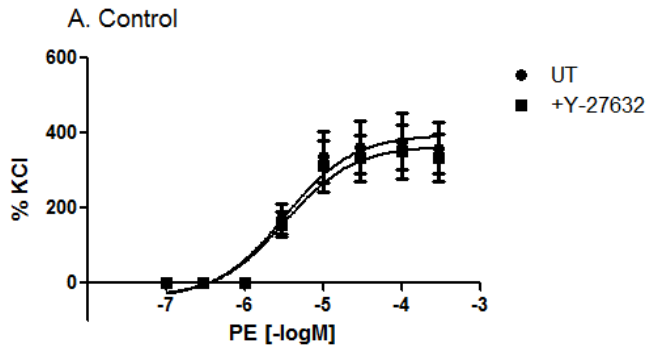

	C	C+Y-27632
LogEC50	-5.50 ± 0.22	-5.49 ± 0.22
Rmax	358.90 ± 33.68	331.59 ± 31.41

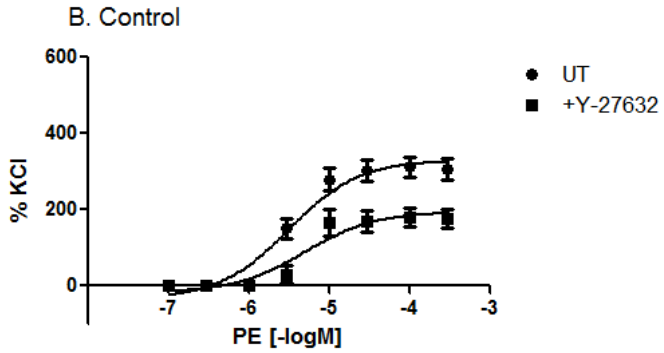

	C	C+Y-27632
LogEC50	-5.51 ± 0.12	-5.31± 0.20
Rmax	304.53 ± 15.66	174.60 ± 16.3 *

Figure 7: PE-induced contractile responses in the absence and presence of 1 μM Y-27632 (A) or 10 μM Y-27632 (B) in mesenteric resistance arteries from control rats. Table shows log EC50 and Rmax derived from non-linear curve fitting of individual concentration-response curves. UT = untreated. Data shown are means ± SEM. N = 5. *, $p < 0.05$ compared to corresponding control group (Student's unpaired t-test).

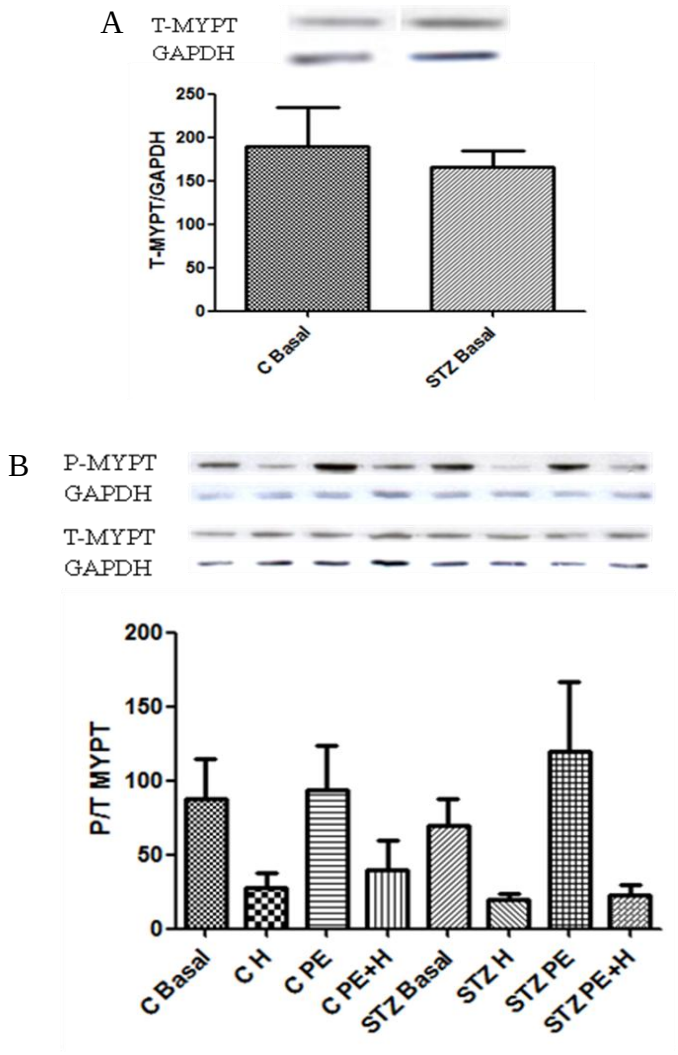

Figure 8: A: Representative Western blot showing total MYPT with GAPDH as a loading control (above). Total MYPT normalized for corresponding GAPDH in the same blot in untreated (Basal) mesenteric resistance arteries from control (C) and STZ rats (bottom). B: Representative Western blot showing total and phosphorylated MYPT at Thr853 with GAPDH as a loading control (above). Ratio of phosphorylated to total MYPT normalized for corresponding GAPDH in the same blot in mesenteric resistance arteries from control (C) and STZ rats with no treatment (Basal), 0.1 µM H-1152 (H), 30 µM PE (PE), and 0.1 µM H-1152 + 30 µM PE (PE+H) (bottom). Data shown are means ± SEM. N = 5. Results were analyzed using Student's unpaired t-test (top) or one-way ANOVA (bottom).

3.1.2 Effect of PE with or without H-1152 on phosphorylation of RhoA in mesenteric resistance arteries

Phosphorylation of RhoA at Ser188 site inactivates it as it enhances the interaction with GDIs, which promotes the release of RhoA from the membrane (Hoffman, Nassar et al. 2000). However, changes in RhoA phosphorylation in mesenteric resistance arteries from STZ-diabetic diabetic animals have not been examined. We wished to determine whether treatment with PE would alter RhoA phosphorylation and whether ROCK inhibition would reverse it in the resistance arteries from STZ-diabetic animals.

As shown in figure 9, no differences were found in either expression or phosphorylation of RhoA in mesenteric resistance arteries from control and diabetic animals and neither PE nor ROCK inhibitor affected its phosphorylation in either control or diabetic animals.

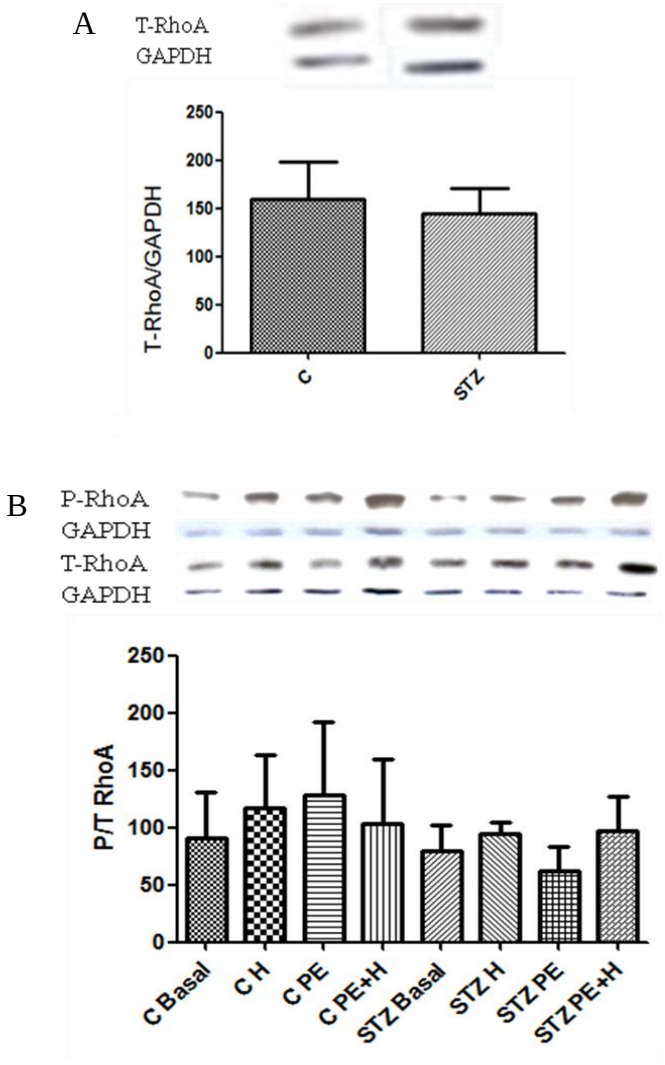

Figure 9: A: Representative Western blot showing total RhoA with GAPDH as a loading control (above). Total RhoA normalized for corresponding GAPDH in the same blot in untreated (Basal) mesenteric resistance arteries from control (C) and STZ rats (bottom). B: Representative Western blot showing total and phosphorylated RhoA at Ser188 with GAPDH as a loading control (above). Ratio of phosphorylated to total RhoA normalized for corresponding GAPDH in the same blot in mesenteric resistance arteries from control (C) and STZ rats with no treatment (Basal), 0.1 μM H-1152 (H), 30 μM PE (PE), and 0.1 μM H-1152 + 30 μM PE (PE+H) (bottom). Data shown are means ± SEM. N = 5. Results were analyzed using Student's unpaired t-test (top) or one-way ANOVA (bottom).

3.1.3 Effect of PE with or without H-1152 on phosphorylation of PKC-ε in mesenteric resistance arteries

Previous work from our laboratory showed that treatment with 1 μM Y-27632 normalized enhancement in agonist-induced activation of PKC-α and -ε measured as the particulate levels or translocation, in STZ-diabetic but not in control superior mesenteric resistance arteries. It has been shown that phosphorylation of PKC isoforms at sites in their catalytic kinase domains is essential for their activation, and phosphorylation at the Thr641 site in PKC-β_2 has been used as an index of activation (Cenni, Doppler et al. 2002; Lin, Brownsey et al. 2009). Here, we determined the phosphorylation of PKC-ε as an index of activation in response to treatment of PE with or without H-1152 in mesenteric resistance arteries from control and STZ-diabetic rats using Western blotting.

As shown in figure 10, basal PKC-ε expression or phosphorylation was similar between control and STZ-diabetic resistance arteries. Treatment with 30 μM PE did not increase phosphorylation of PKC-ε, nor did 0.1 μM H-1152 had any effects on it in either control or STZ-diabetic resistance arteries.

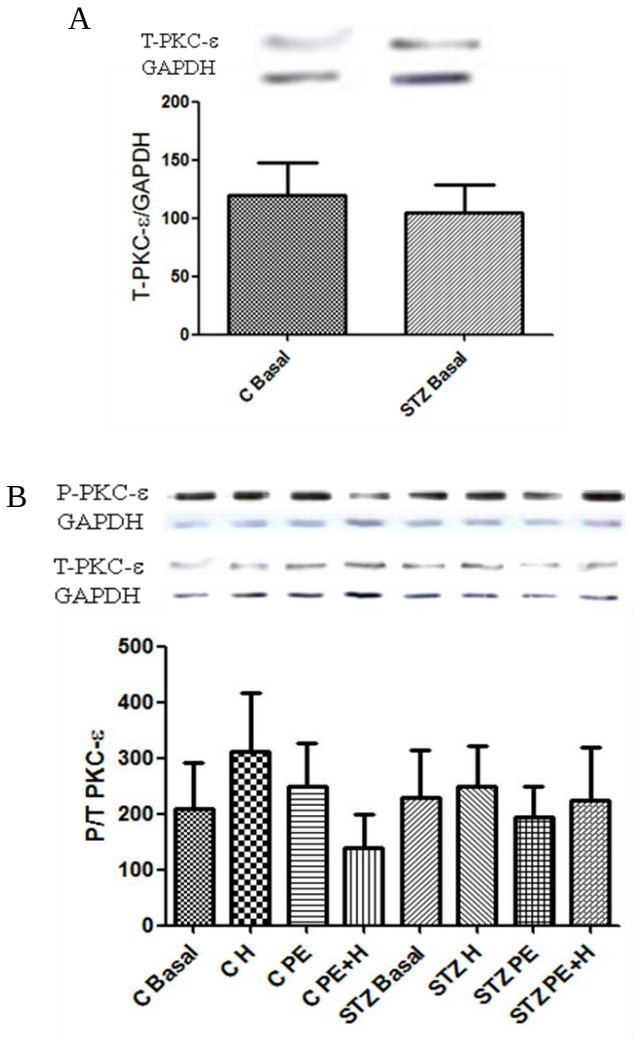

Figure 10: A: Representative Western blot showing total PKC-ε with GAPDH as a loading control (above). Total PKC-ε normalized for corresponding GAPDH in the same blot in untreated (Basal) mesenteric resistance arteries from control (C) and STZ rats (bottom). B: Representative Western blot showing total and phosphorylated PKC-ε at Ser729 with GAPDH as a loading control (above). Ratio of phosphorylated to total PKC-ε normalized for corresponding GAPDH in the same blot in mesenteric resistance arteries from control (C) and STZ rats with no treatment (Basal), 0.1 μM H-1152 (H), 30 μM PE (PE), and 0.1 μM H-1152 + 30 μM PE (PE+H) (bottom). Data shown are means ± SEM. N = 5. Results were analyzed using Student's unpaired t-test (top) or one-way ANOVA (bottom).

3.1.4 Effect of PE with or without Y-27632 on the phosphorylation of CPI-17 at Thr38 in mesenteric resistance arteries

The inhibitor of MLCP, CIP-17, has been shown to be phosphorylated or activated by PKC and ROCK (Mueed, Zhang et al. 2005; Xie, Su et al. 2006). In a previous study published from our lab, CPI-17 phosphorylation at Thr38 was shown to be increased by 30 μM NA, and was normalized by calphostin, a PKC inhibitor, in STZ-diabetic but not in control superior mesenteric arteries, suggesting that in diabetes, CPI-17 regulation is mediated by PKC (Mueed, Zhang et al. 2005). As mentioned in the introduction, there are some studies suggesting that CPI-17 phosphorylation or activation is ROCK-regulated while some demonstrated that this is a PKC-mediated process (Seko, Ito et al. 2003; Pang, Guo et al. 2005; Tsai and Jiang 2006; Xie, Su et al. 2006). Here, we wished to examine the effects of PE on CPI-17 phosphorylation with or without ROCK inhibitor.

In mesenteric resistance arteries, basal CPI-17 expression and phosphorylation were similar between control and STZ-diabetic animals (fig. 11). Phosphorylation of CPI-17 also remained unaffected by treatment with either 30 μM PE or 1 μM Y-27632 in mesenteric resistance arteries from control and STZ-diabetic rats (fig. 11).

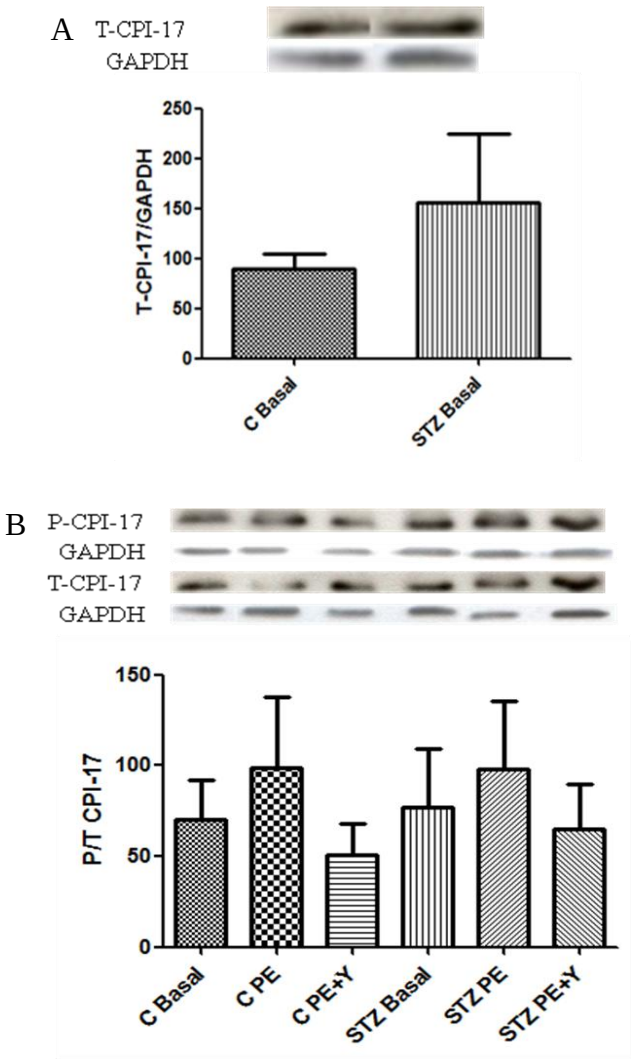

Figure 11: A: Representative Western blot showing total CPI-17 with GAPDH as a loading control (above). Total CPI-17 normalized for corresponding GAPDH in the same blot in untreated (Basal) mesenteric resistance arteries from control (C) and STZ rats (bottom). B: Representative Western blot showing total and phosphorylated CPI-17 at Thr38 with GAPDH as a loading control (above). Ratio of phosphorylated to total CPI-17 normalized for corresponding GAPDH in the same blot in mesenteric resistance arteries from control (C) and STZ rats with no treatment (Basal), 0.1 μM H-1152 (H), 30 μM PE (PE), and 0.1 μM H-1152 + 30 μM PE (PE+H) (bottom). Data shown are means ± SEM. N = 5. Results were analyzed using Student's unpaired t-test (top) or one-way ANOVA (bottom).

3.1.5 Effect of PE with or without Y-27632 on actin polymerization in mesenteric resistance arteries from control rats

The actin filaments resulting from actin polymerization form cross-bridges with MLC, which helps strengthen the entire contractile machinery to facilitate smooth muscle contraction (Gunst and Zhang 2008). A commercially available assay kit was used to isolate and measure the G- and F-actin content from isolated control mesenteric resistance arteries treated with 1 μM Y-27632, 30 μM PE, or 1 μM Y-27632 plus 30 μM PE. As shown in figure 12, in control mesenteric arteries, the F- to G-actin ratio or the degree of actin polymerization significantly increased in response to 30 μM PE, which was substantially attenuated by 1 μM Y-27632.

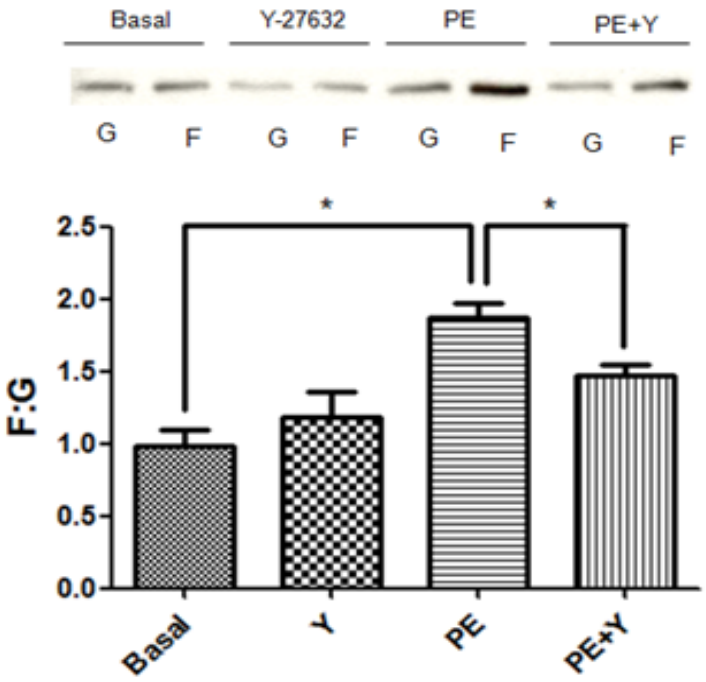

Figure 12: Representative Western blot showing F- to G-actin ratio (actin polymerization) (above). F- to G-actin ratio was calculated by dividing optical densities of F-actin band by corresponding optical densities of G-actin band in mesenteric resistance arteries with no treatment (Basal), 1 μM Y-27632 (Y), 30 μM PE (PE), and 1 μM Y-27632 + 30 μM PE (PE+Y) in control rats (bottom). G = G-actin, F = F-actin. Data shown are means ± SEM. N = 3. *, $p < 0.05$ compared to corresponding control group (one-way ANOVA).

3.2 PE-induced contractile responses in superior mesenteric arteries from control and STZ-diabetic rats

A previous study in our lab showed that 0.1 μM H-1152 or 1 μM Y-27632 was able to inhibit PE-induced contraction in superior mesenteric arteries. To confirm these results, we repeated the experiments. Results from that previous study also showed that PE-induced contractile responses were greater in the superior mesenteric arteries from STZ-diabetic rats than in those from control rats. But in this study, the enhancement in PE-induced contraction in superior arteries from STZ-diabetic rats was not statistically significant (fig. 13A).

As shown in figure 13B and C, 0.1 μM H-1152 successfully attenuated PE-induced contractile responses in superior arteries from control rats by 33%, and in the diabetic rats, PE-induced responses were reduced by 43%, which is consistent with our previous study.

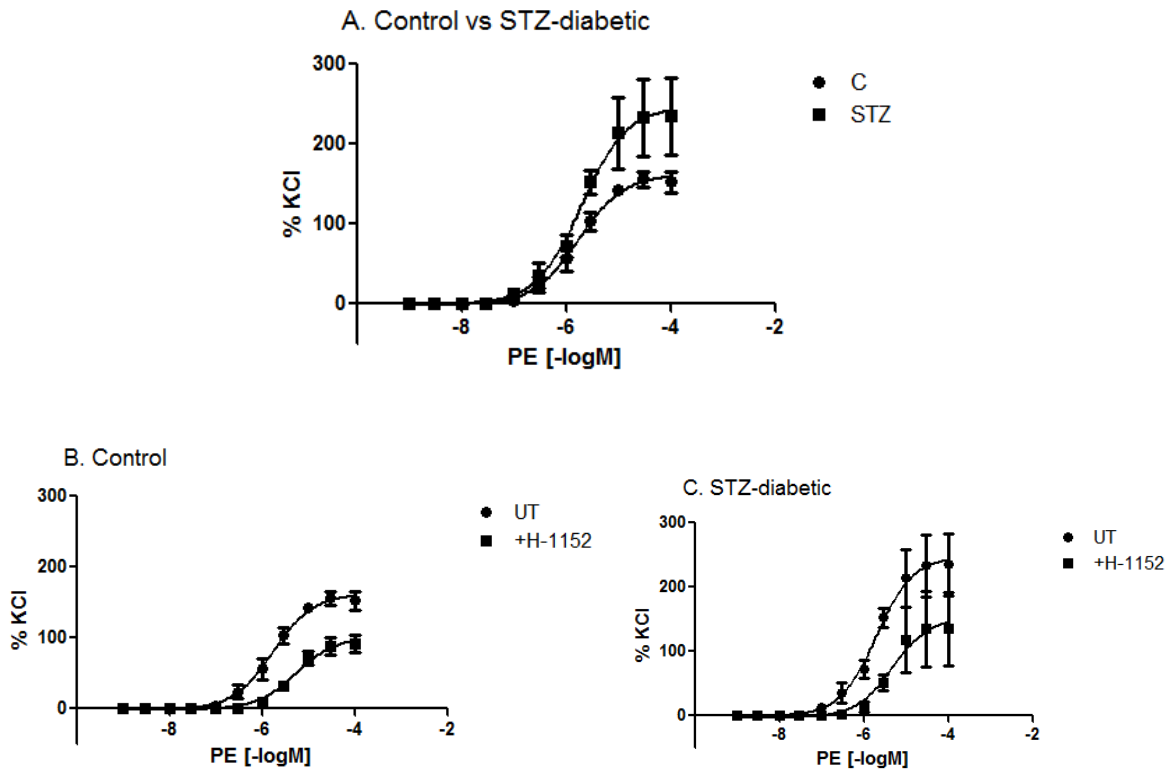

	C	C+H-1152	STZ	STZ+H-1152
LogEC50	-5.77 ± 0.08	-5.27 ± 0.11	-5.71 ± 0.15	-5.33 ± 0.30
Rmax	152.39 ± 5.61	90.93 ± 5.92 *	233.89 ± 16.87	134.69 ± 24.35

Figure 13: A: Comparison of PE-induced contraction in superior mesenteric arteries from control and STZ-diabetic rats. B, C: PE-induced contractile responses in the absence and presence of 0.1 μM H-1152 in superior mesenteric arteries from control and STZ-diabetic rats. Table shows log EC50 and Rmax derived from non-linear curve fitting of individual concentration-response curves. Data shown are means ± SEM. N = 5 in control, 3 in STZ. *, $p < 0.05$ compared to corresponding control group (Student's unpaired t-test).

3.2.1 Effect of PE with or without H-1152 on activity of ROCK in superior mesenteric arteries

In isolated superior arteries, we performed the same treatment as in resistance arteries: 0.1 μM H-1152, 30 μM PE, and 0.1 μM H-1152 plus 30 μM PE. Following the treatment, arteries were homogenized and MYPT phosphorylation was measured using Western blotting. Surprisingly, Western blotting results showed that MYPT expression and basal phosphorylation were similar in mesenteric resistance arteries from control and STZ-diabetic rats, and 30 μM PE did not increase MYPT phosphorylation at Thr853 in either control or diabetic group (fig. 14).

We then did a time-course experiment on PE-induced MYPT phosphorylation as we wanted to determine if MYPT phosphorylation induced by PE was not at peak at 5 minutes. As shown in figure 15, there was a trend to increase MYPT phosphorylation over first 5 minutes, but this increase was not statistical significant.

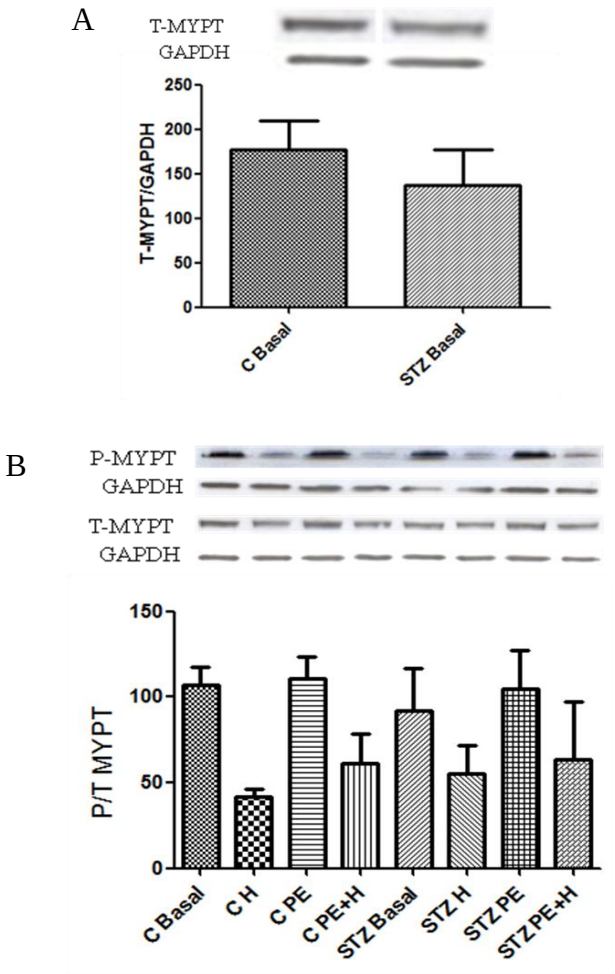

Figure 14: A: Representative Western blot showing total MYPT with GAPDH as a loading control (above). Total MYPT normalized for corresponding GAPDH in the same blot in untreated (Basal) superior mesenteric arteries from control (C) and STZ rats (bottom). B: Representative Western blot showing total and phosphorylated MYPT at Thr853 with GAPDH as a loading control (above). Ratio of phosphorylated to total MYPT normalized for corresponding GAPDH in the same blot in superior mesenteric arteries from control (C) and STZ rats with no treatment (Basal), 0.1 μM H-1152 (H), 30 μM PE (PE), and 0.1 μM H-1152 + 30 μM PE (PE+H) (bottom). Data shown are means ± SEM. N = 5 in control, 3 in STZ. Results were analyzed using Student's unpaired t-test (top) or one-way ANOVA (bottom).

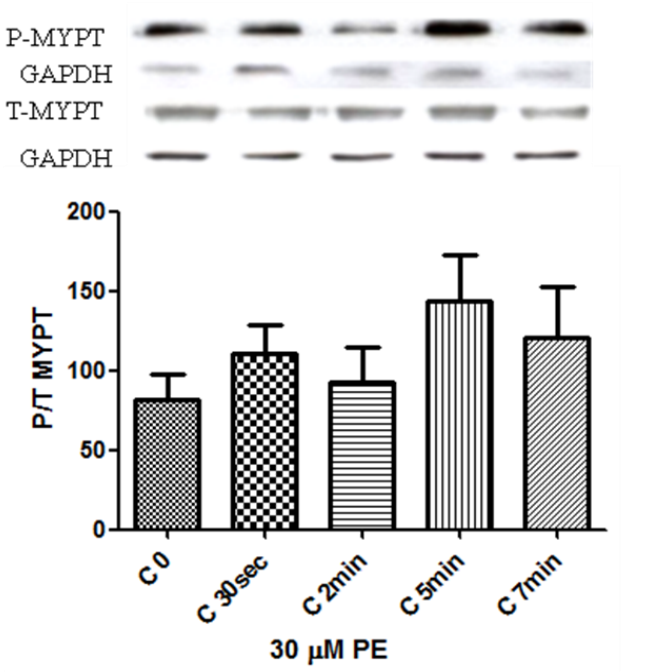

Figure 15: Representative Western blot showing total and phosphorylated MYPT at Thr853 with GAPDH as a loading control (above). Ratio of phosphorylated to total MYPT normalized for corresponding GAPDH in the same blot in superior mesenteric arteries from control rats treated with 30 µM PE at various time points (bottom). Data shown are means ± SEM. N = 8. Results were analyzed using one-way ANOVA.

3.2.2 Effect of PE with or without H-1152 on phosphorylation of PKC-α and -ε in superior mesenteric arteries

Here, we determined the phosphorylation of PKC-α and -ε in response to treatment with PE with or with H-1152 in superior mesenteric arteries from control and STZ-diabetic rats using Western blotting.

Similar to what we found in mesenteric resistance arteries, neither phosphorylation of PKC-α nor -ε showed any significant changes among different treatment groups in superior mesenteric arteries from control or STZ-diabetic rats (fig. 16, 17). Also, expression of either PKC-α or -ε was similar between control and STZ-diabetic arteries (fig. 16, 17).

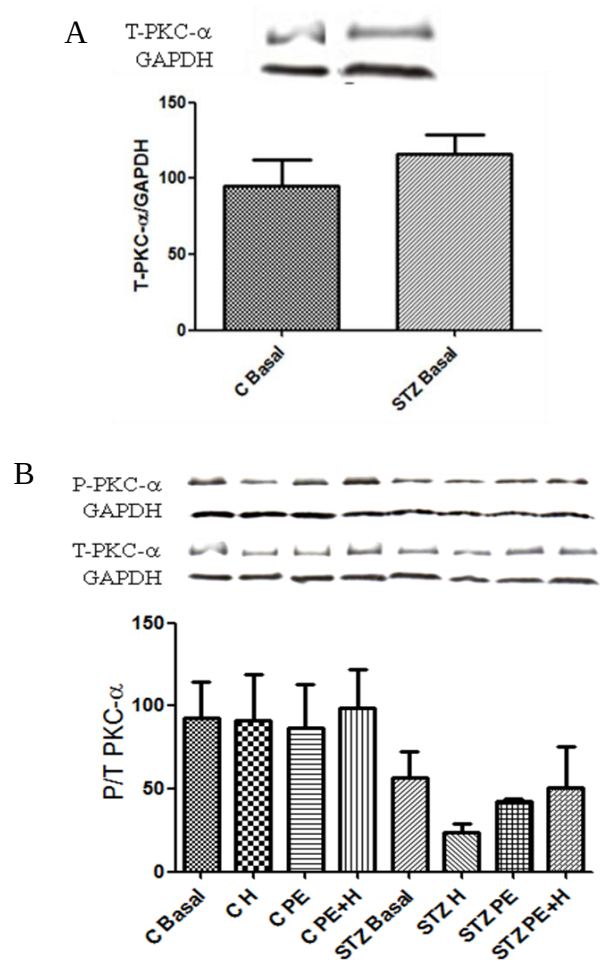

Figure 16: A: Representative Western blot showing total PKC-α with GAPDH as a loading control (above). Total PKC-α normalized for corresponding GAPDH in the same blot in untreated (Basal) superior mesenteric arteries from control (C) and STZ rats (bottom). B: Representative Western blot showing total and phosphorylated PKC-α at Thr638 with GAPDH as a loading control (above). Ratio of phosphorylated to total PKC-α normalized for corresponding GAPDH in the same blot in superior mesenteric arteries from control (C) and STZ rats with no treatment (Basal), 0.1 μM H-1152 (H), 30 μM PE (PE), and 0.1 μM H-1152 + 30 μM PE (PE+H) (bottom). Data shown are means ± SEM. N = 5 in control, 3 in STZ. Results were analyzed using Student's unpaired t-test (top) or one-way ANOVA (bottom).

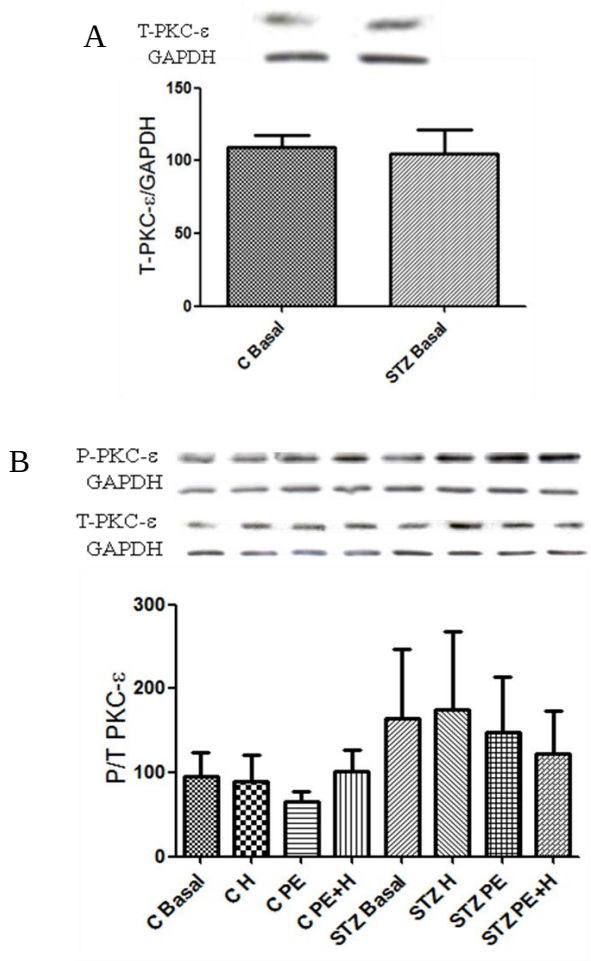

Figure 17: A: Representative Western blot showing total PKC-ε with GAPDH as a loading control (above). Total PKC-ε normalized for corresponding GAPDH in the same blot in untreated (Basal) superior mesenteric arteries from control (C) and STZ rats (bottom). B: Representative Western blot showing total and phosphorylated PKC-ε at Ser729 with GAPDH as a loading control (above). Ratio of phosphorylated to total PKC-ε normalized for corresponding GAPDH in the same blot in superior mesenteric arteries from control (C) and STZ rats with no treatment (Basal), 0.1 μM H-1152 (H), 30 μM PE (PE), and 0.1 μM H-1152 + 30 μM PE (PE+H) (bottom). Data shown are means ± SEM. N = 5 in control, 3 in STZ. Results were analyzed using Student's unpaired t-test (top) or one-way ANOVA (bottom).

3.3 U-46619-induced contractile responses in mesenteric resistance arteries from control and STZ-diabetic rats

We decided to try another agonist that is known to induce contractile responses that are sensitive to ROCK inhibition, as we proposed that contraction is increased in resistance arteries in diabetes due to increased ROCK activity. The compound U-46619 is a thromboxane A_2 mimetic. Upon stimulation by U-46619, thromboxane A_2 receptors couple to $G\alpha_q$ as well as $G\alpha_{12/13}$, resulting in the activation of the RhoA/ROCK pathway (Honma, Saika et al. 2006). It has been shown that the contractile response of carotid arteries to U-46619 was elevated in Ins2(Akita) diabetic mice, an autosomal dominant mutant diabetic model (Yang, Wang et al. 2008). Therefore, we chose to try this compound, U-46619.

As shown in figure 18A, there was no difference in U-46619-induced contraction between control and STZ-diabetic arteries, although there was only a small number of STZ-diabetic animals involved in this study. Treatment with 0.1 μM H-1152 significantly decreased U-46619-induced contractile responses in the mesenteric resistance arteries from control rats by 39%, suggesting that U-46619 may be a suitable agonist to study the involvement of ROCK in resistance artery contractility.

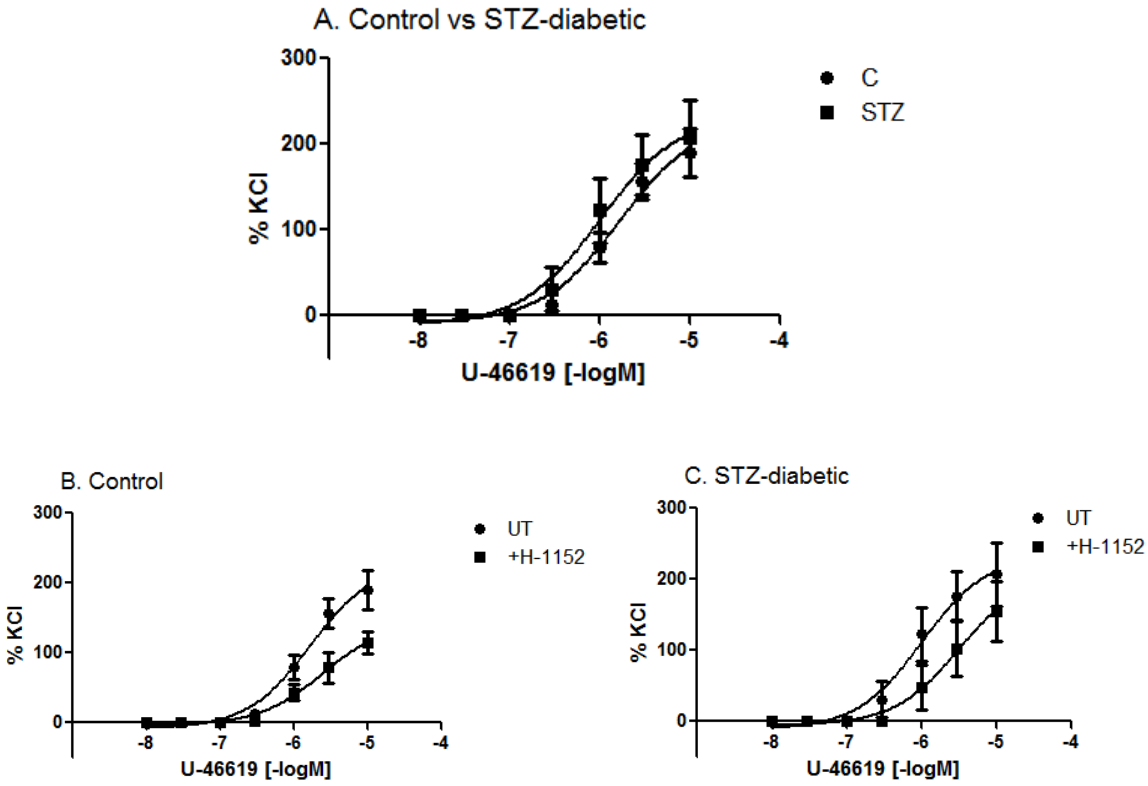

	C	C+H-1152	STZ	STZ+H-1152
LogEC50	-5.77 ±0.15	-5.61 ±0.21	-6.00 ±0.21	-5.51 ±0.30
Rmax	188.98 ±24.76	114.05 ±23.3 *	205.91 ±30.1	154.85 ±52.01

Figure 18: A: Comparison of U-46619-induced contraction in mesenteric resistance arteries from control and STZ-diabetic rats. B, C: U-46619-induced contractile responses in the absence and presence of 0.1 μM H-1152 in mesenteric resistance arteries from control and STZ-diabetic rats. Table shows log EC50 and Rmax derived from non-linear curve fitting of individual concentration-response curves. Data shown are means ± SEM. N = 6 in control, 2 in STZ. *, $p < 0.05$ compared to corresponding control group (Student's unpaired t-test).

3.3.1 Effect of U-46619 with or without H-1152 on activity of ROCK in mesenteric resistance arteries

In isolated mesenteric resistance arteries, we determined MYPT phosphorylation as an index of ROCK activity. The resistance arteries were treated with 0.1 μM H-1152, 10 μM U-46619 (a concentration that induced near maximal contractile response), 0.1 μM H-1152 plus 10 μM U-46619, or were left untreated. Following the treatment, arteries were homogenized and MYPT phosphorylation was measured using Western blotting.

In contrast to PE, 10 μM U-46619 significantly increased MYPT phosphorylation at Thr853, and this was normalized by 0.1 μM H-1152 in mesenteric resistance arteries from both control and STZ-diabetic animals (fig. 19). As found in our previous study, basal MYPT expression and phosphorylation were similar between control and STZ-diabetic resistance arteries. Similarly, there was no difference in the extent of MYPT phosphorylation in response to U-46619 between control and diabetic arteries.

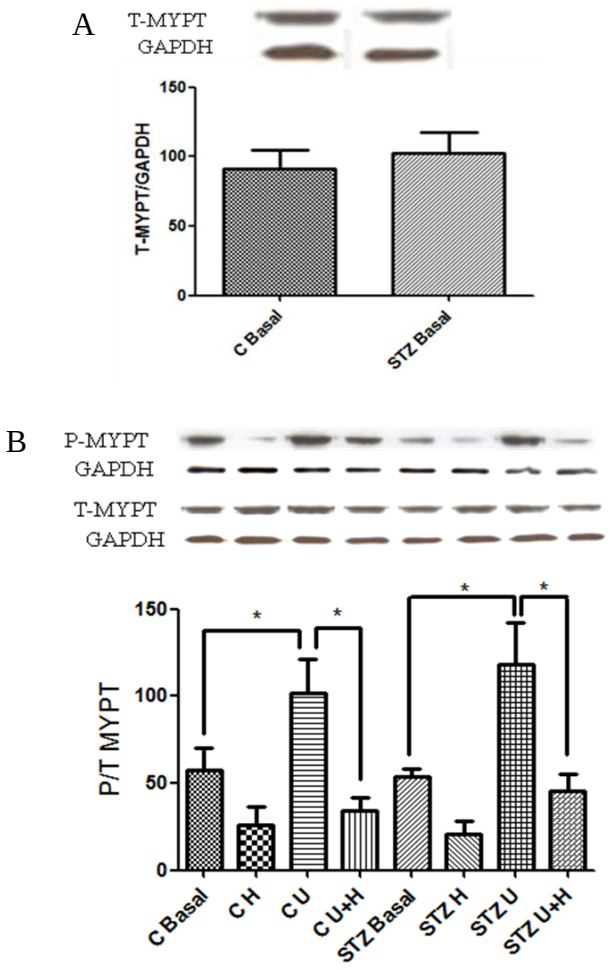

Figure 19: A: Representative Western blot showing total MYPT with GAPDH as a loading control (above). Total MYPT normalized for corresponding GAPDH in the same blot in untreated (Basal) mesenteric resistance arteries from control (C) and STZ rats (bottom). B: Representative Western blot showing total and phosphorylated MYPT at Thr853 with GAPDH as a loading control (above). Ratio of phosphorylated to total MYPT normalized for corresponding GAPDH in the same blot in mesenteric resistance arteries from control (C) and STZ rats with no treatment (Basal), 0.1 µM H-1152 (H), 10 µM U-46619 (U), and 0.1 µM H-1152 + 10 µM U-46619 (U+H) (bottom). Data shown are means ± SEM. N = 5. *, $p < 0.05$ compared to corresponding control group (top: Student's unpaired t-test; bottom: one-way ANOVA).

3.3.2 Expression of ROCK in mesenteric resistance arteries between control and STZ-diabetic rats

We know that ROCK activity was increased in response to U-46619 stimulation and normalized by ROCK inhibitor in control and STZ-diabetic resistance arteries. We wished to determine if there are any differences in ROCK expression between control and STZ-diabetic arteries by performing Western blotting analysis in the same tissue sample lysates. ROCK2 has been shown to be the predominant isoform mediating vascular smooth muscle contraction, and preliminary studies have shown that ROCK2 expression is selectively increased in diabetic rat hearts (Wang, Zheng et al. 2009).

However, as shown in figure 20, ROCK2 expression was similar between control and STZ-diabetic resistance arteries.

3.3.3 Effect of U-46619 with or without H-1152 on phosphorylation of CPI-17 in mesenteric resistance arteries

As shown earlier in figure 11, 30 μM PE didn't increase CPI-17 phosphorylation or activation nor did 0.1 μM H-1152 reduce it in arteries from either control or STZ-diabetic resistance rats. We wanted to examine the effects of U-46619 on phosphorylation or activation of CPI-17. In isolated mesenteric resistance arteries, the same treatments were used: 0.1 μM H-1152, 10 μM U-46619, and 0.1 μM H-1152 plus 10 μM U-46619.

There were no significant differences in basal CPI-17 expression or phosphorylation between control and STZ-diabetic resistance arteries. Neither 10 μM U-46619 nor 0.1 μM H-1152 affected CPI-17 phosphorylation in either control or STZ-diabetic rats (fig. 21).

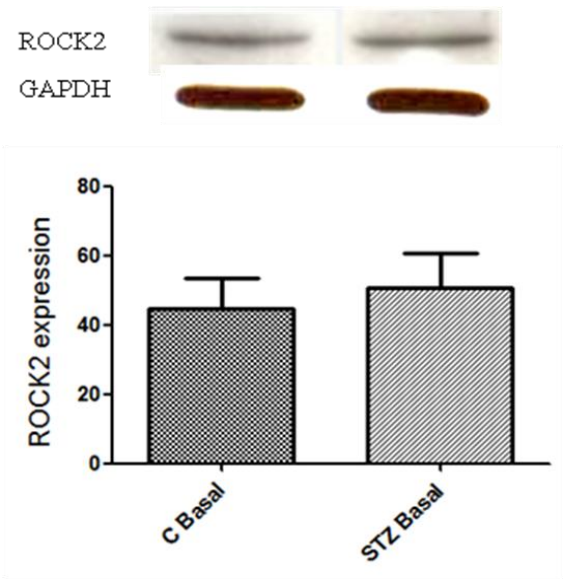

Figure 20: Representative Western blot showing ROCK2 expression with GAPDH as a loading control (above). ROCK2 expression normalized for corresponding GAPDH in the same blot in untreated (Basal) mesenteric resistance arteries from control (C) and STZ rats (bottom). Data shown are means ± SEM. N = 5. Results were analyzed using Student's unpaired t-test.

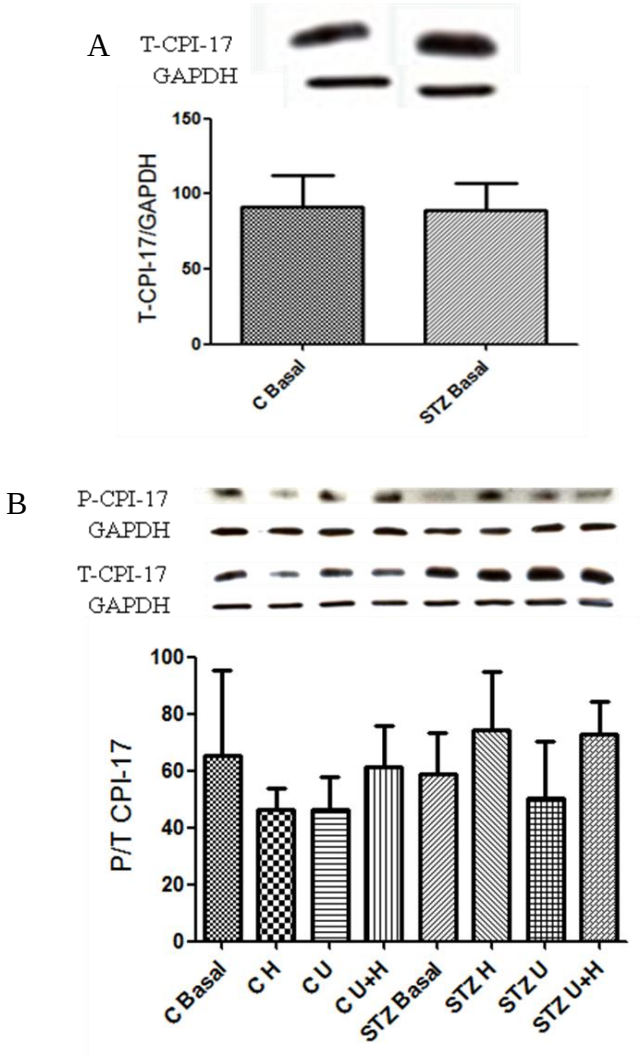

Figure 21: A: Representative Western blot showing total CPI-17 with GAPDH as a loading control (above). Total CPI-17 normalized for corresponding GAPDH in the same blot in untreated (Basal) mesenteric resistance arteries from control (C) and STZ rats (bottom). B: Representative Western blot showing total and phosphorylated CPI-17 at Thr38 with GAPDH as a loading control (above). Ratio of phosphorylated to total CPI-17 normalized for corresponding GAPDH in the same blot in mesenteric resistance arteries from control (C) and STZ rats with no treatment (Basal), 0.1 μM H-1152 (H), 10 μM U-46619 (U), and 0.1 μM H-1152 + 10 μM U-46619 (U+H) (bottom). Data shown are means ± SEM. N = 5. Results were analyzed using Student's unpaired t-test (top) or one-way ANOVA (bottom).

3.4 Main characteristics of control and GK rats

We monitored the body weight of control and GK rats over the 14-week study period, and it was measured every week at the same time after 4 hours of fasting. As shown in figure 22, the body weight of GK rats was significantly lower than that of control rats, and this difference was observed over the entire study.

Glucose and insulin levels were measured in plasma isolated every week at the same time after 4 hours of fasting. There were some variations in glucose levels in GK rats, which ranged from 9.73 mM to 18.10 mM, whereas in control rats, glucose levels ranged from 4.62 mM to 6.83 mM (fig. 23). In general, GK rats had higher blood glucose levels than control rats with exception of weeks 16 and 17, such that the average blood glucose level over the 14 weeks of the study was significantly higher in GK compared to control rats (fig. 23). There was quite a lot of variation in blood insulin levels in both control and GK rats over the course of the sutdy. Insulin levels in GK rats ranged from a low of 0.63 ng/ml to a high of 2.18 ng/ml, and in control rats, insulin levels ranged from 0.41 ng/ml to 1.32 ng/ml when compared on a weekly basis (fig. 24). Insulin levels were not significantly different between control and GK rats except for week 11; however, average insulin levels were significantly higher in GK than in control rats.

Blood pressure was measured biweekly. Similar to what we found in previous studies, GK rats developed mild hypertension (systolic blood pressure 140 mm Hg compared to less than 120 mm Hg in control rats) starting from 14^{th} week onwards (fig. 25). In order to test whether ROCK contributes to elevated blood pressure in GK rats, on week 25, we treated them with fasudil for one week. As shown in figure 25, blood pressure in GK rats measured within 2 hour after fasudil administration was normalized. The average blood pressure in GK

rats then recovered back to the 140 mm Hg level after a 24-hour wash-out period. Therefore, the effect of fasudil on blood pressure appears to have been an acute effect.

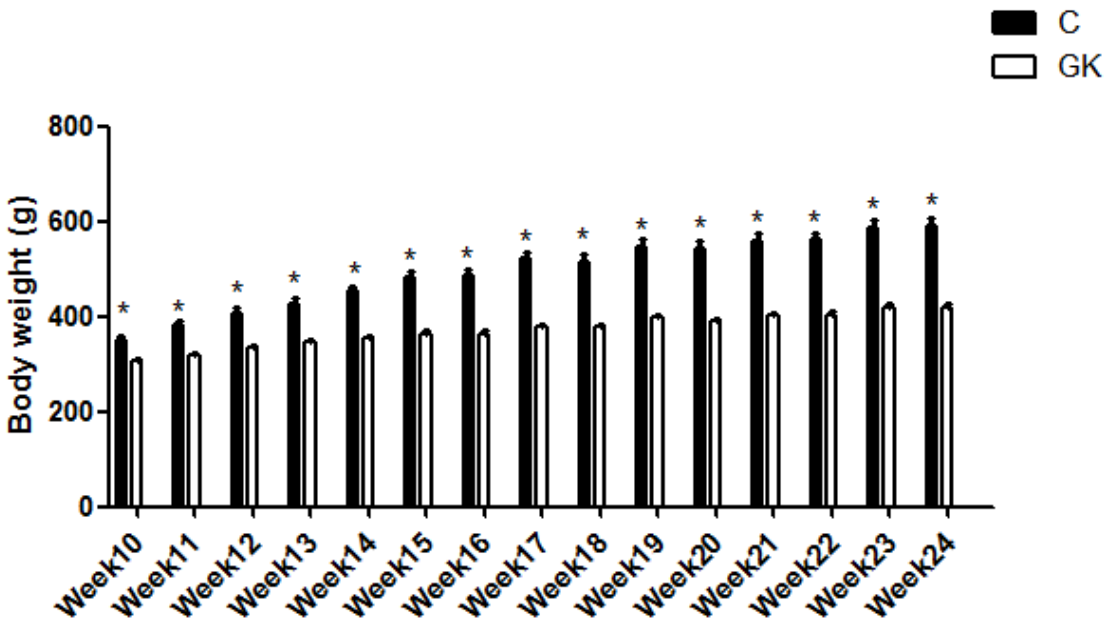

Figure 22: Comparison of body weight of control Wistar and GK rats. Body weight was measured once every week. Results from each measurement were plotted. Data shown are means ± SEM. N = 6 in control and GK. *, $p < 0.05$ compared to corresponding control group (two-way ANOVA followed by the Bonferroni post hoc test).

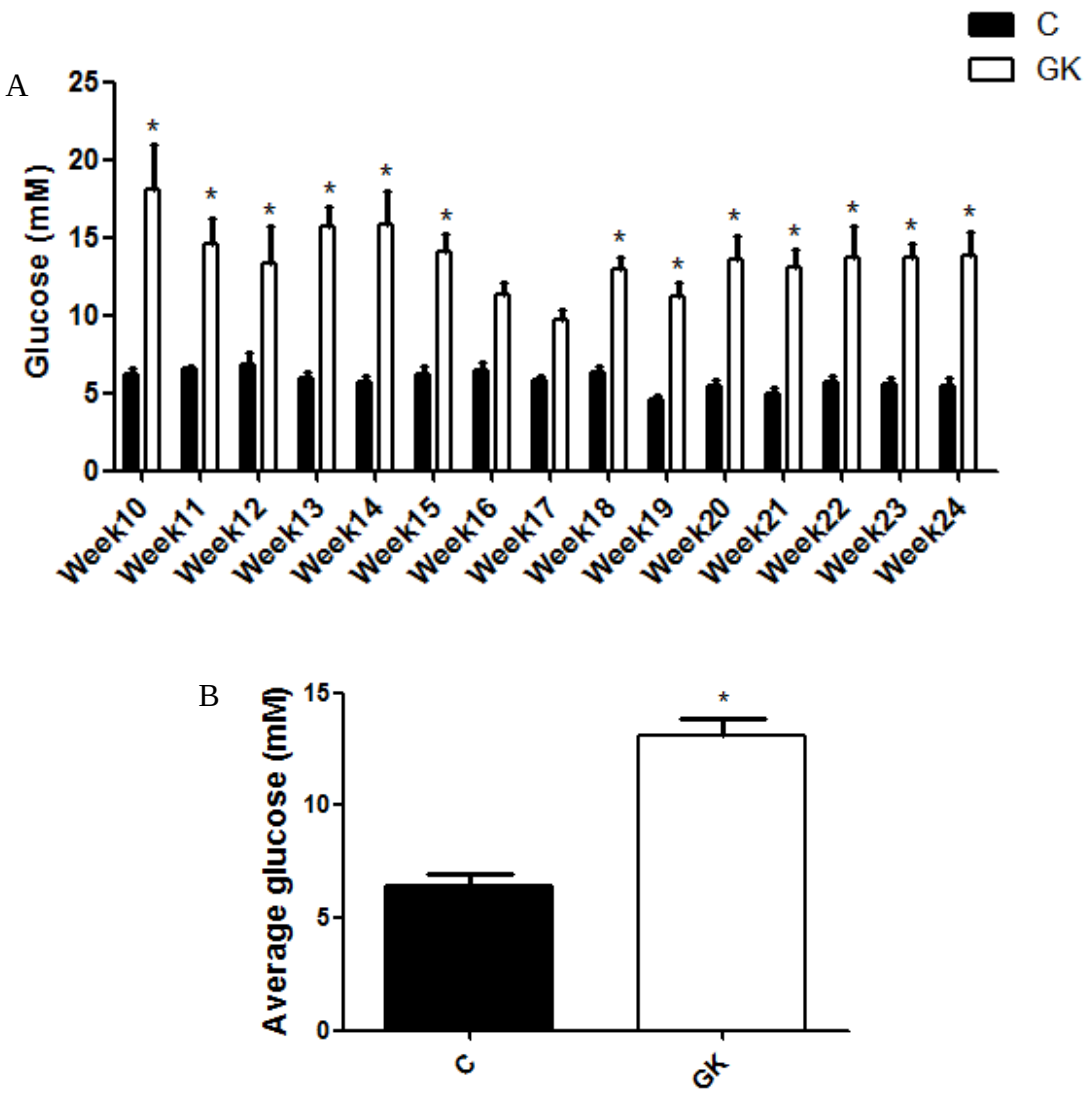

Figure 23: Blood glucose was measured once every week. Results from each measurement were plotted. Data shown are means ± SEM. N = 6 in control and GK. *, $p < 0.05$ compared to corresponding control group. A: Comparison of blood glucose levels each week between control Wistar and GK rats (two-way ANOVA followed by the Bonferroni post hoc test). B: Comparison of average blood glucose levels between control Wistar and GK rats (Student's unpaired t-test).

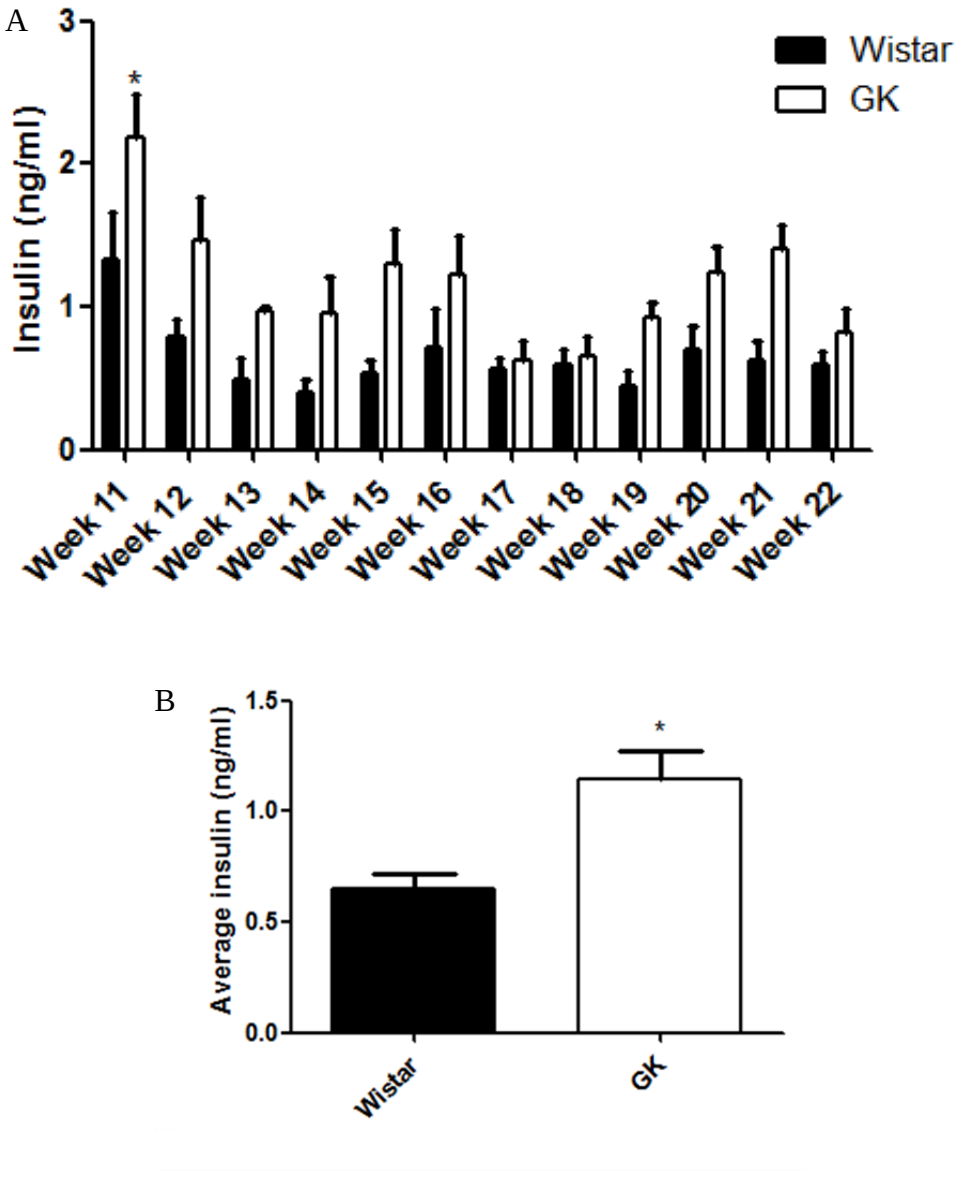

Figure 24: Blood sample was collected once every week, and insulin assay was performed using plasma. Data shown are means ± SEM. N = 6 in control and GK. *, $p < 0.05$ compared to corresponding control group. A: Comparison of plasma insulin levels each week between control Wistar and GK rats (two-way ANOVA followed by the Bonferroni post hoc test). B: Comparison of average insulin levels between control Wistar and GK rats (Student's unpaired t-test).

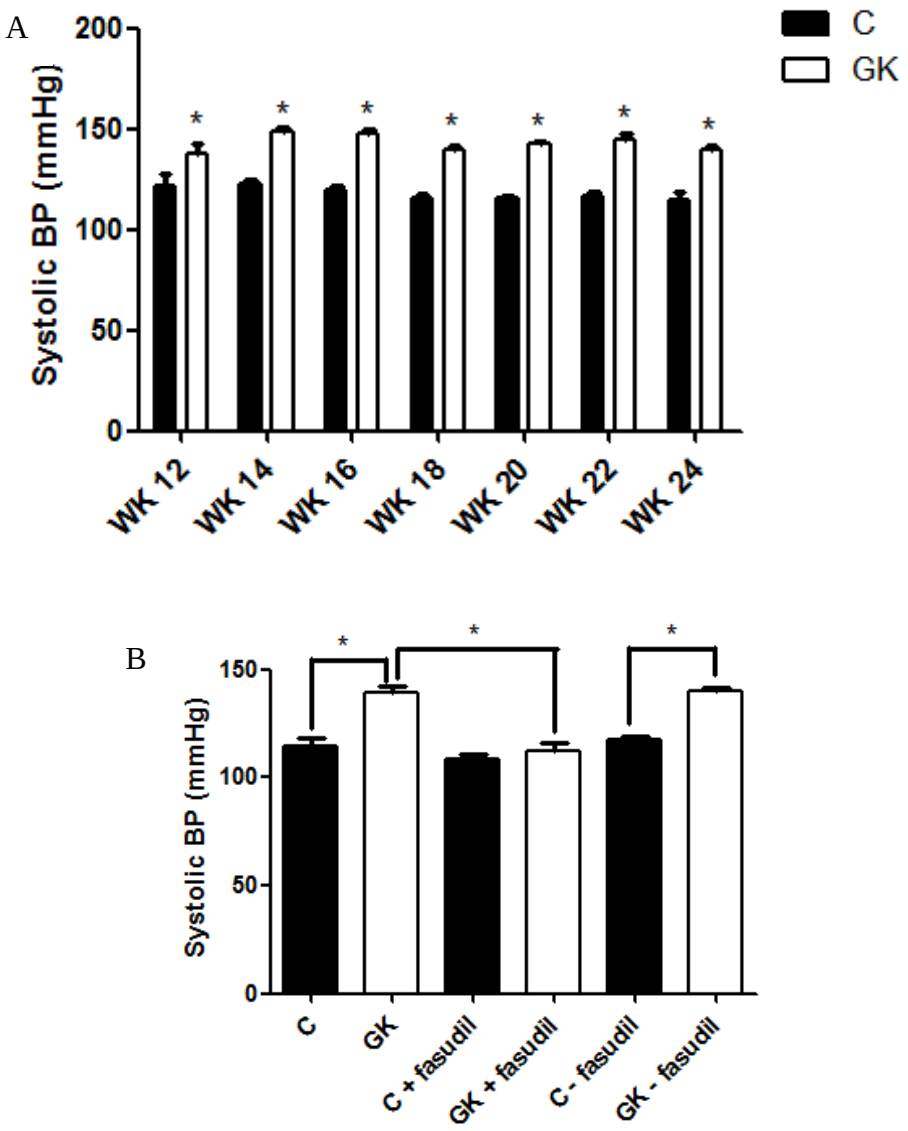

Figure 25: Blood pressure was measured every other week. Data shown are means ± SEM. N = 6 in control and GK. *, $p < 0.05$ compared to corresponding control group. A: Comparison of blood pressure every 2nd week between control Wistar and GK rats (two-way ANOVA followed by the Bonferroni post hoc test). B: Blood pressure measured prior to, during, and 24-hour post fasudil treatment (one-way ANOVA).

3.5 PE-induced contractile responses in mesenteric resistance arteries from control and GK rats

Earlier, we found that PE-induced contractile responses in control and STZ mesenteric arteries were not sensitive to ROCK inhibitors. Here, we examined the involvement of ROCK in PE-induced contractions in GK mesenteric resistance arteries. The degree of contractile response induced by PE was similar between control and GK rats. A non-selective NOS inhibitor, L-NAME, was used to eliminate any role of NO in contractile responses. Treatment with L-NAME significantly shifted the curve to the left to a similar extent in control and GK rats (fig. 26). Pre-treatment with 1 μM Y-27632 did not cause any changes in PE-induced contraction in control mesenteric resistance arteries, which is consistent with what we found earlier (fig. 27A). However, 1μM Y-27632 significantly inhibited PE-induced contractile responses by shifting the curve to the right in GK mesenteric resistance arteries (fig. 27B). Similarly, 0.1 μM H-1152 inhibited PE-induced contraction by shifting the curve to the right in mesenteric resistance arteries from GK but not control rats (fig. 28).

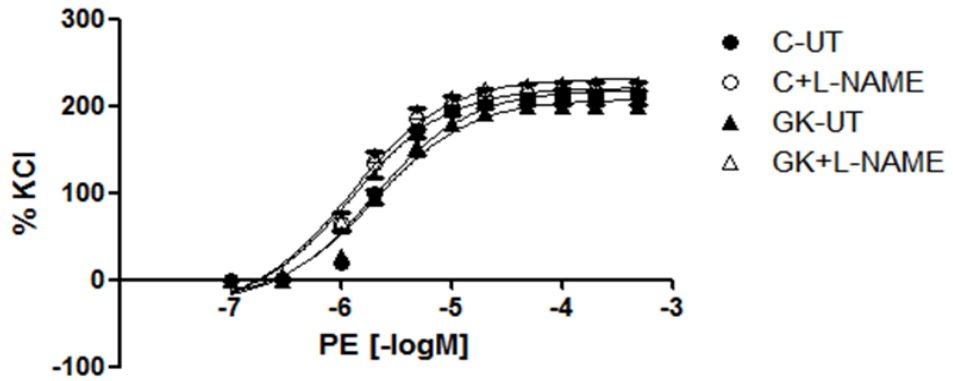

	C-UT	C+L-NAME	GK-UT	GK+L-NAME
LogEC50	-5.72 ±0.056	-5.90 ±0.08 *	-5.69 ±0.052	-5.91 ±0.05 *
Rmax	208.86 ±4.25	213.47 ±5.21 *	199.88 ±3.57	224.34 ±3.58

Figure 26: Comparison of PE-induced contractile responses in the absence (UT) and presence of 100 μM L-NAME in mesenteric resistance arteries from control (C) and GK rats. Table shows log EC50 and Rmax derived from non-linear curve fitting of individual concentration-response curves. Data shown are means ± SEM. T = treated. N = 6. *, $p < 0.05$ compared to corresponding control group (Student's unpaired t-test).

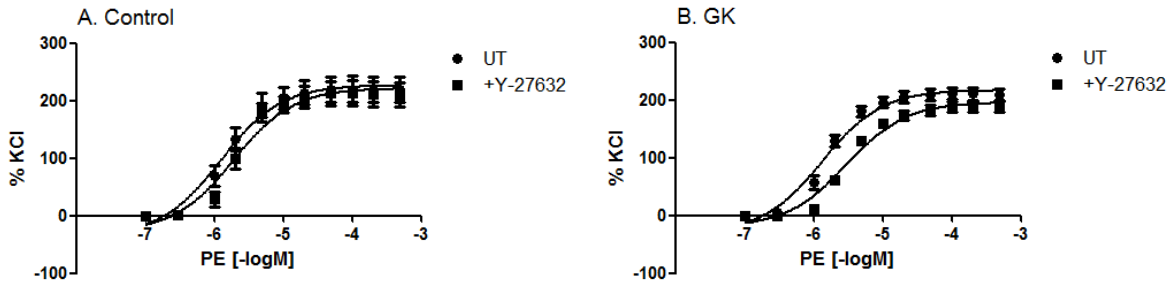

	C-UT	C+Y-27632	GK-UT	GK +Y-27632
LogEC50	-5.91 ±0.12	-5.75 ±0.11	-5.89 ±0.07	-5.54 ±0.06 *
Rmax	219.12 ±8.37	209.51 ±8.23	208.85 ±4.42	188.24 ±3.93

Figure 27: PE-induced contractile responses in the absence (UT) and presence of 1 μM Y-27632 in the presence of L-NAME in mesenteric resistance arteries from control and GK rats. Table shows log EC50 and Rmax derived from non-linear curve fitting of individual concentration-response curves. Data shown are means ± SEM. T = treated. N = 6. *, $p < 0.05$ compared to corresponding control group (Student's unpaired t-test).

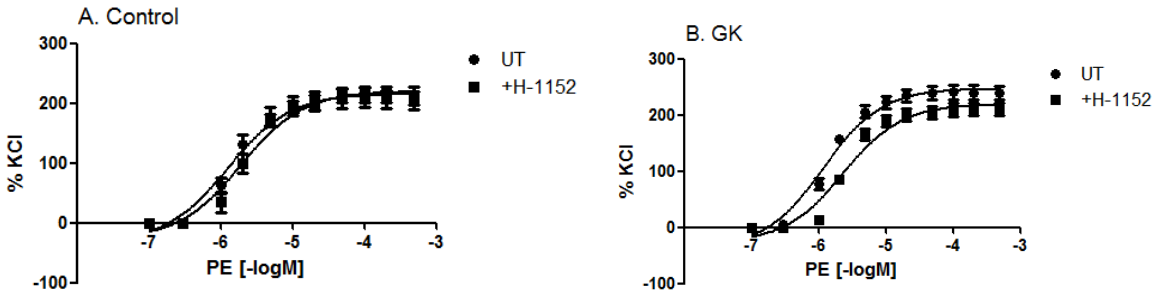

	C-UT	C+H-1152	GK-UT	GK+H-1152
LogEC50	-5.92 ±0.10	-5.76 ±0.08	-5.96 ±0.07	-5.65 ±0.07 *
Rmax	207.82 ±6.69	208.52 ±5.57	239.84 ±4.83	209.52 ±5.16

Figure 28: PE-induced contractile responses in the absence (UT) and presence of 0.1 μM H-1152 in the presence of L-NAME in mesenteric resistance arteries from control and GK rats. Table shows log EC50 and Rmax derived from non-linear curve fitting of individual concentration-response curves. Data shown are means ± SEM. T = treated. N = 6. *, $p < 0.05$ compared to corresponding control group (Student's unpaired t-test).

3.6 U-46619-induced contractile responses in mesenteric resistance arteries from control and GK rats

Based on what we found previously, the thromboxane A_2 mimetic U-46619-induced contractile responses from control and STZ-diabetic rats were sensitive to ROCK inhibition. Contraction induced by U-46619 was then determined in GK mesenteric arteries. As shown in figure 29, the degree of U-46619-induced contractile responses in mesenteric resistance arteries from GK was similar to control rats. Treatment with L-NAME dramatically increased U-46619-induced contraction by shifting the curve to the left as well as increasing maximum contraction in both control and GK animals (fig. 29). Surprisingly, unlike what we found earlier, neither Y-27632 nor H-1152 reduced U-46619-induced contractile responses in control mesenteric arteries (fig. 30A, 31A). In GK mesenteric resistance arteries, H-1152 but not Y-27632 produced a significant right-ward shift in U-46619-induced contractile responses. (fig. 30B, 31B) However, in 5 out of 6 mesenteric resistance artery rings from GK rats, Y-27632 also caused a right-ward shift in U-46619-induced contractile responses.

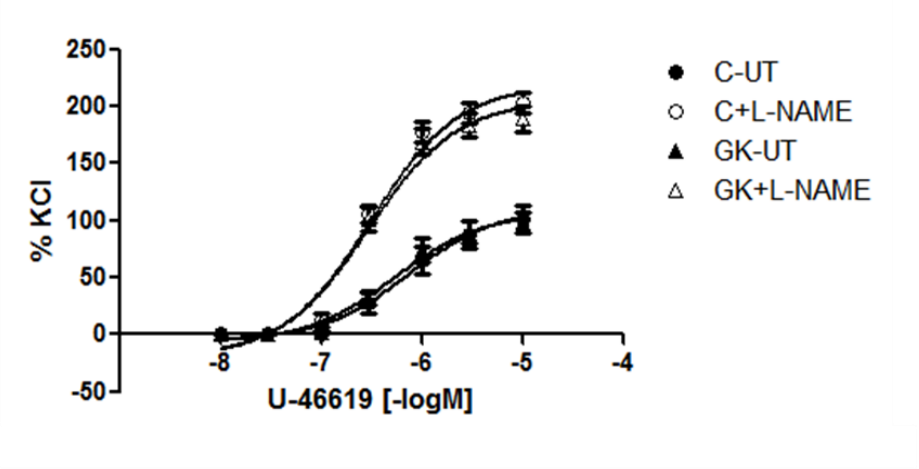

	C-UT	C+L-NAME	GK-UT	GK+L-NAME
LogEC50	-6.08 ± 0.16	-6.52 ± 0.07 *	-6.24 ± 0.12	-6.56 ± 0.09 *
Rmax	101.69 ± 9.57	203.19 ± 7.50 *	97.77 ± 6.70	189.08 ± 8.503 *

Figure 29: Comparison of U-46619-induced contractile responses in the absence (UT) and presence of 100 μM L-NAME in mesenteric resistance arteries from control (C) and GK rats. Table shows log EC50 and Rmax derived from non-linear curve fitting of individual concentration-response curves. Data shown are means ± SEM. N = 6. *, $p < 0.05$ compared to corresponding control group (Student's unpaired t-test).

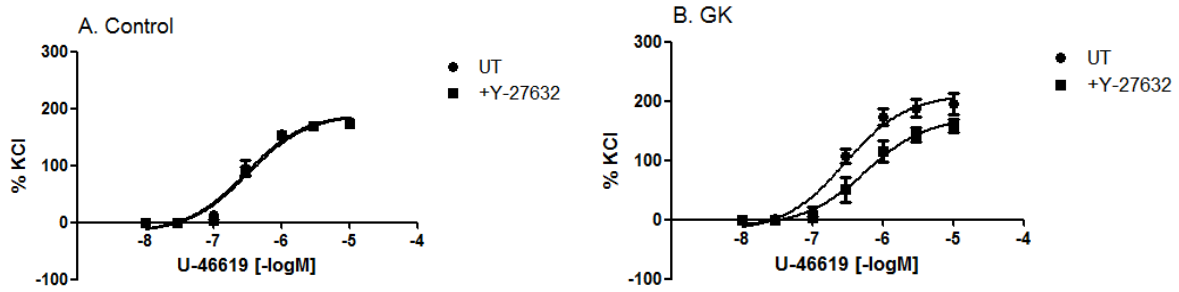

	C-UT	C+Y-27632	GK-UT	GK +Y-27632
LogEC50	-6.53 ± 0.08	-6.49 ± 0.07	-6.54 ± 0.11	-6.25 ± 0.14
Rmax	177.94 ± 6.52	173.43 ± 5.91	195.53 ± 10.53	158.16 ± 12.33

Figure 30: U-46619-induced contractile responses in the absence (UT) and presence of 1 μM Y-27632 in the presence of L-NAME in mesenteric resistance arteries from control and GK rats. Table shows log EC50 and Rmax derived from non-linear curve fitting of individual concentration-response curves. Data shown are means ± SEM. N = 6. Results were analyzed using Student's unpaired t-test.

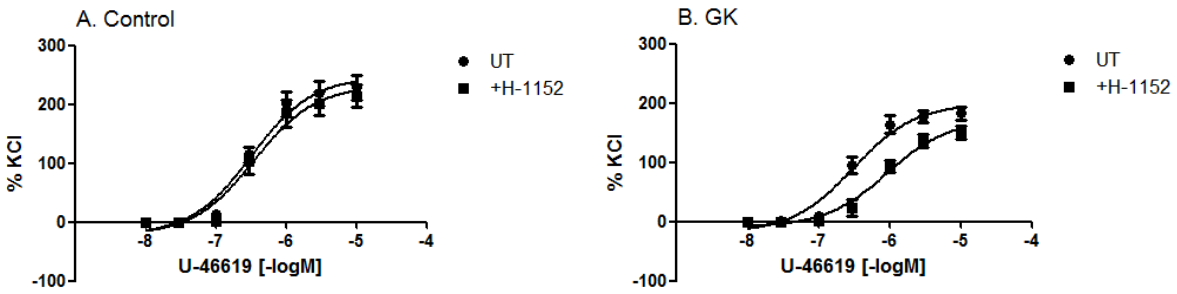

	C-UT	C+H-1152	GK-UT	GK+H-1152
LogEC50	-6.50 ±0.12	-6.43 ±0.14	-6.52 ±0.10	-6.06 ±0.11 *
Rmax	228.43 ±13.24	213.88 ±15.08	182.62 ±9.25	150.31 ±11.20

Figure 31: U-46619-induced contractile responses in the absence (UT) and presence of 0.1 μM H-1152 in the presence of L-NAME in mesenteric resistance arteries from control (C) and GK rats. Data shown are means ± SEM. Table shows log EC50 and Rmax derived from non-linear curve fitting of individual concentration-response curves. N = 6. *, $p < 0.05$ compared to corresponding control group (Student's unpaired t-test).

3.6.1 Expression of ROCK in mesenteric resistance arteries between control and GK rats

Both ROCK 1 and ROCK 2 expression were measured in mesenteric arteries from control and GK rats. The degree of ROCK 1 expression was the same between control and GK rats. The increase in ROCK 2 expression between control and GK resistance arteries was not statistically significant (fig. 32).

3.6.2 Effect of U-46619 with or without H-1152 on activity of ROCK in mesenteric resistance arteries

Phosphorylation of MYPT was measured as an index of ROCK activity. As shown in figure 33, basal expression and phosphorylation of MYPT at Thr853 were similar in mesenteric resistance arteries from GK compared to control animals. Treatment with 10 μM U-46619 substantially increased MYPT phosphorylation by 4.5 and 4.2 fold in control and GK rats, respectively, and this was normalized by 0.1 μM H-1152 in both control and GK rats (fig. 33). L-NAME did not significantly increase MYPT phosphorylation induced by U-46619 in either control or GK rats, but 0.1 μM H-1152 normalized U-46619-induced MYPT phosphorylation in the presence of L-NAME.

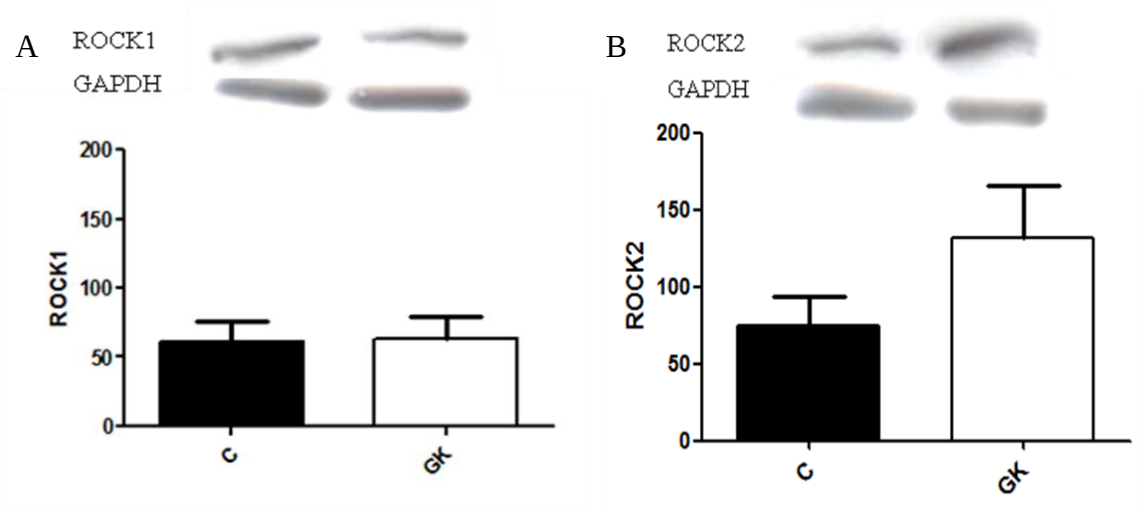

Figure 32: Representative Western blot showing ROCK1 (A) and ROCK2 (B) expression with GAPDH as a loading control (above). ROCK1 (A) and ROCK2 (B) expression normalized for corresponding GAPDH in the same blot in untreated (Basal) mesenteric resistance arteries from control (C) and GK rats (bottom). Data shown are means ± SEM. N = 6. Results were analyzed using Student's unpaired t-test.

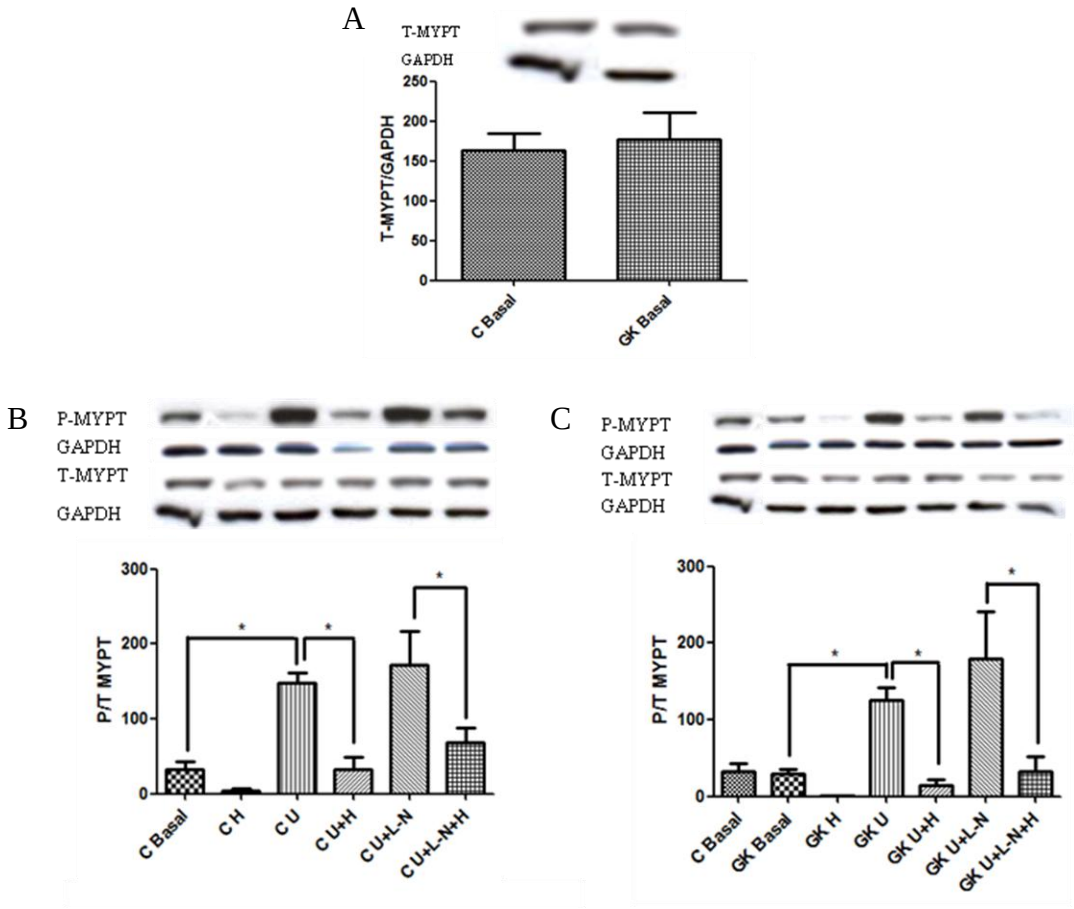

Figure 33: A: Representative Western blot showing total MYPT with GAPDH as a loading control (above). Total MYPT normalized for corresponding GAPDH in the same blot in untreated (Basal) mesenteric resistance arteries from control (C) and GK rats (bottom). B, C: Representative Western blot showing total and phosphorylated MYPT at Thr853 with GAPDH as a loading control (above). Ratio of phosphorylated to total MYPT normalized for corresponding GAPDH in the same blot in mesenteric resistance arteries from control (C) and GK rats with no treatment (Basal), 0.1 μM H-1152 (H), 10 μM U-46619 (U), 0.1 μM H-1152 + 10 μM U-46619 (U+H), 10 μM U-46619 + 100 μM L-NAME (U+L-N), and 0.1 μM H-1152 + 10 μM U-46619 + 100 μM L-NAME (U+L-N+H) (bottom). Data shown are means ± SEM. N = 6. *, $p < 0.05$ compared to corresponding control group (top: Student's unpaired t-test; bottom: one-way ANOVA).

3.6.3 Effect of U-46619 with or without H-1152 on phosphorylation of RhoA in mesenteric resistance arteries

The levels of both RhoA expression and phosphorylation were similar between control and GK mesenteric resistance arteries (fig. 34). Treatment with 10 μM U-46619 seemed to decrease RhoA phosphorylation in mesenteric arteries from GK rats, although this reduction was not statistically significant (fig. 34). Treatment with 0.1 μM H-1152 alone or in the presence of U-46619 or both U-46619 and L-NAME had no effect on RhoA phosphorylation (fig. 34).

3.6.4 Effect of U-46619 with or without H-1152 on phosphorylation of MLC in mesenteric resistance arteries

Phosphorylation of MLC at Ser19 promotes its interaction with actin, thereby increasing contraction in smooth muscle cells (Horowitz, Menice et al. 1996). We tested whether changes produced by U-46619 and ROCK inhibitor in smooth muscle contractile responses were reflected in MLC status. First of all, basal MLC expression and phosphorylation were similar in mesenteric resistance arteries from control and GK rats. U-46619 alone or in the presence of L-NAME did not increase MLC phosphorylation at Ser19 in mesenteric arteries from either control or GK rats (fig. 35). However, H-1152 significantly reduced basal and U-46619-induced MLC phosphorylation in the absence and presence of L-NAME by more than 50% in GK arteries (fig. 35).

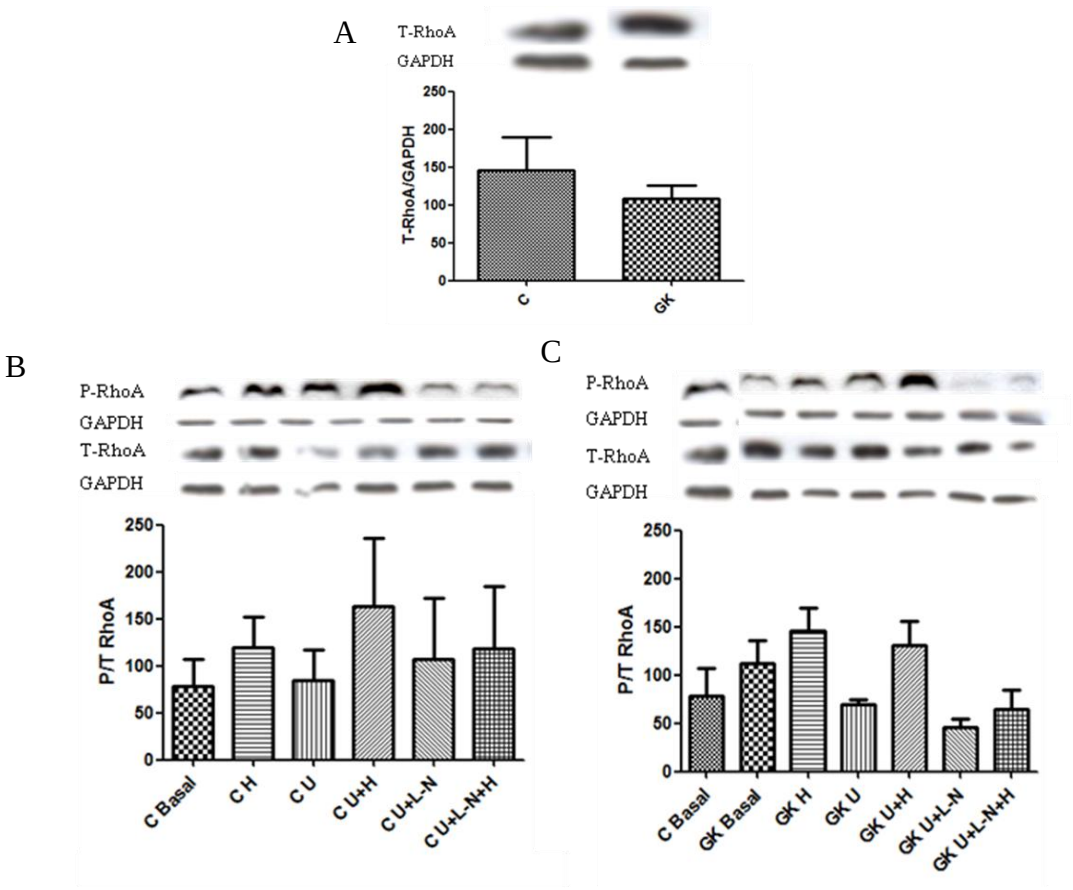

Figure 34: A: Representative Western blot showing total RhoA with GAPDH as a loading control (above). Total RhoA normalized for corresponding GAPDH in the same blot in untreated (Basal) mesenteric resistance arteries from control (C) and GK rats (bottom). B, C: Representative Western blot showing total and phosphorylated RhoA at Ser188 with GAPDH as a loading control (above). Ratio of phosphorylated to total RhoA normalized for corresponding GAPDH in the same blot in mesenteric resistance arteries from control (C) and GK rats with no treatment (Basal), 0.1 μM H-1152 (H), 10 μM U-46619 (U), 0.1 μM H-1152 + 10 μM U-46619 (U+H), 10 μM U-46619 + 100 μM L-NAME (U+L-N), and 0.1 μM H-1152 + 10 μM U-46619 + 100 μM L-NAME (U+L-N+H) (bottom). Data shown are means ± SEM. N = 6. Results were analyzed using Student's unpaired t-test (top) or one-way ANOVA (bottom).

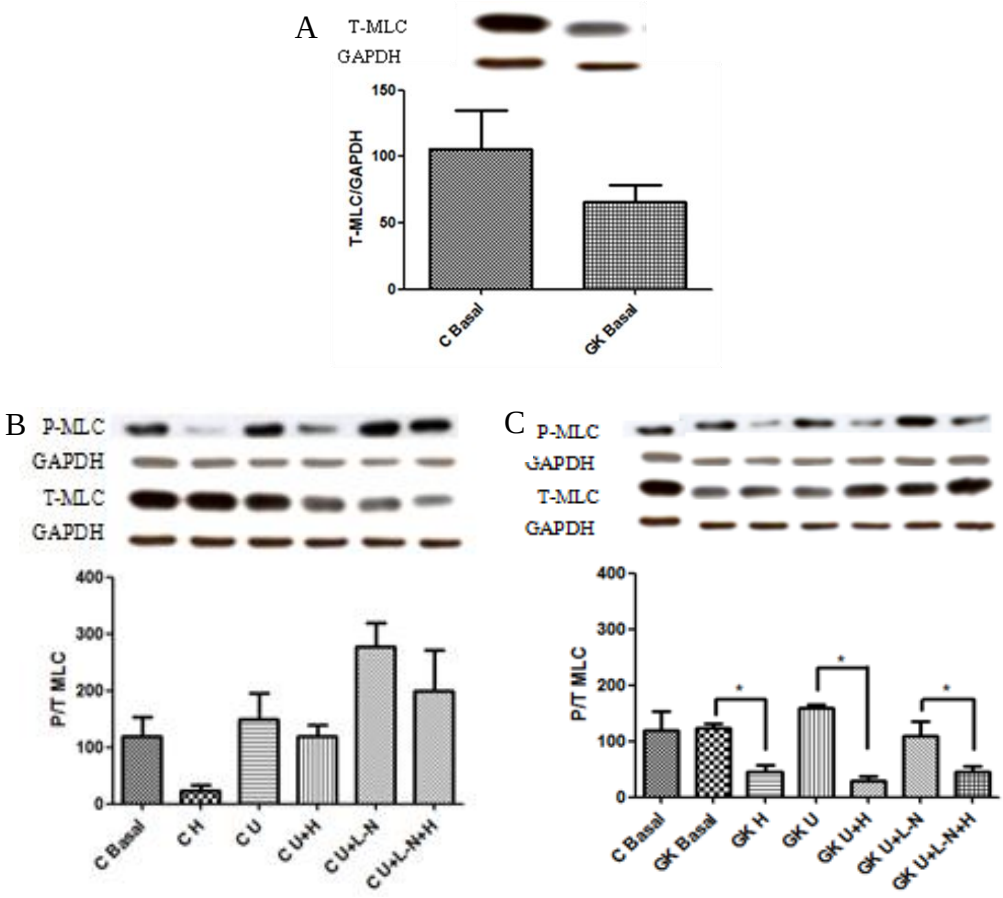

Figure 35: A: Representative Western blot showing total MLC with GAPDH as a loading control (above). Total MLC normalized for corresponding GAPDH in the same blot in untreated (Basal) mesenteric resistance arteries from control (C) and GK rats (bottom). B, C: Representative Western blot showing total and phosphorylated MLC at Ser19 with GAPDH as a loading control (above). Ratio of phosphorylated to total MLC normalized for corresponding GAPDH in the same blot in mesenteric resistance arteries from control (C) and GK rats with no treatment (Basal), 0.1 μM H-1152 (H), 10 μM U-46619 (U), 0.1 μM H-1152 + 10 μM U-46619 (U+H), 10 μM U-46619 + 100 μM L-NAME (U+L-N), and 0.1 μM H-1152 + 10 μM U-46619 + 100 μM L-NAME (U+L-N+H) (bottom). Data shown are means ± SEM. N = 6. *, $p < 0.05$ compared to corresponding control group (top: Student's unpaired t-test; bottom: one-way ANOVA).

3.6.5 Effect of U-46619 with or without H-1152 on phosphorylation of eNOS in mesenteric resistance arteries

As a key source for NO production, eNOS activation was determined by measuring its phosphorylation at Ser 1177 site. U-46619 in the presence and absence of L-NAME had no significant effects on eNOS expression or phosphorylation in either control or GK rats (fig. 36). H-1152 alone or in the presence of U-46619 or U-46619 plus L-NAME did not have any effect on eNOS phosphorylation at Ser1177 in mesenteric arteries from either control or GK group (fig. 36).

3.6.6 Effect of U-46619 with or without H-1152 on phosphorylation of LIM Kinase and cofilin in mesenteric resistance arteries

We measured phosphorylation of LIM kinase and cofilin as they play an important role in the regulation of actin polymerization. When LIM kinase is phosphorylated, it phosphorylates its downstream target cofilin, releasing the inhibitory effect of cofilin on actin polymerization (Bernard 2007). Our results showed that basal expression and phosphorylation of LIM kinase and cofilin were similar in arteries from control and GK rats. Neither LIM kinase or cofilin phosphorylation was altered by U-46619, nor did H-1152 affect their phosphorylation (fig 37, 38).

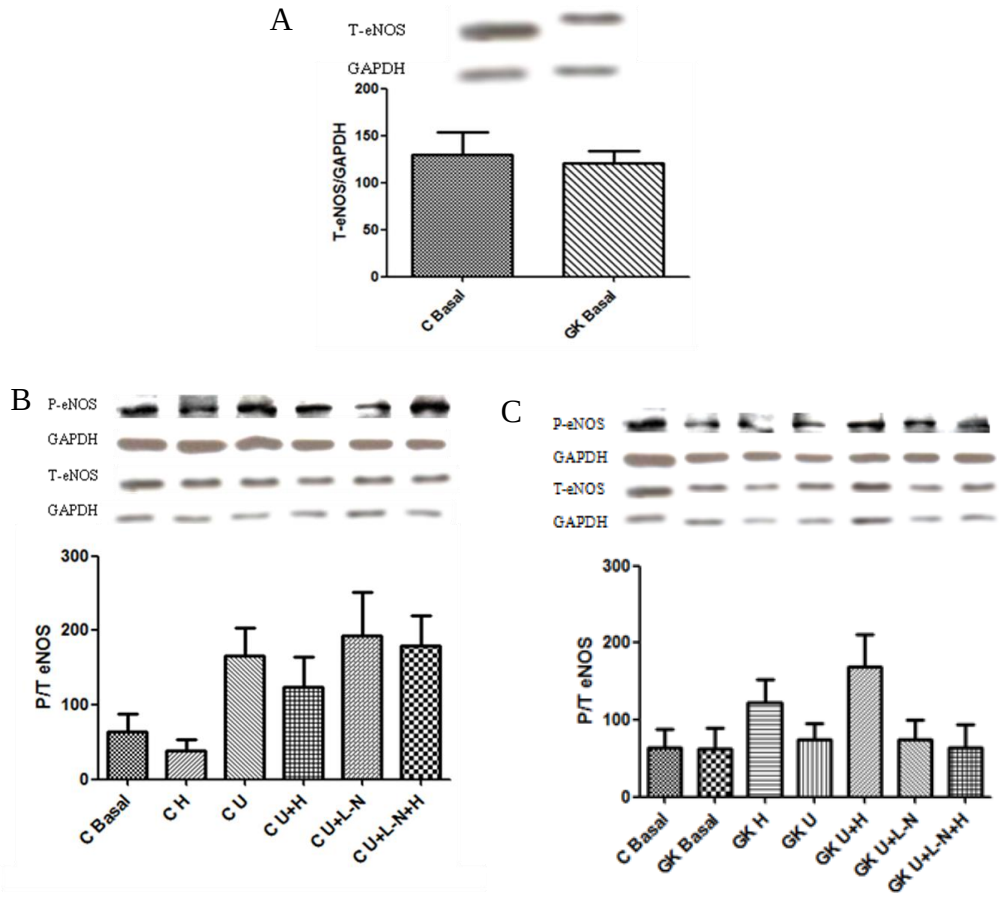

Figure 36: A: Representative Western blot showing total eNOS with GAPDH as a loading control (above). Total eNOS normalized for corresponding GAPDH in the same blot in untreated (Basal) mesenteric resistance arteries from control (C) and GK rats (bottom). B, C: Representative Western blot showing total and phosphorylated eNOS at Ser1177 with GAPDH as a loading control (above). Ratio of phosphorylated to total eNOS normalized for corresponding GAPDH in the same blot in mesenteric resistance arteries from control (C) and GK rats with no treatment (Basal), 0.1 μM H-1152 (H), 10 μM U-46619 (U), 0.1 μM H-1152 + 10 μM U-46619 (U+H), 10 μM U-46619 + 100 μM L-NAME (U+L-N), and 0.1 μM H-1152 + 10 μM U-46619 + 100 μM L-NAME (U+L-N+H) (bottom). Data shown are means ± SEM. N = 6. Results were analyzed using Student's unpaired t-test (top) or one-way ANOVA (bottom).

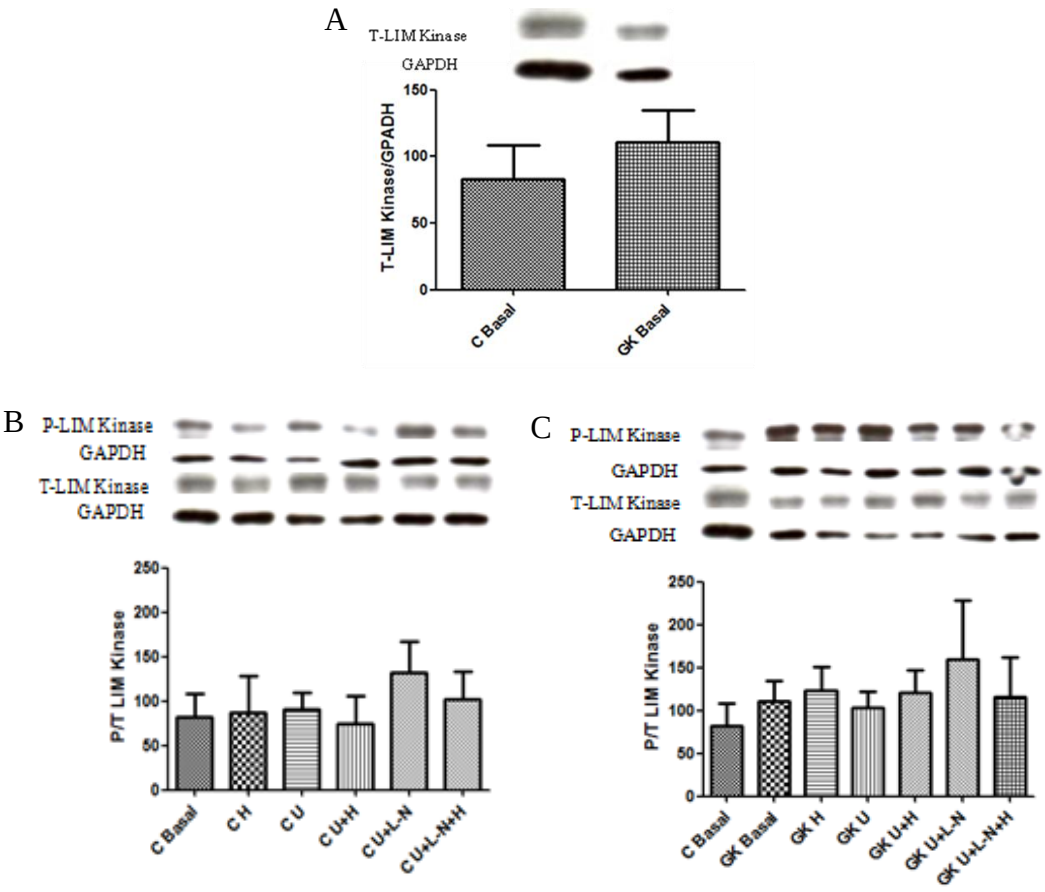

Figure 37: A: Representative Western blot showing total LIM kinase with GAPDH as a loading control (above). Total LIM kinase normalized for corresponding GAPDH in the same blot in untreated (Basal) mesenteric resistance arteries from control (C) and GK rats (bottom). B, C: Representative Western blot showing total and phosphorylated LIM kinase at Thr508/505 with GAPDH as a loading control (above). Ratio of phosphorylated to total LIM kinase normalized for corresponding GAPDH in the same blot in mesenteric resistance arteries from control (C) and GK rats with no treatment (Basal), 0.1 μM H-1152 (H), 10 μM U-46619 (U), 0.1 μM H-1152 + 10 μM U-46619 (U+H), 10 μM U-46619 + 100 μM L-NAME (U+L-N), and 0.1 μM H-1152 + 10 μM U-46619 + 100 μM L-NAME (U+L-N+H) (bottom). Data shown are means ± SEM. N = 6. Results were analyzed using Student's unpaired t-test (top) or one-way ANOVA (bottom).

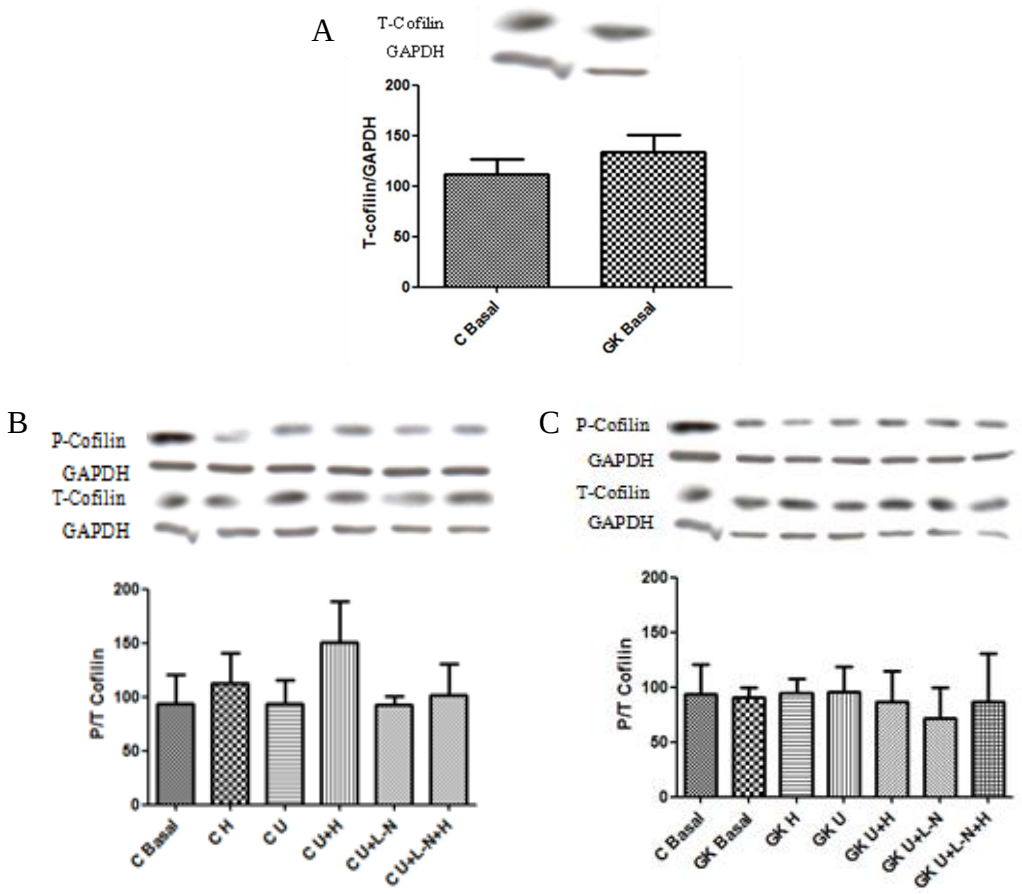

Figure 38: A: Representative Western blot showing total cofilin with GAPDH as a loading control (above). Total cofilin normalized for corresponding GAPDH in the same blot in untreated (Basal) mesenteric resistance arteries from control (C) and GK rats (bottom). B, C: Representative Western blot showing total and phosphorylated cofilin at Ser3 with GAPDH as a loading control (above). Ratio of phosphorylated to total cofilin normalized for corresponding GAPDH in the same blot in mesenteric resistance arteries from control (C) and GK rats with no treatment (Basal), 0.1 μM H-1152 (H), 10 μM U-46619 (U), 0.1 μM H-1152 + 10 μM U-46619 (U+H), 10 μM U-46619 + 100 μM L-NAME (U+L-N), and 0.1 μM H-1152 + 10 μM U-46619 + 100 μM L-NAME (U+L-N+H) (bottom). Data shown are means ± SEM. N = 6. Results were analyzed using Student's unpaired t-test (top) or one-way ANOVA (bottom).

3.6.7 Effect of U-46619 with or without H-1152 on phosphorylation of CPI-17 in mesenteric resistance arteries

To determine whether CPI-17 phosphorylation or activation is directly mediated by ROCK, we measured CPI-17 phosphorylation at Thr38 as an index of its activation. No statistical significant differences were found in basal expression or phosphorylation of CPI-17 between control and GK resistance arteries. Neither treatment with 10 μM U-46619 nor with 0.1 μM H-1152 affected CPI-17 phosphorylation in either control or GK rats (fig. 39). The presence of L-NAME did not alter the effects of U-46619 or H-1152 on CPI-17 phosphorylation in either control or GK rats (fig. 39).

3.7 ACh-induced relaxation in mesenteric resistance arteries from control and GK rats

Endothelial function in mesenteric resistance arteries from control and GK rats was tested by measuring relaxation induced by ACh. The maximum relaxation induced by ACh in arteries from GK animals was slightly less than control, and the dose-response to ACh curve seemed to be slightly shifted to the right (fig. 40). However, there were no statistically significant differences in ACh-induced relaxation between control and GK mesenteric arteries.

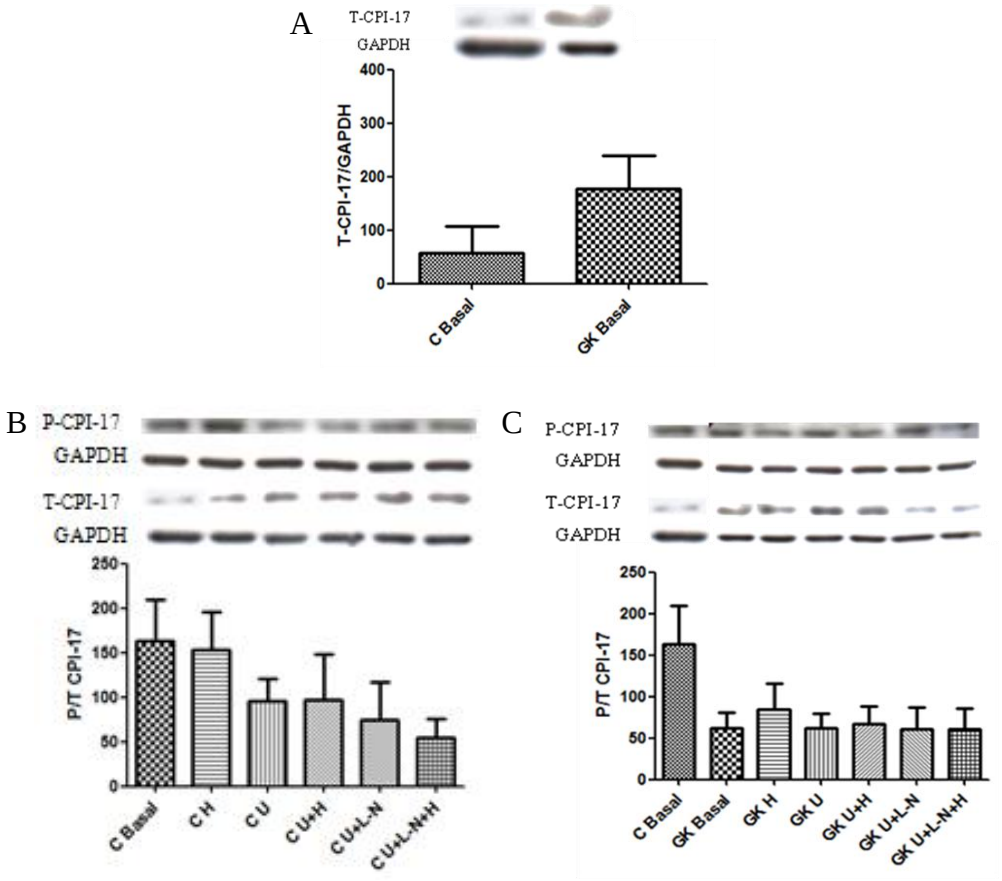

Figure 39: A: Representative Western blot showing total CPI-17 with GAPDH as a loading control (above). Total CPI-17 normalized for corresponding GAPDH in the same blot in untreated (Basal) mesenteric resistance arteries from control (C) and GK rats (bottom). B, C: Representative Western blot showing total and phosphorylated CPI-17 at Thr38 with GAPDH as a loading control (above). Ratio of phosphorylated to total CPI-17 normalized for corresponding GAPDH in the same blot in mesenteric resistance arteries from control (C) and GK rats with no treatment (Basal), 0.1 μM H-1152 (H), 10 μM U-46619 (U), 0.1 μM H-1152 + 10 μM U-46619 (U+H), 10 μM U-46619 + 100 μM L-NAME (U+L-N), and 0.1 μM H-1152 + 10 μM U-46619 + 100 μM L-NAME (U+L-N+H) (bottom). Data shown are means ± SEM. N = 6. Results were analyzed using Student's unpaired t-test (top) or one-way ANOVA (bottom).

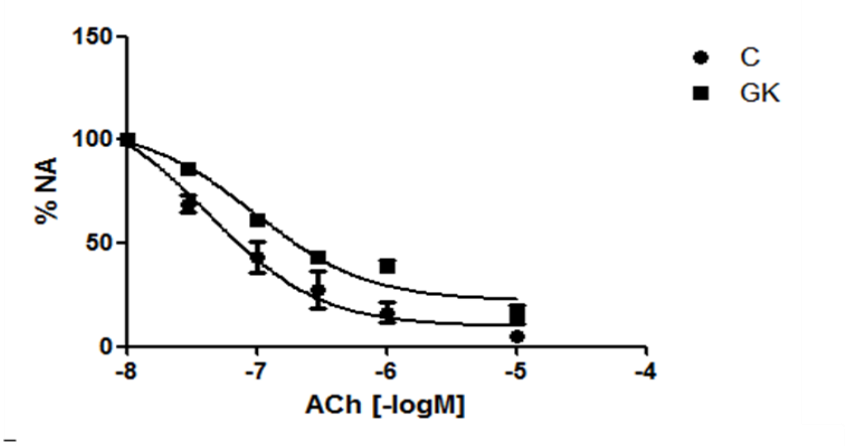

	C	GK
LogEC50	-7.37 ± 0.14	-7.01 ± 0.09
Rmin	5.11 ± 2.47	15.64 ± 2.80

Figure 40: ACh-induced relaxation in mesenteric resistance arteries from control (C) and GK rats. Artery rings were pre-contracted with 3 μM NA. Table shows log EC50 and Rmax derived from non-linear curve fitting of individual concentration-response curves. Data shown are means ± SEM. N = 5. Results were analyzed using Student's unpaired t-test.

Chapter 4: DISCUSSION

Hypertension is one of the major cardiovascular complications associated with diabetes (Tenenbaum, Fisman et al. 1999). It is attributable at least in part to increased vascular smooth muscle tone (Loirand, Guerin et al. 2006). Treatment with ROCK inhibitor has been shown to successfully attenuate contractile responses of vascular smooth muscles and/or phosphorylation of MYPT in arterial tissues from various animal models of hypertension (Mukai, Shimokawa et al. 2001; Weber and Webb 2001; Asano and Nomura 2003; Jin, Ying et al. 2006). Uehata et al. have reported that inhibition of ROCK was able to normalize blood pressure in different animal models of hypertension, and our preliminary studies also showed that elevated blood pressure in GK rats was normalized by ROCK inhibitor, H-1152, together suggesting a role for the RhoA/ROCK pathway in the development of hypertension (Uehata, Ishizaki et al. 1997). A number of studies have demonstrated that agonist-induced vascular smooth muscle contractile responses could be normalized by inhibition of ROCK in isolated arteries from animal models of diabetes, indicating a potential contribution of ROCK to altered vascular contractile function in diabetes (Didion, Lynch et al. 2007; Matsumoto, Kakami et al. 2008; Nuno, Harrod et al. 2009). On the basis of these findings, the major purpose of this study was to determine the contribution of the RhoA/ROCK pathway to the development of diabetes-associated hypertension, and whether this is through enhancing vascular smooth muscle contractile responses to agonist stimulation.

4.1 Mesenteric arteries

Large or superior and small or resistance arteries of rat mesenteric vascular bed are different structurally and functionally. The superior mesenteric arteries are larger arteries that the mesenteric resistance arteries branch out from. The density of smooth muscle cells is higher in small resistance arteries than larger arteries (Pourageaud and De Mey 1997). It has been reported that resistance arteries have tight myoendothelial junctions, which facilitate the transport of substances to the organs (Hwa, Ghibaudi et al. 1994). The superior mesenteric arteries are conduit arteries that are important in supplying blood flow to the intestines, whereas the mesenteric resistance arteries are mainly involved in tissue perfusion (Pourageaud and De Mey 1997). The resistance arteries also play an important role in the cardiovascular system, as they are essential in the peripheral control of blood pressure (Christensen and Mulvany 2001). In general, the recommended size of mesenteric resistance arteries used for contractile measurement is under 400 μM in diameter (Fronhoffs, Mengden et al. 1999; Christensen and Mulvany 2001). Besides their difference in size, superior and small mesenteric arteries also differ in terms of their contractile responses to agonists (Taylor, McCarthy et al. 1992; Budzyn, Paull et al. 2006).

4.2 Control and STZ-diabetic rats

4.2.1 Role of ROCK in agonist-induced contractile responses and changes in protein expression/activity in mesenteric resistance arteries from control rats

We started with PE, a well-known α_1-adrenoceptor agonist, as the agonist to induce contractile responses in mesenteric resistance arteries. α1-Adrenoceptors located in vascular smooth muscle have been shown to play a pivotal role in the regulation of peripheral resistance (Jarajapu, Johnston et al. 2001; Zacharia, Hillier et al. 2004). The concentrations of ROCK inhibitors used in this study were higher than the IC50 values that are suggested to be ROCK selective, but our concentrations were still much lower than the IC50 values for other kinases (Tamura, Nakao et al. 2005). However, the IC50 values were determined in vitro, and it is possible that they may be higher in intact organs. Moreover, the concentrations of ROCK inhibitors used in our study were similar to or even lower than ones used in most of the studies involving ROCK inhibitors. Thus, any effect resulted from treatment with ROCK inhibitor in this project was believed to be mainly through ROCK. We found that either 0.1 μM H-1152 or 1 μM Y-27632 was not able to reduce contractile responses induced by PE in mesenteric resistance arteries from control rats, and that PE did not enhance MYPT phosphorylation or ROCK activity (Sasaki, Suzuki et al. 2002). These results suggest that PE-induced contractile responses in mesenteric resistance arteries from control rats may not be regulated by increased ROCK activity. A study has also reported that the same concentration of Y-27632 did not inhibit PE-induced contraction in mesenteric resistance arteries, which agrees with our findings that in mesenteric resistance arteries, ROCK may not be the major player in the

regulation of PE-induced contraction; however, MYPT phosphorylation was not measured in that study (Budzyn, Paull et al. 2006). In contrast, another study has shown that phosphorylation of MYPT was significantly increased by PE, and that was eliminated by treatment with ROCK inhibitor in rat tail arteries (Tsai and Jiang 2006). Differences observed may be due to different tissue types. Results reported by Budzyn et al. suggested that PKC is important in PE-induced contraction in mesenteric resistance arteries (Budzyn, Paull et al. 2006). Moreover, the Ohanian group has found that treatment with PLC inhibitor significantly attenuated NA-induced contractile responses in rat mesenteric resistance arteries, suggesting that NA-induced contraction in small mesenteric arteries may be regulated by the PLC/PKC pathway (Clarke, Forman et al. 2008). Another study done by the Ohanian group has suggested that tyrosine phosphorylation of paxillin and the ERK pathway are also important in NA-induced contraction in rat mesenteric small arteries (Ward, Alder et al. 2002). These imply that pathways other than the RhoA/ROCK pathway may play a role in regulating contraction induced by α_1 stimulation in rat mesenteric resistance arteries.

Interestingly, contraction induced by the thromboxane A_2 mimetic, U-46619, in mesenteric resistance arteries from control animals was significantly attenuated by inhibition of ROCK. In addition, phosphorylation of MYPT was also substantially enhanced by U-46619, and it was normalized by ROCK inhibitor. These together indicate that U-46619-induced contractile responses in mesenteric resistance arteries were likely to be mediated at least in part by increased ROCK activity. These results also suggest that the concentration of ROCK inhibitor we used was sufficient enough to inhibit ROCK activity. Tsai et al. have reported that U-46619 increased contraction as well as MYPT

phosphorylation in rat tail artery smooth muscle, and this was inhibited by ROCK inhibitor, suggesting the regulation of contractile responses by ROCK, which is consistent with our findings (Tsai and Jiang 2006). Another study has also shown that U-46619-induced contractile responses were normalized by ROCK inhibitor in mesenteric resistance arteries from Ang II-induced hypertensive rats, further suggesting the involvement of ROCK in U-46619-induced contraction in mesenteric resistance arteries (Hilgers, Todd et al. 2007). Stimulation of thromboxane A_2 receptor by U-46619 has been shown to couple to $G\alpha_q$ as well as $G\alpha_{12/13}$, resulting in the activation of the RhoA/ROCK pathway (Honma, Saika et al. 2006). $G\alpha_q$ stimulation not only leads to the activation of the RhoA/ROCK pathway, but also the PLC pathway, leading to subsequent activation of PKC. $G\alpha_{12/13}$ stimulation on the other hand, activates only the RhoA/ROCK pathway (Somlyo and Somlyo 2003). Therefore, it is possible that in rat mesenteric resistance arteries, contractions induced by U-46619 were mainly through activation of ROCK, whereas contractions induced by PE were mostly through activation of the PLC and subsequent PKC pathway, since activated α_1-adrenoceptors couple to $G\alpha_q$.

Previous studies from our lab have shown increased RhoA expression in hearts from STZ-diabetic rats compared to control rats. In this study, we wanted to see whether RhoA expression is also upregulated in vasculature tissues from STZ-diabetic rats. Our results suggest that unlike in cardiac tissues from STZ-diabetic rats, RhoA expression was not higher in mesenteric resistance arteries compared to control rats. RhoA phosphorylation at Ser188, as mentioned, enhances the interaction with GDI, which promotes its inactivation (Ellerbroek, Wennerberg et al. 2003). Kitazawa et al. has reported that PE significantly attenuated Ser188 phosphorylation in RhoA in rabbit femoral arteries,

suggesting that RhoA phosphorylation can be regulated by agonist stimulation (Kitazawa, Semba et al. 2009). Thus, we determined whether PE had any effect on RhoA phosphorylation at Ser188 in mesenteric resistance arteries. Based on our results, PE did not alter phosphorylation of RhoA in mesenteric resistance arteries from control animals. The Loirand group has reported that RhoA was phosphorylated at Ser188 by NO/cGMP-dependent protein kinase (PKG), leading to the inactivation of RhoA (Sauzeau, Le Jeune et al. 2000). Moreover, phosphorylation of Ser188 in RhoA has also been suggested to be mediated by cAMP-dependent protein kinase (PKA) (Lang, Gesbert et al. 1996). These suggest that PKA and PKG may be the major proteins in the regulation of RhoA phosphorylation. On the other hand, ROCK inhibitor also did not affect RhoA phosphorylation in mesenteric resistance arteries from control animals. Since RhoA is upstream of ROCK, it is possible that inhibiting its downstream target ROCK has no effect on its phosphorylation.

Activation of PKC is first initiated by phosphorylation of multiple phosphorylation motifs to achieve catalytic competence, followed by the binding of DAG and Ca^{2+} (only in conventional PKCs) to the regulatory domains to fully activate the enzyme by inducing its translocation to the plasma membrane (Carmena and Sardini 2007). Therefore, we measured PKC phosphorylation as an index of activation to investigate whether PKC is activated by PE. A study published from our lab has suggested that PKC-ε is activated by NA, and this is likely to contribute to NA-induced contraction in mesenteric arteries (Mueed, Zhang et al. 2005). Hence, we chose to examine this particular PKC isoform. Phosphorylation of PKC-ε was not increased by PE, suggesting that PKC is not likely to contribute to PE-induced contraction in rat mesenteric resistance arteries. To confirm this,

we then investigated a downstream effector of PKC, CPI-17, which is a known MLCP inhibitor that promotes MLC phosphorylation and thereby vascular smooth muscle contraction (Somlyo and Somlyo 2003). Our results showed that CPI-17 phosphorylation or activation also did not increase in response to PE, further suggesting that the PKC/CPI-17 pathway may not play a role in PE-induced contraction in mesenteric resistance arteries from control rats.

As introduced earlier, actin polymerization has been implicated in PE-induced vascular smooth muscle contraction through a ROCK-mediated mechanism (Tsai and Jiang 2006). Thus, we were interested in examining the role of actin polymerization in PE-induced contractile responses in mesenteric resistance arteries. We found that the ratio of F- to G-actin as a measure of actin polymerization was increased by PE, and it was normalized by ROCK inhibitor, suggesting that this process is ROCK mediated. However, the same concentration of ROCK inhibitor did not block PE-induced contraction in mesenteric resistance arteries, indicating that any effect of ROCK on actin cytoskeleton may not be contributing to contractile responses induced by PE in mesenteric resistance arteries.

4.2.2 Role of ROCK in agonist-induced contractile responses and changes in protein expression/activity in mesenteric resistance arteries from STZ-diabetic rats

A study done by Makino and Kamata has shown that the contractile responses to α_1 agonist methoxamine in endothelium denuded mesenteric resistance artery was attenuated in STZ-diabetic compared to control rats, indicating an impairment in vascular

smooth muscle contractility in mesenteric resistance arteries from STZ-diabetic rats (Makino and Kamata 1998). Moreover, Lee et al. have reported diminished contraction induced by α_1 stimulation in endothelium denuded mesenteric resistance arteries from hypotensive STZ-diabetic rats (Lee, Bahk et al. 2011). On the other hand, in mesenteric resistance arteries with intact endothelium from STZ-diabetic rats, NA-induced contractile responses have been reported to be enhanced compared to control rats, and treatment with L-NAME, a NOS inhibitor, dramatically increased contractile responses to NA in control but not in STZ-diabetic rats (Taylor, Oon et al. 1994). This suggests that the enhanced contractile responses to NA in mesenteric resistance arteries from STZ-diabetic rats is likely to be due to impaired NO production or endothelial function (Taylor, Oon et al. 1994). In our study, we also observed a slightly reduced contraction in response to PE in endothelium-denuded mesenteric resistance arteries from STZ-diabetic rats; however, this was not statistically significant. In general, due to individual differences, such as health status, among different animals, studies involving animals usually face large variation, resulting in relatively large standard errors. This may have contributed to our failure to find significant differences among data in this study.

Similar to control rats, PE-induced contraction in mesenteric resistance arteries was not likely to be modulated by ROCK. As was found in arteries from control rats, contractile responses induced by U-46619 in mesenteric resistance arteries from STZ-rats seemed to be mediated by ROCK, but the study did not have enough power to show any statistical significance.

4.2.3 Role of ROCK in agonist-induced contractile responses and changes in protein expression/activity in superior mesenteric arteries from control rats

Preliminary results from our lab have suggested that PE-induced contractile responses in rat superior mesenteric arteries were sensitive to ROCK inhibition. Therefore, we wanted to confirm these results. Consistently, we found that PE-induced contraction in superior mesenteric arteries from control rats was significantly attenuated by the same concentration of ROCK inhibitor used in mesenteric resistance arteries, suggesting the involvement of ROCK in PE-induced contraction in superior mesenteric arteries. The results are supported by a study done by Budzyn et al., in that PE-induced contraction in superior mesenteric arteries but not in mesenteric resistance arteries was sensitive to ROCK inhibition (Budzyn, Paull et al. 2006). Surprisingly, ROCK activity measured as MYPT phosphorylation was not increased by PE in superior mesenteric arteries from control rats. A time course experiment revealed that MYPT phosphorylation already seemed to be at peak after treatment with PE for 5 minutes, so the reason for the discrepancy we encountered remains unclear. One possibility is that the artery rings used for Western blotting analysis were different from those used in the wire myograph

apparatus. The artery rings used for contraction measurement were under tension and endothelium denuded, whereas those isolated for Western blotting had intact endothelium and were not stretched.

Mueed et al. have reported that NA-induced contractile responses in superior mesenteric arteries were reduced by PKC inhibitor, and NA also increased particulate levels or translocation (an index of activation) of PKC-ε and –α (only in diabetic rats), together suggesting regulation by PKC. Therefore, we measured PKC activation in superior mesenteric arteries to test whether PKC plays a role in PE-induced contractile responses. Our results showed that phosphorylation of PKC-α and -ε as an index of activation was not increased by PE in superior mesenteric arteries from control rats. Again, the discrepancy may be due to different ways of sample processing for Western blotting analysis. Also, phosphorylation of PKC may not be a good measure of short-term PKC activation, as phosphorylated PKC is competent for activation but only activated when translocated to the plasma membranes (Carmena and Sardini 2007). In fact, most of studies determined agonist-induced or short-term PKC activation by measuring particulate levels of PKC, whereas phosphorylation of PKC was rarely used as a measure of PKC activation (Wang, Rolfe et al. 2003; Turrell, Rodrigo et al. 2011).

4.2.4 Role of ROCK in agonist-induced contractile responses and changes in protein expression/activity in superior mesenteric arteries from STZ-diabetic rats

Contractile responses induced by PE in superior mesenteric arteries from STZ-diabetic rats were not reduced by inhibition of ROCK. This is likely to be due to a low

number of animals used in the study as there was lot of variation. Our previous study has also shown increased contraction induced by α_1 stimulation in superior mesenteric arteries from STZ-diabetic rats compared to those from control rats (Mueed, Zhang et al. 2005). A recent study has reported that contractile responses induced by α_1 stimulation in endothelium denuded mesenteric resistance arteries from hypotensive STZ-diabetic rats were reduced, where the α_1 stimulation-induced contraction in superior mesenteric arteries was increased (Lee, Bahk et al. 2011). These results suggest a difference in agonist-induced contraction between superior and small mesenteric arteries, and this difference may be caused by the involvement of different types of vessels in blood pressure regulation. Since the small mesenteric arteries have been implicated in peripheral control of blood pressure, it is possible that the reduced agonist-induced contraction in these arteries reflect the hypotensive characteristic of STZ-diabetic rats. Our results agree with these previous findings reported from other studies that contractile responses induced by α_1 stimulation were different in mesenteric resistance from superior arteries. However, the enhancement of PE-induced contractile responses in superior mesenteric arteries from STZ-diabetic rats was not statistically significant, again perhaps because the study did not have enough power.

The enhancement in contractile responses induced by NA in superior mesenteric arteries from STZ-diabetic rats has been shown to be associated with an increase in NA-induced particulate levels of PKC-α and -ε (Mueed, Zhang et al. 2005). Activation of PKC isoforms measured as phosphorylation in our study was not augmented by PE in superior mesenteric arteries from STZ-diabetic rats. As discussed above, phosphorylation of PKC may not be a good measure of acute PKC activation.

4.3 Control and GK rats

4.3.1 Main characteristics of control and GK rats

The STZ-diabetic rat model has been used extensively in our lab. Based on our previous work, the body weight of STZ-diabetic rats generally was only almost 50% of control rats, and they had an average glucose level of 25 mM. Similar to STZ-diabetic rats, the body weight of GK rats was significantly lower compared to corresponding control rats. The average glucose and insulin levels of GK rats were significantly higher than that of control rats throughout the time of the study, which is consistent with the GK rat model being a type 2 diabetic model.

Over the whole period of study, GK rats consistently had substantially higher blood pressure compared to control rats, which agrees with our previous studies as well as other reports that GK rats were mild hypertensive (Witte, Jacke et al. 2002; Gronholm, Cheng et al. 2005). To investigate whether the elevation in blood pressure in GK rats was due to increased ROCK activity, we treated them with a well known ROCK inhibitor, fasudil, for one week. Our results showed that one week treatment with fasudil significantly normalized blood pressure in GK rats to control levels, suggesting that the elevation in blood pressure in GK rats was mainly due to increased ROCK pathway.

4.3.2 Contribution of the RhoA/ROCK pathway to elevated blood pressure in GK rats

Surprisingly, the degree of contractile responses induced by either PE or U-46619 in GK mesenteric resistance arteries was similar to that in control, although GK rats exhibited mild hypertension. Moreover, opposite to what we observed in our preliminary studies, ROCK and RhoA expression in mesenteric resistance arteries was similar between control and GK rats, and no differences were found in basal MYPT or MLC phosphorylation in mesenteric resistance arteries between control and GK rats. These results do not support the conclusion that elevated blood pressure in GK rats was due to enhanced RhoA/ROCK pathway, at least in the mesenteric resistance arteries. The concentration of fasudil used in this study was high, at least within the first hour after administration, which could potentially inhibit other pathways, as fasudil at a high concentration has been found to be non-selective toward other kinases (Tamura, Nakao et al. 2005). Alternatively, it has been shown that RhoA expression and ROCK activity in brainstem from spontaneously hypertensive rats (SHR) were increased compared to control rats, and that either microinjection of ROCK inhibitor or adenovirus vector encoding dominant-negative ROCK was able to decrease blood pressure, heart rate, and renal sympathetic nerve activity in both animal groups but to a greater extent in SHRs (Ito, Hirooka et al. 2003). Results from that study suggest that the RhoA/ROCK pathway in brainstem may contribute to the regulation of blood pressure via the sympathetic nerve system; however, specific mechanisms remain unknown (Ito, Hirooka et al. 2003). It is also worthwhile to point out that our studies were done in vitro, which did not perfectly resemble the in vivo environment. Factors such as fats, connective tissues and growth

hormones, normally present under physiological conditions, were not present in vitro, which may have contributed to the discrepancy that we encountered.

4.3.3 Role of ROCK in PE-induced contractile responses and changes in protein expression/activity in mesenteric resistance arteries from control and GK rats

Different from earlier studies, the endothelium remained intact in these animals. The removal of endothelium was found incomplete sometimes, as some vessels still responded to ACh. In this study, we used a non-selective NOS inhibitor, L-NAME, to block the synthesis of NO. Evidence suggests that NO is the major player involved in endothelium-dependent relaxation in superior mesenteric arteries, whereas in mesenteric resistance arteries, other factors known as endothelium-derived hyperpolarizing factors (EDHFs) may play an important role in relaxation (Hwa, Ghibaudi et al. 1994). However, relaxation mediated by NO but not EDHF was reduced in mesenteric resistance arteries from rat models of renovascular hypertension (Christensen, Stankevicius et al. 2007). Moreover, reduction in NO release has also been evidenced in mesenteric resistance arteries from diabetic mice (Lagaud, Masih-Khan et al. 2001). These indicate an impairment in NO but not EDHF production or activity in mesenteric resistance arteries from animal models of hypertension or diabetes. Therefore, by blocking NO production, any potential differences in contribution of NO to contractile responses in mesenteric resistance arteries would be eliminated. Similar to before, PE-induced contractile responses in mesenteric resistance arteries from control rats were not attenuated by either 0.1 μM H-1152 or 1 μM Y-27632 in the presence of L-NAME. We did not measure

MYPT phosphorylation in response to PE due to limited number animals. Therefore, ROCK activity was not determined to confirm the involvement of ROCK in PE-induced contraction in mesenteric resistance arteries from control rats.

Interestingly, PE-induced contractile responses in mesenteric resistance arteries from GK rats were inhibited by either 0.1 μM H-1152 or 1 μM Y-27632 in the presence of L-NAME, indicating a contribution of ROCK to PE-induced contraction in mesenteric resistance arteries from GK rats. The results suggest that unlike in control rats, PE-induced contractile responses in mesenteric arteries from GK rats were likely to be mediated in part by increased ROCK activity. However, ROCK activity was not measured due to a small number of animals.

4.3.4 Role of ROCK in U-46619-induced contractile responses and changes in protein expression/activity in mesenteric resistance arteries from control rats

Surprisingly, U-46619-induced contractile responses in mesenteric resistance arteries from control rats were no longer blocked by ROCK inhibition in the presence of L-NAME. It is possible that endothelium was not removed completely from mesenteric resistance arteries in earlier experiments, and that in the absence of NO, U-46619-induced contraction in control mesenteric arteries became insensitive to ROCK inhibition. It has been reported that Y-27632 enhanced eNOS phosphorylation at Ser1177 as well as Akt phosphorylation at Ser473 in human umbilical vein endothelial cells [44]. Phosphorylation of Ser1177 in eNOS is required for its activation (Fulton, Gratton et al. 2001). Thus, ROCK inhibitor could have attenuated U-46619-induced contractile

responses by increasing eNOS phosphorylation/activation and thereby increasing NO availability in mesenteric resistance arteries from control rats; this effect would be lost in the presence of L-NAME. However, this explanation is not consistent with our observation that phosphorylation of eNOS at Ser1177 was not increased by H-1152 in mesenteric resistance arteries from control rats. Furthermore, the magnitude of contraction induced by U-46619 was similar between endothelium-denuded and L-NAME treated arteries from control rats, suggesting a similar degree of NO removal by endothelium denudation and L-NAME treatment. Interestingly, H-1152 still attenuated U-46619-induced MYPT phosphorylation in the presence of L-NAME in mesenteric resistance arteries from control rats. The discrepancy between contractile responses and MYPT phosphorylation may be because the artery rings used for Western blotting were not those used for contractile measurement in the wire myograph; they were treated differently, as the artery rings in myograph chambers were under tension, so that the biochemical results may not truly reflect the contractile responses. Also, in the presence of L-NAME, the contractile responses but not MYPT phosphorylation induced by U-46619 were robustly increased in control animals, indicating that the enhancement in agonist-induced contraction by treatment with L-NAME may not be through increasing MLCP phosphorylation or ROCK activity. It has been known that NO can induce vascular smooth muscle relaxation by numerous pathways including reduction of intracellular Ca^{2+} (Lowenstein, Dinerman et al. 1994). Hence, enhancement in agonist-induced contraction in the absence of NO is not necessarily through increased ROCK activity.

We then measured phosphorylation of MLC, a downstream target of MLCP, to further investigate the involvement of ROCK in U-46619-induced contractile responses in mesenteric resistance arteries from control rats. Phosphorylation of MLC has been shown to promote contraction in vascular smooth muscle cells (Somlyo and Somlyo 2003). Interestingly, despite the increase in MYPT phosphorylation produced by U-46619, there was no significant increase in the phosphorylation of MLC at the ser19 site. This may be due to technical difficulties in obtaining Western blotting results of MLC phosphorylation. Moreover, it has been reported that ROCK can enhance phosphorylation of MLC at both Ser19 and Thr18 sites either directly or indirectly by inhibiting MLCP (Amano, Ito et al. 1996; Getz, Dangelmaier et al. 2010). Therefore, it is possible that MLC phosphorylation at Thr18 but not Ser19 was augmented by U-46619.

As mentioned earlier, Ser188 in RhoA can be phosphorylated by the NO/PKG pathway (Sauzeau, Le Jeune et al. 2000). In our study, we did not observe any changes in RhoA phosphorylation in the absence of NO achieved by treatment with L-NAME. This suggests that RhoA phosphorylation may not be regulated by NO in mesenteric resistance arteries from control rats. Similar to PE, U-46619 also did not affect phosphorylation of RhoA in mesenteric resistance arteries from control rats.

We then measured phosphorylation of LIM kinase and cofilin, two major proteins involved in actin polymerization pathway to investigate the contribution of actin polymerization to U-46619-induced contractile responses in mesenteric resistance arteries. Neither phosphorylation of LIM kinase nor cofilin was increased by stimulation with U-46619 or decreased by H-1152, implying that in mesenteric resistance arteries from control rats, actin polymerization may not contribute to U-46619-inudced contraction.

We measured CPI-17 phosphorylation or activation to determine the involvement of the PKC/CPI-17 pathway in U-46619-induced contractile responses in mesenteric resistance arteries. The PKC/CPI-17 pathway has been implicated in agonist-induced contractile responses in mesenteric resistance arteries (Budzyn, Paull et al. 2006; Clarke, Forman et al. 2008). In this study, phosphorylation of CPI-17 was not increased by U-46619, suggesting that the PKC/CPI-17 may not play a role in U-46619-induced contractile responses in mesenteric resistance arteries from control rats. Similar observations have been found in a study from Tsai et al., in that U-46619 also did not promote CPI-17 phosphorylation in rat tail artery smooth muscles (Tsai and Jiang 2006). Treatment with H-1152 did not affect CPI-17 phosphorylation in resistance arteries, implying that CPI-17 phosphorylation or activation is not ROCK-mediated.

4.3.5 Role of ROCK in U-46619-induced contractile responses and changes in protein expression/activity in mesenteric resistance arteries from GK rats

Interestingly, unlike in control rats, U-46619-induced contractile responses in mesenteric resistance arteries from GK rats were sensitive to ROCK inhibition in the presence of L-NAME. Furthermore, MYPT phosphorylation as a measure of ROCK activity was increased by U-46619 both in the absence and presence of L-NAME compared to basal MYPT phosphorylation, and this was attenuated by ROCK inhibitor. These suggest that U-46619-induced contraction in mesenteric resistance arteries from GK rats in the presence of L-NAME was likely to be mediated by ROCK through enhanced MLCP activity. Although the degree of MYPT phosphorylation induced by U-

46619 in GK rats was not greater than in control rats, it is possible that the response of mesenteric arteries from GK rats to U-46619 was more dependent on ROCK activity than that of arteries from control animals.

Similar to control rats, MLC phosphorylation at Ser19 was not enhanced by U-46619 in mesenteric resistance arteries from GK rats. However, H-1152 significantly attenuated basal MLC phosphorylation, implying that basal phosphorylation of MLC is regulated by ROCK in mesenteric resistance arteries from GK rats.

4.3.6 Endothelial function in mesenteric resistance arteries from control and GK rats

Endothelial dysfunction has been observed in mesenteric arterial rings from GK rats (Cheng, Vaskonen et al. 2001). Therefore, in this study, we wanted to test endothelial function in control and GK rats by comparing relaxation induced by ACh. We observed a small reduction in ACh-induced relaxation in GK mesenteric resistance arteries, indicating a slightly impaired endothelial function in GK rats. However, this reduction was not statistically significant.

Interestingly, the degree of increase in agonist-induced contractile responses by L-NAME in mesenteric resistance arteries was the same between control and GK groups, suggesting that the involvement of NO in contraction is similar between control and GK animals. This was further supported by similar levels of eNOS phosphorylation between control and GK rats. Furthermore, a study has reported that basal NOS activity in mesenteric resistance arteries was similar between control and GK animals (Matsumoto, Ishida et al. 2009). These results indicate that the contribution of NO to agonist-induced

contractile responses in mesenteric resistance arteries may be similar between control and GK rats.

4.4 Summary and conclusions

In this thesis, we focused on the contribution of the RhoA/ROCK pathway in vascular smooth muscle contractility in diabetes-associated hypertension. We have concluded the following main points:

1. Contractile responses induced by PE in superior mesenteric arteries were more likely to be mediated by ROCK as compared to those in mesenteric resistance arteries.
2. Contractile responses induced by U-46619 in mesenteric resistance arteries may be through increased ROCK activity.
3. The PKC/CPI-17 pathway may not play a role in agonist-induced contraction in mesenteric resistance or superior arteries from control or STZ-diabetic rats, but phosphorylation of PKC may not be a good measure of PKC activation in response to agonist stimulation.
4. The effects of ROCK on actin cytoskeleton are not likely to contribute to PE-induced contractile responses in mesenteric resistance arteries from control rats.
5. Fasudil normalized elevated blood pressure in GK rats, suggesting that hypertension in GK rats was due to increased ROCK activity. However, contractile responses and ROCK expression and activity in GK rats were not increased compared to those in control rats. The reason for this discrepancy remains unclear. Based a previous report, it may be

possible that the RhoA/ROCK pathway in brainstem regulates blood pressure via sympathetic nerve activity.

6. PE- or U-46619-induced contractile responses in the presence of L-NAME in mesenteric resistance arteries from GK rats were likely to be mediated by ROCK.

Based on our findings from the GK rat study, our hypothesis that activation of the RhoA/ROCK pathway contributes to the development of diabetes-associated hypertension in GK rats by enhancing vascular smooth muscle contractile responses is not supported.

4.5 Future directions

1. To further investigate the effects of fasudil on blood pressure, vascular smooth muscle contractile responses, and protein expression/activity changes in diabetic animals, a more ROCK selective ROCK inhibitor is needed.
2. Phosphorylation of Thr18 in MLC in response to agonist stimulation should also be measured.
3. Particulate levels of PKC isoforms should be considered as a measure of their activation. Alternatively, a commercially available kit, which is based on the ability of PKC to phosphorylate a synthetic peptide substrate, may be used to measure PKC isoform activity.
4. To further confirm the involvement of actin polymerization in U-46619-induced contractile responses in mesenteric resistance arteries from GK rats, F- to G-actin ratio should be measured, as it directly reflects the degree of actin polymerization.

REFERENCE

Abebe, W., K. H. Harris, et al. (1990). "Enhanced contractile responses of arteries from diabetic rats to alpha 1-adrenoceptor stimulation in the absence and presence of extracellular calcium." J Cardiovasc Pharmacol **16**(2): 239-248.

Abebe, W. and K. M. MacLeod (1991). "Enhanced arterial contractility to noradrenaline in diabetic rats is associated with increased phosphoinositide metabolism." Can J Physiol Pharmacol **69**(3): 355-361.

Aittaleb, M., C. A. Boguth, et al. (2010). "Structure and function of heterotrimeric G protein-regulated Rho guanine nucleotide exchange factors." Mol Pharmacol **77**(2): 111-125.

Amano, M., K. Chihara, et al. (1999). "The COOH terminus of Rho-kinase negatively regulates rho-kinase activity." J Biol Chem **274**(45): 32418-32424.

Amano, M., Y. Fukata, et al. (2000). "Regulation and functions of Rho-associated kinase." Exp Cell Res **261**(1): 44-51.

Amano, M., M. Ito, et al. (1996). "Phosphorylation and activation of myosin by Rho-associated kinase (Rho-kinase)." J Biol Chem **271**(34): 20246-20249.

Asano, M. and Y. Nomura (2003). "Comparison of inhibitory effects of Y-27632, a Rho kinase inhibitor, in strips of small and large mesenteric arteries from spontaneously hypertensive and normotensive Wistar-Kyoto rats." Hypertens Res **26**(1): 97-106.

Banting, F. G., C. H. Best, et al. (1922). "Pancreatic Extracts in the Treatment of Diabetes Mellitus." Can Med Assoc J **12**(3): 141-146.

Bernard, O. (2007). "Lim kinases, regulators of actin dynamics." Int J Biochem Cell Biol **39**(6): 1071-1076.

Bernards, A. and J. Settleman (2004). "GAP control: regulating the regulators of small GTPases." Trends Cell Biol **14**(7): 377-385.

Bos, J. L., H. Rehmann, et al. (2007). "GEFs and GAPs: critical elements in the control of small G proteins." Cell **129**(5): 865-877.

Brondum, E., H. Kold-Petersen, et al. (2008). "Increased contractility to noradrenaline and normal endothelial function in mesenteric small arteries from the Goto-Kakizaki rat model of type 2 diabetes." J Physiol Sci **58**(5): 333-339.

Broustas, C. G., N. Grammatikakis, et al. (2002). "Phosphorylation of the myosin-binding subunit of myosin phosphatase by Raf-1 and inhibition of phosphatase activity." J Biol Chem **277**(4): 3053-3059.

Budzyn, K., P. D. Marley, et al. (2006). "Targeting Rho and Rho-kinase in the treatment of cardiovascular disease." Trends Pharmacol Sci **27**(2): 97-104.

Budzyn, K., M. Paull, et al. (2006). "Segmental differences in the roles of rho-kinase and protein kinase C in mediating vasoconstriction." J Pharmacol Exp Ther **317**(2): 791-796.

Bugger, H. and E. D. Abel (2009). "Rodent models of diabetic cardiomyopathy." Dis Model Mech **2**(9-10): 454-466.

Carmena, D. and A. Sardini (2007). "Lifespan regulation of conventional protein kinase C isotypes." Biochem Soc Trans **35**(Pt 5): 1043-1045.

Cenni, V., H. Doppler, et al. (2002). "Regulation of novel protein kinase C epsilon by phosphorylation." Biochem J **363**(Pt 3): 537-545.

Chen, X., K. Pavlish, et al. (2006). "Effects of chronic portal hypertension on agonist-induced actin polymerization in small mesenteric arteries." Am J Physiol Heart Circ Physiol **290**(5): H1915-1921.

Chen, Y. H., M. X. Chen, et al. (1994). "Molecular cloning of cDNA encoding the 110 kDa and 21 kDa regulatory subunits of smooth muscle protein phosphatase 1M." FEBS Lett **356**(1): 51-55.

Cheng, X., X. S. Cheng, et al. (2004). "Inhibition of iNOS augments cardiovascular action of noradrenaline in streptozotocin-induced diabetes." Cardiovasc Res **64**(2): 298-307.

Cheng, Z. J., T. Vaskonen, et al. (2001). "Endothelial dysfunction and salt-sensitive hypertension in spontaneously diabetic Goto-Kakizaki rats." Hypertension **37**(2 Part 2): 433-439.

Chitaley, K., D. Weber, et al. (2001). "RhoA/Rho-kinase, vascular changes, and hypertension." Curr Hypertens Rep **3**(2): 139-144.

Christensen, F. H., E. Stankevicius, et al. (2007). "Flow- and acetylcholine-induced dilatation in small arteries from rats with renovascular hypertension--effect of tempol treatment." Eur J Pharmacol **566**(1-3): 160-166.

Christensen, K. L. and M. J. Mulvany (2001). "Location of resistance arteries." J Vasc Res **38**(1): 1-12.

Cipolla, M. J., N. I. Gokina, et al. (2002). "Pressure-induced actin polymerization in vascular smooth muscle as a mechanism underlying myogenic behavior." FASEB J **16**(1): 72-76.

Clarke, C. J., S. Forman, et al. (2008). "Phospholipase C-delta1 modulates sustained contraction of rat mesenteric small arteries in response to noradrenaline, but not endothelin-1." Am J Physiol Heart Circ Physiol **295**(2): H826-834.

Collado-Mesa, F., H. M. Colhoun, et al. (1999). "Prevalence and management of hypertension in type 1 diabetes mellitus in Europe: the EURODIAB IDDM Complications Study." Diabet Med **16**(1): 41-48.

Corteling, R. L., S. E. Brett, et al. (2007). "The functional consequence of RhoA knockdown by RNA interference in rat cerebral arteries." Am J Physiol Heart Circ Physiol **293**(1): H440-447.

Del Valle, G. O., C. D. Adair, et al. (1997). "Interpretation of the TDx-FLM fluorescence polarization assay in pregnancies complicated by diabetes mellitus." Am J Perinatol **14**(5): 241-244.

Didion, S. P., C. M. Lynch, et al. (2005). "Impaired endothelium-dependent responses and enhanced influence of Rho-kinase in cerebral arterioles in type II diabetes." Stroke **36**(2): 342-347.

Didion, S. P., C. M. Lynch, et al. (2007). "Cerebral vascular dysfunction in TallyHo mice: a new model of Type II diabetes." Am J Physiol Heart Circ Physiol **292**(3): H1579-1583.

Dong, M., B. P. Yan, et al. (2010). "Rho-kinase inhibition: a novel therapeutic target for the treatment of cardiovascular diseases." Drug Discov Today **15**(15-16): 622-629.

El-Omar, M. M., Z. K. Yang, et al. (2004). "Cardiac dysfunction in the Goto-Kakizaki rat. A model of type II diabetes mellitus." Basic Res Cardiol **99**(2): 133-141.

Ellerbroek, S. M., K. Wennerberg, et al. (2003). "Serine phosphorylation negatively regulates RhoA in vivo." J Biol Chem **278**(21): 19023-19031.

Feng, J., M. Ito, et al. (1999). "Rho-associated kinase of chicken gizzard smooth muscle." J Biol Chem **274**(6): 3744-3752.

Fronhoffs, S., T. Mengden, et al. (1999). "Cholesterol enhances contractile responses in isolated small mesenteric arteries of normotensive and spontaneously hypertensive rats." J Hypertens **17**(12 Pt 2): 1941-1947.

Fulton, D., J. P. Gratton, et al. (2001). "Post-translational control of endothelial nitric oxide synthase: why isn't calcium/calmodulin enough?" J Pharmacol Exp Ther **299**(3): 818-824.

Getz, T. M., C. A. Dangelmaier, et al. (2010). "Differential phosphorylation of myosin light chain (Thr)18 and (Ser)19 and functional implications in platelets." J Thromb Haemost **8**(10): 2283-2293.

Gong, M. C., A. Fuglsang, et al. (1992). "Arachidonic acid inhibits myosin light chain phosphatase and sensitizes smooth muscle to calcium." J Biol Chem **267**(30): 21492-21498.

Grassie, M. E., L. D. Moffat, et al. (2011). "The myosin phosphatase targeting protein (MYPT) family: A regulated mechanism for achieving substrate specificity of the catalytic subunit of protein phosphatase type 1delta." Arch Biochem Biophys **510**(2): 147-159.

Gronholm, T., Z. J. Cheng, et al. (2005). "Vasopeptidase inhibition has beneficial cardiac effects in spontaneously diabetic Goto-Kakizaki rats." Eur J Pharmacol **519**(3): 267-276.

Grundy, S. M., I. J. Benjamin, et al. (1999). "Diabetes and cardiovascular disease: a statement for healthcare professionals from the American Heart Association." Circulation **100**(10): 1134-1146.

Gunst, S. J. and W. Zhang (2008). "Actin cytoskeletal dynamics in smooth muscle: a new paradigm for the regulation of smooth muscle contraction." Am J Physiol Cell Physiol **295**(3): C576-587.

Hattori, T., H. Shimokawa, et al. (2004). "Long-term inhibition of Rho-kinase suppresses left ventricular remodeling after myocardial infarction in mice." Circulation **109**(18): 2234-2239.

Hilgers, R. H., J. Todd, Jr., et al. (2007). "Increased PDZ-RhoGEF/RhoA/Rho kinase signaling in small mesenteric arteries of angiotensin II-induced hypertensive rats." J Hypertens **25**(8): 1687-1697.

Hoffman, G. R., N. Nassar, et al. (2000). "Structure of the Rho family GTP-binding protein Cdc42 in complex with the multifunctional regulator RhoGDI." Cell **100**(3): 345-356.

Honma, S., M. Saika, et al. (2006). "Thromboxane A2 receptor-mediated G12/13-dependent glial morphological change." Eur J Pharmacol **545**(2-3): 100-108.

Horowitz, A., C. B. Menice, et al. (1996). "Mechanisms of smooth muscle contraction." Physiol Rev **76**(4): 967-1003.

Hwa, J. J., L. Ghibaudi, et al. (1994). "Comparison of acetylcholine-dependent relaxation in large and small arteries of rat mesenteric vascular bed." Am J Physiol **266**(3 Pt 2): H952-958.

Ito, K., Y. Hirooka, et al. (2003). "Rho/Rho-kinase pathway in brain stem contributes to blood pressure regulation via sympathetic nervous system: possible involvement in neural mechanisms of hypertension." Circ Res **92**(12): 1337-1343.

Ito, M., T. Nakano, et al. (2004). "Myosin phosphatase: Structure, regulation and function." Molecular and Cellular Biochemistry **259**(1-2): 197-209.

Jarajapu, Y. P., F. Johnston, et al. (2001). "Functional characterization of alpha1-adrenoceptor subtypes in human subcutaneous resistance arteries." J Pharmacol Exp Ther **299**(2): 729-734.

Jin, L., Z. Ying, et al. (2006). "Increased RhoA/Rho-kinase signaling mediates spontaneous tone in aorta from angiotensin II-induced hypertensive rats." J Pharmacol Exp Ther **318**(1): 288-295.

Kitazawa, T., M. Eto, et al. (2003). "Phosphorylation of the myosin phosphatase targeting subunit and CPI-17 during Ca2+ sensitization in rabbit smooth muscle." J Physiol **546**(Pt 3): 879-889.

Kitazawa, T., S. Semba, et al. (2009). "Nitric oxide-induced biphasic mechanism of vascular relaxation via dephosphorylation of CPI-17 and MYPT1." J Physiol **587**(Pt 14): 3587-3603.

Kobayashi, T., T. Matsumoto, et al. (2004). "Differential expression of alpha2D-adrenoceptor and eNOS in aortas from early and later stages of diabetes in Goto-Kakizaki rats." Am J Physiol Heart Circ Physiol **287**(1): H135-143.

Kosako, H., H. Goto, et al. (1999). "Specific accumulation of Rho-associated kinase at the cleavage furrow during cytokinesis: cleavage furrow-specific phosphorylation of intermediate filaments." Oncogene **18**(17): 2783-2788.

Kozasa, T. (2001). "Regulation of G protein-mediated signal transduction by RGS proteins." Life Sci **68**(19-20): 2309-2317.

Kozasa, T., X. Jiang, et al. (1998). "p115 RhoGEF, a GTPase activating protein for Galpha12 and Galpha13." Science **280**(5372): 2109-2111.

Krolewski, A. S., J. H. Warram, et al. (1987). "Epidemiologic approach to the etiology of type I diabetes mellitus and its complications." N Engl J Med **317**(22): 1390-1398.

Laemmli, U. K. (1970). "Cleavage of structural proteins during the assembly of the head of bacteriophage T4." Nature **227**(5259): 680-685.

Lagaud, G. J., E. Masih-Khan, et al. (2001). "Influence of type II diabetes on arterial tone and endothelial function in murine mesenteric resistance arteries." J Vasc Res **38**(6): 578-589.

Lago, R. M., P. P. Singh, et al. (2007). "Diabetes and hypertension." Nat Clin Pract Endocrinol Metab **3**(10): 667.

Lang, P., F. Gesbert, et al. (1996). "Protein kinase A phosphorylation of RhoA mediates the morphological and functional effects of cyclic AMP in cytotoxic lymphocytes." EMBO J **15**(3): 510-519.

Lee, D. L., R. C. Webb, et al. (2004). "Hypertension and RhoA/Rho-kinase signaling in the vasculature: highlights from the recent literature." Hypertension **44**(6): 796-799.

Lee, J. H., J. H. Bahk, et al. (2011). "The diabetes-induced functional and distributional changes of the alpha 1-adrenoceptor of the abdominal aorta and distal mesenteric

artery from streptozotocin-induced diabetic rats." Korean J Anesthesiol **60**(4): 272-281.

Leung, T., X. Q. Chen, et al. (1996). "The p160 RhoA-binding kinase ROK alpha is a member of a kinase family and is involved in the reorganization of the cytoskeleton." Mol Cell Biol **16**(10): 5313-5327.

Leung, T., E. Manser, et al. (1995). "A novel serine/threonine kinase binding the Ras-related RhoA GTPase which translocates the kinase to peripheral membranes." J Biol Chem **270**(49): 29051-29054.

Lin, G., R. W. Brownsey, et al. (2009). "Regulation of mitochondrial aconitase by phosphorylation in diabetic rat heart." Cell Mol Life Sci **66**(5): 919-932.

Loirand, G., P. Guerin, et al. (2006). "Rho kinases in cardiovascular physiology and pathophysiology." Circ Res **98**(3): 322-334.

Longenecker, K., P. Read, et al. (1999). "How RhoGDI binds Rho." Acta Crystallogr D Biol Crystallogr **55**(Pt 9): 1503-1515.

Lowenstein, C. J., J. L. Dinerman, et al. (1994). "Nitric oxide: a physiologic messenger." Ann Intern Med **120**(3): 227-237.

MacDonald, J. A., M. A. Borman, et al. (2001). "Identification of the endogenous smooth muscle myosin phosphatase-associated kinase." Proc Natl Acad Sci U S A **98**(5): 2419-2424.

Maekawa, M., T. Ishizaki, et al. (1999). "Signaling from Rho to the actin cytoskeleton through protein kinases ROCK and LIM-kinase." Science **285**(5429): 895-898.

Makino, A. and K. Kamata (1998). "Possible modulation by endothelin-1, nitric oxide, prostaglandin I2 and thromboxane A2 of vasoconstriction induced by an alpha-agonist in mesenteric arterial bed from diabetic rats." Diabetologia **41**(12): 1410-1418.

Matsui, T., M. Amano, et al. (1996). "Rho-associated kinase, a novel serine/threonine kinase, as a putative target for small GTP binding protein Rho." EMBO J **15**(9): 2208-2216.

Matsumoto, T., K. Ishida, et al. (2009). "Involvement of NO and MEK/ERK pathway in enhancement of endothelin-1-induced mesenteric artery contraction in later-stage type 2 diabetic Goto-Kakizaki rat." Am J Physiol Heart Circ Physiol **296**(5): H1388-1397.

Matsumoto, T., K. Ishida, et al. (2010). "Mechanisms underlying the losartan treatment-induced improvement in the endothelial dysfunction seen in mesenteric arteries from type 2 diabetic rats." Pharmacol Res.

Matsumoto, T., M. Kakami, et al. (2008). "Gender differences in vascular reactivity to endothelin-1 (1-31) in mesenteric arteries from diabetic mice." Peptides **29**(8): 1338-1346.

Moriki, N., M. Ito, et al. (2004). "RhoA activation in vascular smooth muscle cells from stroke-prone spontaneously hypertensive rats." Hypertens Res **27**(4): 263-270.

Mueed, I., L. Zhang, et al. (2005). "Role of the PKC/CPI-17 pathway in enhanced contractile responses of mesenteric arteries from diabetic rats to alpha-adrenoceptor stimulation." Br J Pharmacol **146**(7): 972-982.

Mukai, Y., H. Shimokawa, et al. (2001). "Involvement of Rho-kinase in hypertensive vascular disease: a novel therapeutic target in hypertension." FASEB J **15**(6): 1062-1064.

Muranyi, A., J. A. MacDonald, et al. (2002). "Phosphorylation of the myosin phosphatase target subunit by integrin-linked kinase." Biochem J **366**(Pt 1): 211-216.

Muranyi, A., R. Zhang, et al. (2001). "Myotonic dystrophy protein kinase phosphorylates the myosin phosphatase targeting subunit and inhibits myosin phosphatase activity." FEBS Lett **493**(2-3): 80-84.

Nagareddy, P. R., J. H. McNeill, et al. (2009). "Chronic inhibition of inducible nitric oxide synthase ameliorates cardiovascular abnormalities in streptozotocin diabetic rats." Eur J Pharmacol **611**(1-3): 53-59.

Nakagawa, O., K. Fujisawa, et al. (1996). "ROCK-I and ROCK-II, two isoforms of Rho-associated coiled-coil forming protein serine/threonine kinase in mice." FEBS Lett **392**(2): 189-193.

Niiro, N. and M. Ikebe (2001). "Zipper-interacting protein kinase induces Ca(2+)-free smooth muscle contraction via myosin light chain phosphorylation." J Biol Chem **276**(31): 29567-29574.

Niiro, N., Y. Koga, et al. (2003). "Agonist-induced changes in the phosphorylation of the myosin- binding subunit of myosin light chain phosphatase and CPI17, two regulatory factors of myosin light chain phosphatase, in smooth muscle." Biochem J **369**(Pt 1): 117-128.

Nishimatsu, H., E. Suzuki, et al. (2005). "Endothelial dysfunction and hypercontractility of vascular myocytes are ameliorated by fluvastatin in obese Zucker rats." Am J Physiol Heart Circ Physiol **288**(4): H1770-1776.

Noma, K., N. Oyama, et al. (2006). "Physiological role of ROCKs in the cardiovascular system." Am J Physiol Cell Physiol **290**(3): C661-668.

Nuno, D. W., J. S. Harrod, et al. (2009). "Sex-dependent differences in Rho activation contribute to contractile dysfunction in type 2 diabetic mice." Am J Physiol Heart Circ Physiol **297**(4): H1469-1477.

Pang, H., Z. Guo, et al. (2005). "RhoA-Rho kinase pathway mediates thrombin- and U-46619-induced phosphorylation of a myosin phosphatase inhibitor, CPI-17, in vascular smooth muscle cells." Am J Physiol Cell Physiol **289**(2): C352-360.

Pimenta, W., M. Korytkowski, et al. (1995). "Pancreatic beta-cell dysfunction as the primary genetic lesion in NIDDM. Evidence from studies in normal glucose-tolerant individuals with a first-degree NIDDM relative." JAMA **273**(23): 1855-1861.

Pourageaud, F. and J. G. De Mey (1997). "Structural properties of rat mesenteric small arteries after 4-wk exposure to elevated or reduced blood flow." Am J Physiol **273**(4 Pt 2): H1699-1706.

Prentki, M. and C. J. Nolan (2006). "Islet beta cell failure in type 2 diabetes." J Clin Invest **116**(7): 1802-1812.

Puetz, S., L. T. Lubomirov, et al. (2009). "Regulation of smooth muscle contraction by small GTPases." Physiology (Bethesda) **24**: 342-356.

Rattan, S. and C. A. Patel (2008). "Selectivity of ROCK inhibitors in the spontaneously tonic smooth muscle." Am J Physiol Gastrointest Liver Physiol **294**(3): G687-693.

Riento, K. and A. J. Ridley (2003). "Rocks: multifunctional kinases in cell behaviour." Nat Rev Mol Cell Biol **4**(6): 446-456.

Rossini, A. A., J. P. Mordes, et al. (1988). "Speculations on etiology of diabetes mellitus. Tumbler hypothesis." Diabetes **37**(3): 257-261.

Rossman, K. L., L. Cheng, et al. (2003). "Multifunctional roles for the PH domain of Dbs in regulating Rho GTPase activation." J Biol Chem **278**(20): 18393-18400.

Sasaki, Y., M. Suzuki, et al. (2002). "The novel and specific Rho-kinase inhibitor (S)-(+)-2-methyl-1-[(4-methyl-5-isoquinoline)sulfonyl]-homopiperazine as a probing molecule for Rho-kinase-involved pathway." Pharmacol Ther **93**(2-3): 225-232.

Sauzeau, V., H. Le Jeune, et al. (2000). "Cyclic GMP-dependent protein kinase signaling pathway inhibits RhoA-induced Ca2+ sensitization of contraction in vascular smooth muscle." J Biol Chem **275**(28): 21722-21729.

Schaan, B. D., P. Dall'Ago, et al. (2004). "Relationship between cardiovascular dysfunction and hyperglycemia in streptozotocin-induced diabetes in rats." Braz J Med Biol Res **37**(12): 1895-1902.

Seko, T., M. Ito, et al. (2003). "Activation of RhoA and inhibition of myosin phosphatase as important components in hypertension in vascular smooth muscle." Circ Res **92**(4): 411-418.

Shimizu, H., M. Ito, et al. (1994). "Characterization of the myosin-binding subunit of smooth muscle myosin phosphatase." J Biol Chem **269**(48): 30407-30411.

Sin, W. C., X. Q. Chen, et al. (1998). "RhoA-binding kinase alpha translocation is facilitated by the collapse of the vimentin intermediate filament network." Mol Cell Biol **18**(11): 6325-6339.

Smith, J. M., D. J. Paulson, et al. (1997). "Inhibition of nitric oxide synthase by L-NAME improves ventricular performance in streptozotocin-diabetic rats." J Mol Cell Cardiol **29**(9): 2393-2402.

Solaro, R. J. (2000). "Myosin light chain phosphatase: a Cinderella of cellular signaling." Circ Res **87**(3): 173-175.

Somlyo, A. P. and A. V. Somlyo (1994). "Signal transduction and regulation in smooth muscle." Nature **372**(6503): 231-236.

Somlyo, A. P. and A. V. Somlyo (2000). "Signal transduction by G-proteins, rho-kinase and protein phosphatase to smooth muscle and non-muscle myosin II." J Physiol **522 Pt 2**: 177-185.

Somlyo, A. P. and A. V. Somlyo (2003). "Ca2+ sensitivity of smooth muscle and nonmuscle myosin II: modulated by G proteins, kinases, and myosin phosphatase." Physiol Rev **83**(4): 1325-1358.

Somlyo, A. P., X. Wu, et al. (1999). "Pharmacomechanical coupling: the role of calcium, G-proteins, kinases and phosphatases." Rev Physiol Biochem Pharmacol **134**: 201-234.

Sowers, J. R. and M. Epstein (1995). "Diabetes mellitus and associated hypertension, vascular disease, and nephropathy. An update." Hypertension **26**(6 Pt 1): 869-879.

Szkudelski, T. (2001). "The mechanism of alloxan and streptozotocin action in B cells of the rat pancreas." Physiol Res **50**(6): 537-546.

Takizawa, N., Y. Koga, et al. (2002). "Phosphorylation of CPI17 and myosin binding subunit of type 1 protein phosphatase by p21-activated kinase." Biochem Biophys Res Commun **297**(4): 773-778.

Takizawa, N., N. Niiro, et al. (2002). "Dephosphorylation of the two regulatory components of myosin phosphatase, MBS and CPI17." FEBS Lett **515**(1-3): 127-132.

Tamura, M., H. Nakao, et al. (2005). "Development of specific Rho-kinase inhibitors and their clinical application." Biochim Biophys Acta **1754**(1-2): 245-252.

Taylor, P. D., A. L. McCarthy, et al. (1992). "Endothelium-dependent relaxation and noradrenaline sensitivity in mesenteric resistance arteries of streptozotocin-induced diabetic rats." Br J Pharmacol **107**(2): 393-399.

Taylor, P. D., B. B. Oon, et al. (1994). "Prevention by insulin treatment of endothelial dysfunction but not enhanced noradrenaline-induced contractility in mesenteric

resistance arteries from streptozotocin-induced diabetic rats." Br J Pharmacol **111**(1): 35-41.

Tenenbaum, A., E. Z. Fisman, et al. (1999). "Prevalence and prognostic significance of unrecognized systemic hypertension in patients with diabetes mellitus and healed myocardial infarction and/or stable angina pectoris." Am J Cardiol **84**(3): 294-298.

Tsai, M. H. and M. J. Jiang (2006). "Rho-kinase-mediated regulation of receptor-agonist-stimulated smooth muscle contraction." Pflugers Arch **453**(2): 223-232.

Turrell, H. E., G. C. Rodrigo, et al. (2011). "Phenylephrine preconditioning involves modulation of cardiac sarcolemmal K(ATP) current by PKC delta, AMPK and p38 MAPK." J Mol Cell Cardiol **51**(3): 370-380.

Uehata, M., T. Ishizaki, et al. (1997). "Calcium sensitization of smooth muscle mediated by a Rho-associated protein kinase in hypertension." Nature **389**(6654): 990-994.

Vega, G. L. (2001). "Results of Expert Meetings: Obesity and Cardiovascular Disease. Obesity, the metabolic syndrome, and cardiovascular disease." Am Heart J **142**(6): 1108-1116.

Wang, L., M. Rolfe, et al. (2003). "Ca(2+)-independent protein kinase C activity is required for alpha1-adrenergic-receptor-mediated regulation of ribosomal protein S6 kinases in adult cardiomyocytes." Biochem J **373**(Pt 2): 603-611.

Wang, Y., X. R. Zheng, et al. (2009). "ROCK isoform regulation of myosin phosphatase and contractility in vascular smooth muscle cells." Circ Res **104**(4): 531-540.

Ward, D. T., A. C. Alder, et al. (2002). "Noradrenaline-induced paxillin phosphorylation, ERK activation and MEK-regulated contraction in intact rat mesenteric arteries." J Vasc Res **39**(1): 1-11.

Weber, D. S. and R. C. Webb (2001). "Enhanced relaxation to the rho-kinase inhibitor Y-27632 in mesenteric arteries from mineralocorticoid hypertensive rats." Pharmacology **63**(3): 129-133.

Wibberley, A., Z. Chen, et al. (2003). "Expression and functional role of Rho-kinase in rat urinary bladder smooth muscle." Br J Pharmacol **138**(5): 757-766.

Witte, K., K. Jacke, et al. (2002). "Dysfunction of soluble guanylyl cyclase in aorta and kidney of Goto-Kakizaki rats: influence of age and diabetic state." Nitric Oxide **6**(1): 85-95.

Woodsome, T. P., A. Polzin, et al. (2006). "Agonist- and depolarization-induced signals for myosin light chain phosphorylation and force generation of cultured vascular smooth muscle cells." J Cell Sci **119**(Pt 9): 1769-1780.

Xie, Z., M. C. Gong, et al. (2010). "Role of calcium-independent phospholipase A2beta in high glucose-induced activation of RhoA, Rho kinase, and CPI-17 in cultured vascular smooth muscle cells and vascular smooth muscle hypercontractility in diabetic animals." J Biol Chem **285**(12): 8628-8638.

Xie, Z., W. Su, et al. (2006). "Up-regulation of CPI-17 phosphorylation in diabetic vasculature and high glucose cultured vascular smooth muscle cells." Cardiovasc Res **69**(2): 491-501.

Yang, X. Q., Y. Y. Wang, et al. (2008). "Increased superoxide contributes to enhancement of vascular contraction in Ins2(Akita) diabetic mice, an autosomal dominant mutant model." Clin Exp Pharmacol Physiol **35**(9): 1097-1103.

Zacharia, J., C. Hillier, et al. (2004). "Alpha1-adrenoceptor subtypes involved in vasoconstrictor responses to exogenous and neurally released noradrenaline in rat femoral resistance arteries." Br J Pharmacol **141**(6): 915-924.

Zemlickova, E., F. J. Johannes, et al. (2004). "Association of CPI-17 with protein kinase C and casein kinase I." Biochem Biophys Res Commun **316**(1): 39-47.